NASA/CR-2000-210112

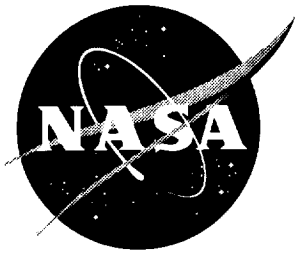

Validation of Aircraft Noise Prediction Models at Low Levels of Exposure

Juliet A. Page, Christopher M. Hobbs, Kenneth J. Plotkin, and Eric Stusnick
Wyle Laboratories, Arlington, Virginia

National Aeronautics and
Space Administration

Langley Research Center
Hampton, Virginia 23681-2199

Prepared for Langley Research Center
under Contract NAS1-20103, Task 22

April 2000

Available from:

NASA Center for AeroSpace Information (CASI)
7121 Standard Drive
Hanover, MD 21076-1320
(301) 621-0390

National Technical Information Service (NTIS)
5285 Port Royal Road
Springfield, VA 22161-2171
(703) 605-6000

Table of Contents

List of Figures

List of Tables

List of Tables (Continued)

1 Introduction

For purposes of community planning and environmental assessments, the trend is toward prediction and analysis of aircraft noise at increasing distances from airports. Noise levels around airports and airbases in the United States are computed using the Federal Aviation Administration's (FAA's) Integrated Noise Model (INM)[1,2,3] or the Air Force's NOISEMAP (NMAP) software[4]. Historically, noise contours are expressed in terms of day-night average sound level (DNL or L_{dn}) in the vicinity of the airport. The aforementioned noise models were conceived and developed for use within the 65-dB L_{dn} contour. However, environmental assessments, community planning, and even en-route noise issues are forcing the use of these models to and beyond the 55-dB L_{dn} contour line. For a medium or large airport, the 55-dB L_{dn} contour line can be as much as 15 miles away from the runway threshold.

Previous studies[5] undertaken by Wyle Laboratories considered the accuracy of INM and NOISEMAP out to the 55-dB L_{dn} contour line, or approximately six to seven miles away from the airport. Statistical analysis of more than 300 correlated noise events, using INM and field measurements, demonstrated the applicability of the fundamental acoustic methodologies between the 65- and 55-dB L_{dn} contours. The current study considers noise prediction well beyond the 55-dB L_{dn} contour at Denver International Airport[6] (DIA) for distances up to 25 miles from the runway threshold.

Several significant analysis improvements were made during the course of this study, namely the development of a thrust prediction methodology and an improved "track first" noise correlation process. The basic premise is to model the aircraft in the exact location, with the most accurate representation of speed and power possible, allowing the only remaining issues to be the acoustic and atmospheric modeling and the noise source data utilized by the noise model. During the course of this study DIA, United Airlines (UAL) and Delta Airlines (DL) cooperated extensively, allowing Wyle Laboratories to develop a power prediction methodology, as well as obtain detailed flight information such as position, speed, takeoff gross weights and historical airframe/ engine equipment usage.

Table 1-1 itemizes the required information for prediction of aircraft noise:

Aircraft Noise Prediction Data Requirements
Aircraft Position
Aircraft Speed
Aircraft Engine State
Noise Source Data as a Function of Power, Speed, and Distance
Atmospheric Conditions Between Source and Receiver
Terrain and Ground Cover States

Table 1-1

For the current study, data was gathered in sufficient detail to fulfill all of the above noise prediction requirements (Table 1-2).

Data Availability for the Current Noise Study	
Requirement	**Data Obtained**
Aircraft Position Aircraft Speed	ARTS IIIA Radar Data
Aircraft Engine State (Power Setting) Percent of Flights Not Derated	Detailed Performance and Historical Operational Data from United Airlines and Delta Airlines
Noise Source Data	INM Internal Noise Database N-P-D Curves
Atmospheric Conditions Between Source and Receiver	Hourly Ground Weather Data and Twice-Daily Upper Air Data
Terrain and Ground Cover States	USGS* Terrain and Elevation Data and Noise Monitoring Site Surveys

Note: *U.S. Geological Survey

Table 1-2

During the study, the following assumptions and simplifications were made due to data unavailability or task scope restrictions:

- Vertical atmospheric profile parameters were linearly interpolated from twice-daily balloon launch data.
- A given aircraft departure was assumed to perform a derated thrust takeoff if such option was available, based on the local current atmospheric information and takeoff gross weight of the aircraft. Historical derate percentiles were applied only to the final analysis correlation parameters.
- Power schedules and net corrected installed thrust were calculated based on flight-specific atmospheric conditions, although INM allows only one set of atmospheric conditions per study.
- Estimation of thrust levels was only performed for departures. Arrivals, where pilots are often "jockeying" the throttles, were not considered in the current study, since existing simple thrust from velocity or descent gradient methods do not address such significant random pilot throttle variations.

Chapter 2 of this report documents the measurement planning and the decisions made regarding airport selection and site location as well as details of the measurements themselves and the data acquisition process. Presentation of the acquired data is given in Chapter 3. Analysis of the data correlation between predicted and measured noise levels and documentation of the power prediction methodology is contained in Chapter 4. Interpretation of the results is contained in Chapter 5, while conclusions and recommendations for future work are made in Chapter 6.

2 Measurement Program and Data Acquisition

2.1 Introduction

Building on experiences gained in the previous Dulles Noise Study[5], a high priority was placed on the enlistment of airline cooperation to ensure that accurate power and throttle settings could be evaluated for all points in the profile. Airline cooperation was also deemed critically necessary for obtaining detailed actual "as-flown" fleet airframe/engine combinations as well as takeoff weights. Assumptions were made regarding equipment usage in the prior study and were based on fleet average assessments with destinations based on the *Official Airline Guide* (OAG). For this study, we considered it necessary to obtain exact detailed, indisputable airframe/engine information directly from the FAA-mandated airline maintenance archives, as well as detailed takeoff and climb thrust performance data.

2.2 Airport Selection

During the planning phase for this study, the following criteria shown in Table 2-1 were developed to aid in the selection of the measurement airport.

Airport Site Selection Criteria
1. Availability of ARTS Radar Data
2. Cooperation of Airlines with a significant number of operations at the airport.
3. Low background noise levels in the surrounding community, especially in areas beyond the 55-dB L_{dn} contour line.
4. Cooperation with the local noise abatement office and access to existing noise monitoring system data.

Table 2-1

After research and coordination efforts, Denver International Airport (DIA) was selected and approved by NASA as the study site.[6]

2.3 Measurement Site Selection

The DIA Noise Abatement Office provided to Wyle Laboratories a series of official L_{dn} contours surrounding the airport (Figure 2-1). Several days of sample radar tracking data were also provided to aid in the monitor location selection process. As shown in Figure 2-1, DIA has an extensive noise monitoring system in place, to which access was

granted for obtaining noise measurement data. Additional temporary monitoring stations were selected to supplement the DIA permanent monitoring system.

Supplementary site locations were identified after consideration of the following:

- expected L_{dn} noise contour locations
- flight track-based analysis of sample radar data
- likelihood and levels of background noise
- equipment security
- location accessibility

An on-location survey of the proposed sites led to the final selection. This survey identified specific locations and considered local noise sources such as automobile traffic, construction, as well as site accessibility and security. Permission from the landowners to install and maintain equipment was obtained for all locations.

All but one of the supplementary sites were located outside or near the 65-dB L_{dn} contour. The monitors installed by Wyle were located east of Runway 08/26 and south of the airport. Using flight tracks as a guide, the noise monitors were located under the densest air traffic. The distances between the airport origin and the DIA and Wyle noise monitoring sites are listed in Table 2-2.

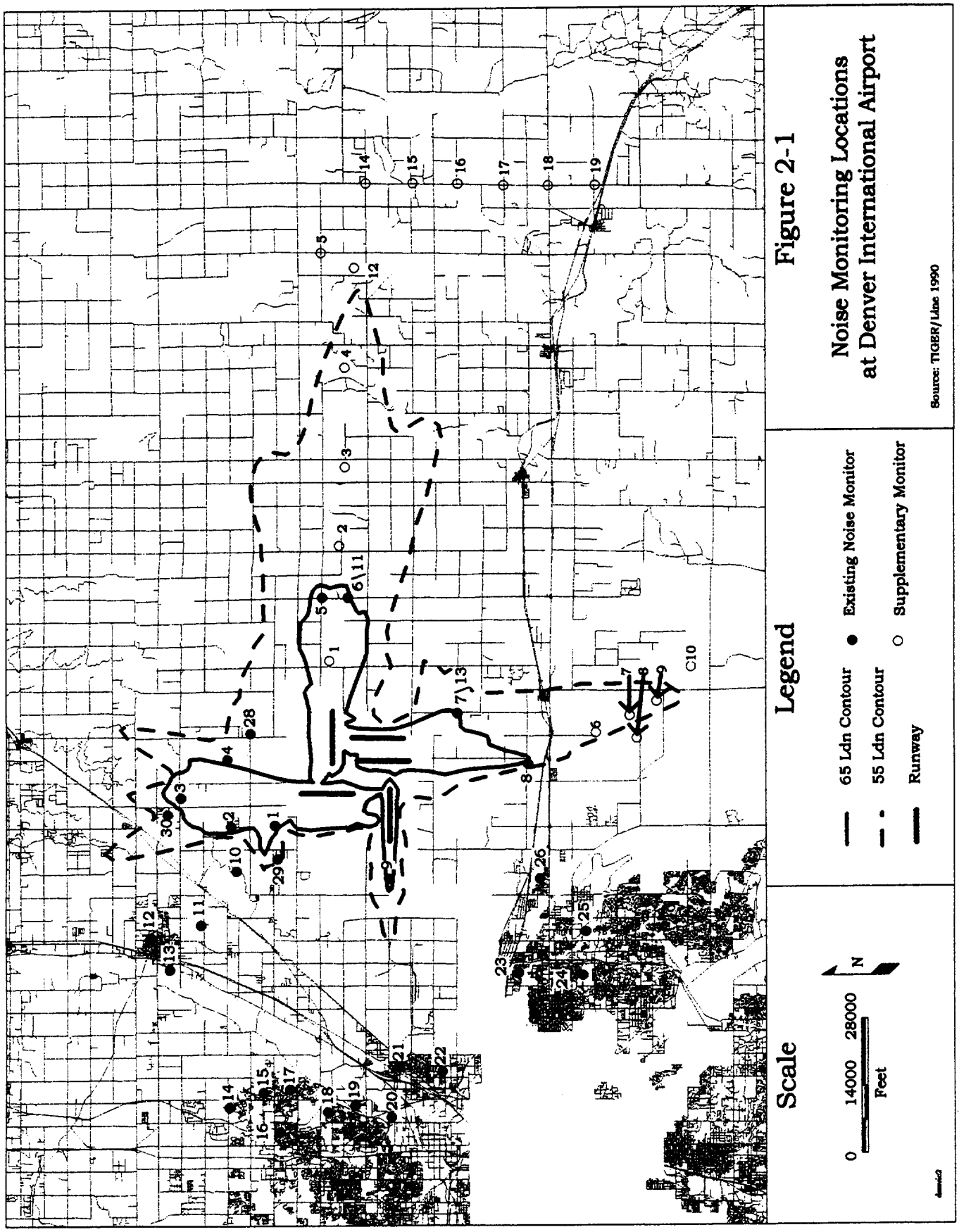
Figure 2-1
Noise Monitoring Locations
at Denver International Airport
Source: TIGER/Line 1990
Legend
65 Ldn Contour
55 Ldn Contour
Runway
Existing Noise Monitor
Supplementary Monitor
Scale
0
14000
28000
Feet
N

DIA (S) and Wyle (W) Noise Monitor Site Distances					
Monitor Site	Distance, nmi	Monitor Site	Distance, nmi	Monitor Site	Distance, nmi
S10	5.18	S27	21.90	W04	18.49
S11	7.22	S28	5.77	W05	22.39
S12	9.10	S29	3.56	W06	9.36
S13	9.12	S30	7.55	W07	10.86
S14	11.74	S31	22.57	W08	11.03
S15	10.70	S01	3.51	W09	12.21
S16	11.95	S02	5.14	W10	13.91
S17	10.28	S03	7.14	W11	8.89
S18	10.81	S04	5.96	W12	21.88
S19	10.46	S05	9.02	W13	5.63
S20	10.95	S06	8.89	W14	24.49
S21	9.09	S07	5.63	W15	24.55
S22	9.60	S08	6.58	W16	24.70
S23	7.87	S09	2.00	W17	24.98
S24	9.88	W01	6.58	W18	25.36
S25	9.15	W02	10.68	W19	25.89
S26	6.78	W03	14.34		

Table 2-2

Coordinates for the monitor locations are shown in Table 2-3. DIA officials provided the coordinates for the Denver sites (denoted with an S). The Wyle sites (denoted with a W) were determined by locating the site on 7.5 x 7.5-minute USGS maps and verifying in the field with a global positioning system. The margin of error is 150 feet in the horizontal plane and 20 feet in the vertical direction.

Noise Monitor Site Coordinates and Elevations							
Site	Latitude	Longitude	Elevation	Site	Latitude	Longitude	Elevation
S01	39.913417	-104.71386	5,243	W01	39.86975	-104.57708	5,380
S02	39.940714	-104.71449	5,158	W02	39.87658	-104.48877	5,238
S03	39.972091	-104.69054	5,112	W03	39.868474	-104.40838	5,233
S04	39.943126	-104.65899	5,279	W04	39.869266	-104.31845	5,140
S05	39.88391	-104.52659	5,266	W05	39.883978	-104.23518	5,095
S06	39.867579	-104.52661	5,299	W06	39.710779	-104.64083	5,711
S07	39.797821	-104.62164	5,423	W07	39.690147	-104.62097	5,772
S08	39.753662	-104.66348	5,604	W08	39.682132	-104.63654	5,810
S09	39.841317	-104.75777	5,292	W09	39.667582	-104.6151	5,870
S10	39.937485	-104.75127	5,098	W10	39.647203	-104.58455	5,970
S11	39.959605	-104.79585	5,046	W11	39.867946	-104.5267	5,306
S12	39.990732	-104.80629	4,977	W12	39.852291	-104.24486	5,110
S13	39.979036	-104.83249	4,967	W13	39.797821	-104.62164	5,423
S14	39.941792	-104.9463	5,338	W14	39.855233	-104.18819	4,979
S15	39.920678	-104.93377	5,171	W15	39.826166	-104.18839	5,021
S16	39.910657	-104.96674	5,325	W16	39.797211	-104.18929	5,056
S17	39.904312	-104.93136	5,203	W17	39.768049	-104.1913	5,101
S18	39.880582	-104.94985	5,249	W18	39.739084	-104.19081	5,163
S19	39.863181	-104.94443	5,121	W19	39.710338	-104.19086	5,225
S20	39.839967	-104.95437	5,125	ASR	39.854986	-104.7183	5,431
S21	39.834983	-104.91327	5,151				
S22	39.807386	-104.91656	5,181				
S23	39.759972	-104.83585	5,335				
S24	39.718379	-104.8378	5,459				
S25	39.716632	-104.80171	5,450				
S26	39.746086	-104.75819	5,459				
S27	39.494244	-104.6437	5,900				
S28	39.928624	-104.63775	5,200				
S29	39.911728	-104.74136	5,243				
S30	39.980388	-104.70447	5,112				
S31	39.483224	-104.64222	5,900				

Table 2-3

Note that use of the current L_{dn} contours in Figure 2-1 was for the purpose of providing a reference noise environment to aid in the selection of the noise monitoring locations. The L_{dn} contours are an interpretation of the official contours in that they were digitized from the original exhibit and registered in a geographic information system (GIS). These modified contours are a good representation of the originals so far as the shape and extent of the footprint; however, due to the digitization process, the contour lines are not as smooth as the originals. These contours should not be considered the official L_{dn} contours for DIA nor should they be used for any land-use planning purposes. As Figure 2-1 indicates, most of the noise monitoring sites span and exceed the space between the 55- and 65-dB contours, consistent with the main objective of the study: to examine the predictive capabilities of INM at low-levels of exposure, out to and beyond the 55-dB L_{dn} contour.

2.4 Noise Monitor Installation and Instrumentation

Noise monitoring was conducted during the period from 13 May through 13 June 1997. DIA operates 30 noise monitors in and around the metropolitan area. They are noted as existing noise monitors in Figure 2-1 and their coordinates are denoted with an S in Tables 2-2 and 2-3. Wyle installed an additional 12 monitors (denoted as Supplementary Monitors in Figure 2-1 and with a W in Tables 2-2 and 2-3) for the duration of the measurements. Six additional monitors, numbered 14 through 19 in Figure 2-1, were put in place the afternoon of 12 June and ran for approximately 24 hours. The purpose of this lateral array was to assess the data quantity and quality over extremely long slant ranges and low elevation angles. Decisions regarding future long-range lateral attenuation studies can make use of this data. Two sets of site numbers side by side in Figure 2-1 (6/11 and 7/13) indicate that a Wyle monitor was placed next to a Denver monitor. This was an effort to ensure that the data gathered from the two different systems, utilizing different brands of monitors, microphones, and calibration techniques, agreed with each other.

2.5 Measurement Program Execution

Each site chosen for noise monitoring was serviced every two to three days. This schedule was sufficient to ensure near continuous operation from 13 May to 13 June 1997. The only down time occurred during the approximately 20-minute monitor site servicing. Visits to a site included downloading the field data directly to a laptop computer, checking and replacing the external batteries, and calibrating to ensure the system was operating within tolerance. Records of the visit were made in a site log. A sample site log entry is shown in Figure 2-2.

Immediately following field data collection, the binary files downloaded from the monitors were transmitted via modem to the home office for analysis.

DENVER MONITORING PROGRAM (J/N 19110)

Date: May 25th Name: CH

Site # 9 Serial # 63 Arrival Time: 9:35 Restart Time: 9:50

Free Memory 31.82%

No. Exceedances -

Threshold - Changed? Yes ___ No / New Threshold ___

External Batt 163% (12.27V) Replaced? Yes ___ No /

Internal Batt 96% Replaced? Yes ___ No /

Calibration Check 94.1 dB

Binary Data File S09525.bin

Wind slow 9.6 mph, max gusting Temp 56°F Precip none

Comments: Mic is dry. 1 landing north of site + 1 landing west (coming from the west) + 1 landing coming from overhead + 1 landing west + 1 1 passby overhead. Reset data. Reset time (3s slow) + 1 landing north.

Site # 8 Serial # 78 Arrival Time: 9:57 Restart Time: 10:10

Free Memory 31.22%

No. Exceedances -

Threshold - Changed? Yes ___ No / New Threshold ___

External Batt 164% (12.33V) Replaced? Yes ___ No /

Internal Batt 106% Replaced? Yes ___ No /

Calibration Check 94.1 dB

Binary Data File S09525.bin

Wind mild 11.3 mph, max gusting Temp ~59°F Precip none

Comments: lot of noise (small propeler plane + motorcycles + cars)

1 landing north of site + 1 passingby overhead + 1 landing west

1 landing north + 1 west + 1 passby + 1 landing to the north-est + 1 landing nor

reset data + time (1s slow) + 1 west (landing)

ambiant (with ultra light plane) : 63dB

jet air plane afterwards : 59 dB

Figure 2-2. Sample Site Log

2.6 Instrumentation

Larson Davis Model 820 sound level meters were used to collect one-second, slow response, A-weighted equivalent sound levels (L_{eq}s) with single-digit precision. Bruel & Kjaer Model 4176 (type I) microphones attached to Larson Davis Model 827 preamplifiers were covered with a windscreen and secured so that the microphone face was four feet above the ground. See Figure 2-3 for a typical setup. The monitor and external battery were secured in an environmental box. A cable led from the preamplifier to the monitor. It is important to note that the Denver monitors are 16 feet above the ground. Wyle monitor 11 was placed on a tower 6 inches from Denver monitor 6. Both monitors were 16 feet above the ground. Figure 2-4 is a picture of Denver/Wyle sites 6/11. Examples of the time records downloaded from the monitors can be seen in Figure 2-5. Note the excellent agreement between the two systems. An example summary report from a monitor is reproduced in Figure 2-6.

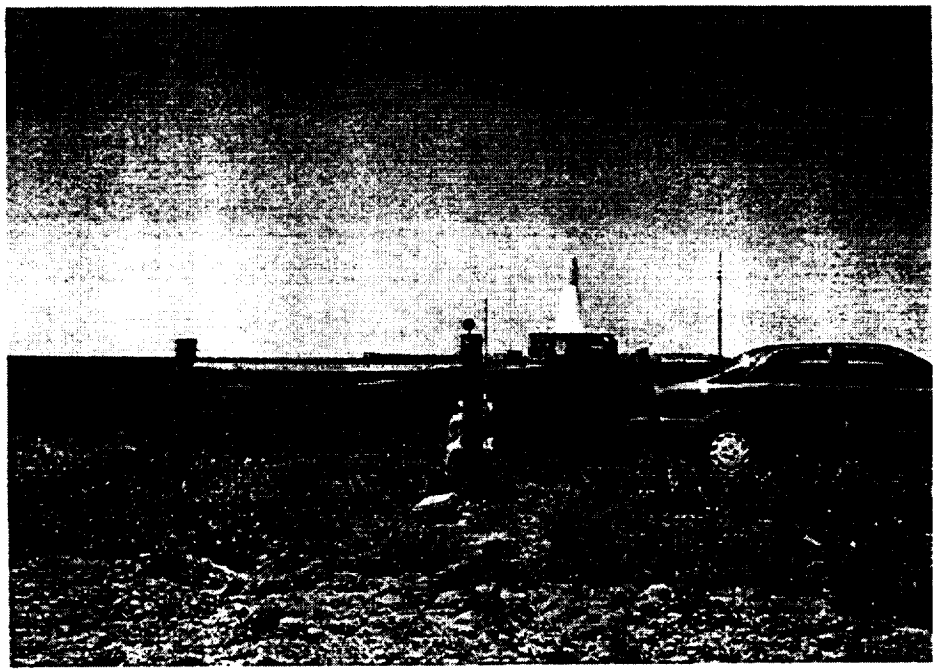

Figure 2-3. Typical Site Instrumentation Setup

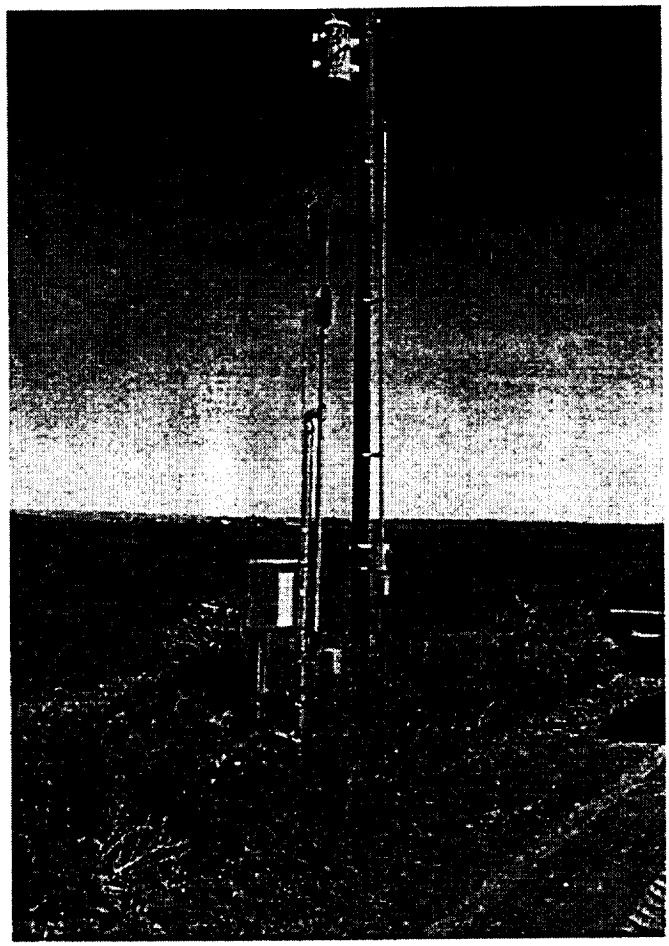

Figure 2-4. Co-located Denver Site 6 and Wyle Site 11

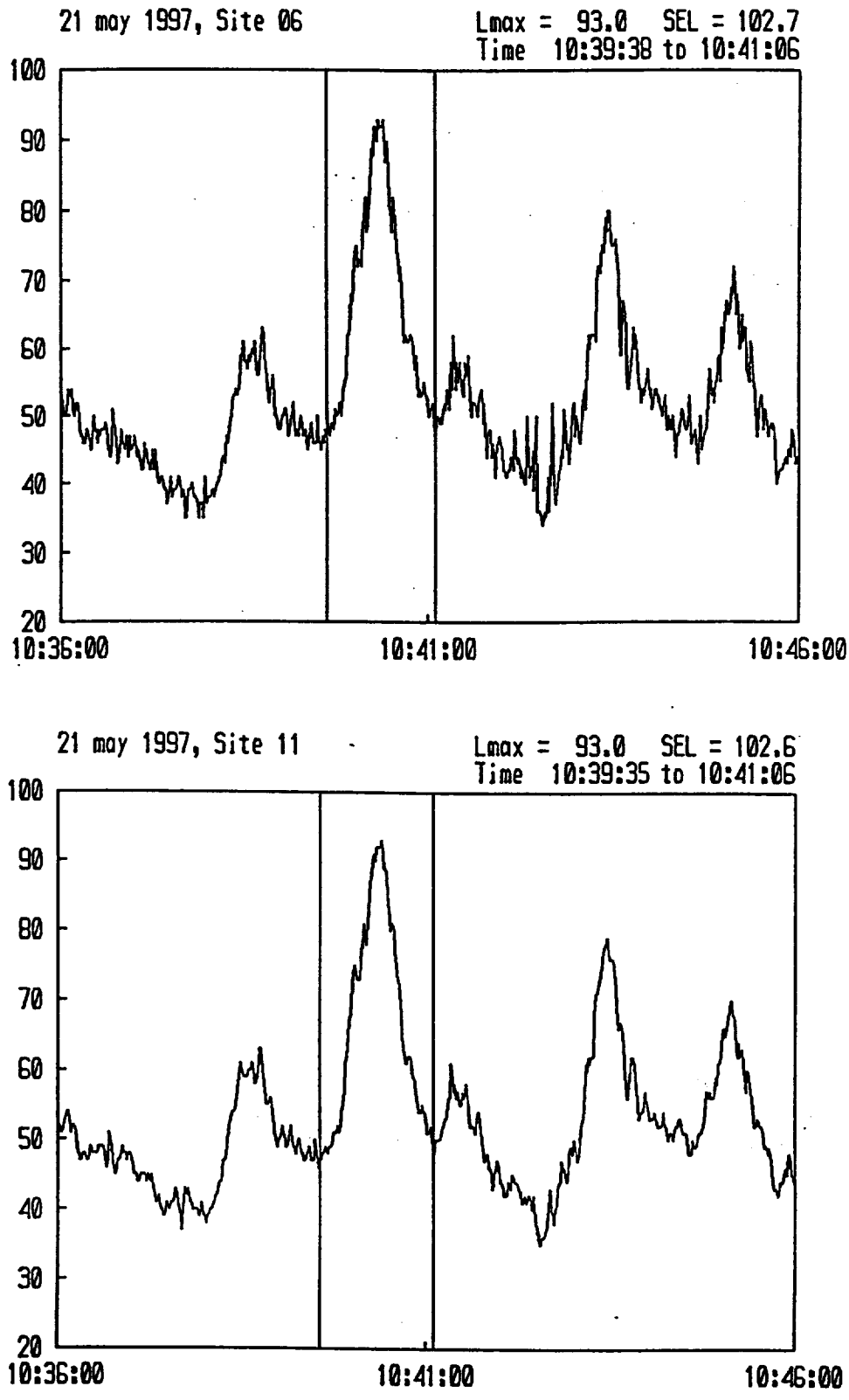

Figure 2-5. Example Time Records for Co-located Denver Site S06 and Wyle Site W11

```
D:\NOISEX2\S01527.bin    Summary Data
-----------------------------------------------------------------

Site:          0     Model: 820
Location:
Date:        25May 97 11:22:51

                        Overall                  Current
Run Time                51:25:27.3               00:00:00.0
Start Time            25May 97 11:22:51          27May 97 14:50:26
Leq                       72.1                   Leq    0.0
SEL                      124.7                          0.0
Lmax                     104.4                          0.0
Lmax Time             27May 97 10:50:10          31Jan 00 00:00:00
Lmin                      21.7                          0.0
Lmin Time             27May 97 01:36:05          31Jan 00 00:00:00
Peak                     121.2                          0.0
Peak Time             25May 97 19:31:40          31Jan 00 00:00:00
Unweighted Peak          124.2                          0.0
Uwpk Time             25May 97 19:31:40          31Jan 00 00:00:00
Dose                       0.0                          0.0
Projected Dose             0.0                          0.0
Threshold                  0                            0
Criterion                  0                            0
Ln values
   L 1 =  82.7   L10 =  62.6   L33 =  48.3
   L50 =  43.3   L90 =  26.6   L99 =  23.7

Ldn               72.5      Event Leq         72.1
Cnel              73.4      Event Time     50:37:38.5
Sound Exposure     0.3      Background Leq    65.7
Overloads            0      Background Time   00:47:48.8
Pause Time       00:00:00.0

Records:
Run/Stop        2    Daily               0
Event           0    Calibration         1
Interval       52    Time History   185130
```

Figure 2-6. Sample Monitor Summary Report

2.7 Site Visit

When visiting a monitor site, the temperature and wind speed were recorded. These weather records agreed with the surface data measured at the airport. The condition of the external battery was checked. If the voltage was low, it was replaced with a newly charged battery. The amount of memory used since the last download was recorded. The calibration was checked with a Bruel & Kjaer Model 4231 calibrator. Any deviation of the measured level of the calibration tone from what it should be was recorded. The monitor's clock was reset to the correct time. The difference between the correct time and the monitor's clock time, if any, was recorded. Generally, it was found that the monitor's time differed from the correct time by less than three seconds. The correct time was taken as that transmitted by the Naval Observatory.

2.8 Analysis

All data were received at each site continuously with few exceptions. The monitor at Denver site 7/Wyle site 13 was moved to Denver site 6/Wyle site 11 on 20 May. The road leading to this site was treacherous. Were there any rains, it would have been impassable. A monitor at site 9 on 21 May was not operating because of equipment failure. It was replaced. During a period of approximately two hours on 4 June none of the monitors were operating. Their memories were filled and data had ceased to be taken. Otherwise, one-second L_{eq}s were being recorded by the Wyle monitors at all times during the measurement period except during each 20-minute monitor-servicing period.

From 13 May to 21 May, the windscreens of all monitors were covered with plastic to protect the microphones from moisture. Laboratory measurements showed no change in sound levels between a wrapped and unwrapped windscreen. After 21 May, the wraps were not replaced over the windscreen because they were deemed unnecessary. None of the microphones exhibited adverse effects from exposure. The unwrapped windscreens protected the microphones from the rain. There was no equipment failure as a result of this action; therefore.

3 Presentation of Data Acquired

Data were obtained from several sources and required the cooperation of numerous organizations and agencies. This cooperation enabled Wyle Laboratories to accumulate an extremely detailed, broadly comprehensive set of acoustic, atmospheric, and operational data. Data gathering fell into five general areas:

1. weather and atmospheric conditions
2. radar tracking data
3. noise monitoring data
4. operational information
5. performance and power data

Table 3-1 provides a summary of overall operations at DIA during the measurement period.

Sections 3.1 to 3.5 give descriptions of each of these data types. Section 3.6 includes, in addition to the basic measurement program, data from a mini-lateral array at sites W14 to W19, as described in Section 2.4.

3.1 Weather and Atmospheric Data

Two types of atmospheric data were acquired:

- hourly surface weather data from DIA
- vertical profile data from twice-daily balloon launches at Denver-Stapleton Airport

Airport surface weather data was geared to pilot requirements and included such information as:

- wind speed and direction
- gust information
- temperature
- barometric pressure
- dew point
- relative humidity
- precipitation
- atmospheric observations such as cloud cover and visibility

Summary Data From Radar Tracking			
Start Date: 19970515 Ending Date: 19970613 Total Tracks: 14,992			
Aircraft Type	**Total Number**	**Operator**	**# Operations – Arrival and Departure**
B727	1,903		
B737	4,790	American	427
B757	1,335	Delta	415
B767	80	General Aviation	2,069
B757	101	NorthWest	213
B777	119	TWA	129
BA46	274	United	6,306
DC10	317	UPS	61
DC8	67	US Air	140
DC9	101	Other	5,232
MD80	682		
MD88	108		
GA & other	5,115		
Total	14,992	Total	14,992

Runway/Operations	
Runway	**Operations**
7/Arrival	249
7/Departure	2
8/Arrival	0
8/Departure	4,486
16/Arrival	420
16/Departure	5
17L/Arrival	3
17L/Departure	611
17R/Arrival	243
17R/Departure	2,077
26/Arrival	1
26/Departure	15
25/Arrival	0
25/Departure	1,414
34/Arrival	0
34/Departure	1,673
35L/Arrival	186
35L/Departure	535
35R/Arrival	79
35R/Departure	1
ASR/Arrival	226
ASR/Departure	2,703
Overflights	63
Total	14,992

Table 3-1

Table 3-2 contains a partial report of hourly surface weather data. Barometric pressures reported in this data are actually the reference pressure or altimeter setting for the pilots.

This is the setting, in inches of mercury, at which the airplane's altimeter will read actual geometric airport altitude for the given atmospheric conditions.

Sample upper air weather data from the balloon launches is presented in Table 3-3. Contained within these reports for the reporting altitudes is the atmospheric pressure in millibars, wind speed and direction, temperature, dew point, and humidity. As the balloon rises, data is reported at irregular intervals.

DENVER AP, (DEN), HOURLY SURFACE AIRWAYS OBERVATIONS, 14 MAY - 15 JUNE 1997

Key: TIME(GMT and MDT) = ddhhmm where dd=day, hh=hour, and mm=minute.
VISIBILITY = ddSM where dd is the visibility in statute miles. (Precipitation code: RA=rain,SN=snow, BR=mist, TS=thunderstorm, GS=small hail/snow pellets, FG=fog, FC=funnel cloud; - = light, + = heavy; +FC = tornado/water spout.)
CLOUD COVER = dddhhh where ddd=descriptor (FEW=few, SCT=scattered, BKN=broken) and hhh is height in hundreds of feet. (Example: FEW050 = few clouds at 5000 ft., SCT100 = scattered clouds at 10000 ft., BKN250 = broken clouds at 25000 ft.)
TEMP = tt/dd where tt is the air temperature in degrees Centigrade and dd is the dew point temperature in degrees Centigrade (Note: M stands for 'minus'; thus, M05 means -5°C.)
ALTIMITER = Aaaaa where aaaa is the altimeter setting in hundredths of an inch of mercury.
RMK = remark follows; AO2=automatic, SLP=sea level pressure in millibars (SLP024 means 1024 millibars).

	Time		Wind Speed			Visibility		Temp/Dew	Altimiter	
Date	GMT	MDT	Dir	Av.(kts)	Gusts(kts)	(st.mi.)	Cloud Cover	Pt. (°C)	.01"Hg	Remarks
970514	132353	131753	360	22	G27	10SM	SCT120 OVC250	19/03	A2996	RMK AO2 PK
970514	140053	131853	350	11		10SM	SCT120 OVC250	17/03	A2998	RMK AO2 PK WND
970514	140153	131953	360	9		10SM	SCT100 OVC250	16/03	A3000	.RMK AO2 SLP101
970514	140253	132053	40	6		10SM	SCT100 BKN250	12/03	A3002	RMK AO2 SLP107
970514	140353	132153	50	3		10SM	SCT100 BKN250	13/02	A3005	RMK AO2 SLP111
970514	140453	132253	60	5		10SM	FEW100 SCT250	10/01	A3007	RMK AO2 SLP123
970514	140553	132353	110	3		10SM	FEW100 SCT250	09/00.	A3008	RMK AO2 SLP130
970514	140653	140053	160	6		10SM	FEW250	08/M01	A3008	RMK AO2 SLP129
970514	140753	140153	170	7		10SM	FEW250	07/M01	A3007	RMK AO2 SLP128
970514	140853	140253	170	8		10SM	FEW250	07/M02	A3006	RMK AO2 SLP125
970514	140953	140353	250	5		10SM	FEW250	06/M02	A3005	RMK AO2 SLP127
970514	141053	140453	170	5		10SM	FEW250	03/M02	A3004	RMK AO2 SLP132
970514	141153	140553	160	5		10SM	SCT250	02/M03	A3003	RMK AO2 SLP134
970514	141253	140653	200	7		10SM	FEW250	07/00.	A3004	RMK AO2 SLP128
970514	141353	140753	140	5		10SM	BKN250	10/02	A3005	RMK AO2 SLP130
970514	141453	140853	150	7		10SM	FEW110 BKN250	16/01	A3005	RMK AO2 SLP126
970514	141553	140953	70	5		10SM	BKN120 BKN250	17/02	A3006	RMK AO2 SLP127
970514	141653	141053	120	3		10SM	BKN140 BKN250	17/02	A3007	RMK AO2 SLP135
970514	141753	141153	VRB	3		10SM	SCT100 BKN250	18/02	A3007	RMK AO2 SLP133
970514	141853	141253	360	16		8SM -RA	BKN042 OVC055	14/08	A3009	RMK AO2
970514	141853	141253	360	16		8SM -RA	BKN042 OVC055	14/08	A3009	RMK AO2
970514	141953	141353	60	13		10SM	BKN055 BKN120	15/06	A3006	RMK AO2
970514	142053	141453	VRB	3		10SM	SCT070TCU SCT120 BKN250	18/06	A3007	RMK

Table 3-2

DENVER, STAPLETON AP, CO. UPPER AIR DATA, 14-20 MAY 1997.

Station: 72469
Time: 97051400

Typ	Prs mb	Ht m	Theta K	Temp C	DewPt C	RH %	Dir deg	Spd kt
b	1000	54						
b	925	732						
b	850	1456						
G	835	1608	309.3	20.6	2.6	30	40	20
s	821	1753	308.0	18.0	-1.0	28		
w		1828					35	18
w		2133					15	17
w		2438					350	20
s	750	2519	310.5	12.8	-5.2	28		
w		2742					350	18
m	700	3090	310.7	7.4	-6.6	36	350	15
w		3352					350	14
w		3656					320	12
w		4266					280	20
s	568	4764	312.5	-7.3	-12.3	67		
w		4875					280	32
s	528	5328	312.8	-12.5	-14.0	89		
s	521	5430	313.6	-12.9	-15.9	78		
m	500	5740	314.3	-15.3	-18.1	79	300	33
w		6094					300	32
s	469	6220	315.9	-18.7	-20.2	88		
m	400	7390	320.5	-26.5	-29.3	77	315	38
w		7617					320	43
w		7922					325	47
s	345	8443	324.8	-33.5	-39.5	55		
w		9141					315	55
m	300	9410	326.8	-41.5	-46.5	58	315	54
m	250	10620	329.1	-51.7	-56.7	55	310	58
w		10664					315	59
m	200	12030	333.3	-62.7	-67.7	51	320	57
w		12492					325	56
s	183	12572	335.4	-66.7	-71.4	51		
T	153	13644	346.8	-70.3	-74.8	52	315	42
w		13711					315	42
m	150	13760	348.5	-70.5	-75.2	50	315	43
s	140	14177	368.7	-62.9	-69.9	38		
s	132	14540	376.1	-62.3	-71.3	29		
w		14625					330	32
s	128	14732	386.2	-58.5	-68.5	26		
w		15235					310	19
w		15539					295	19
s	112	15562	392.3	-63.3	-77.3	13		
w		16149					305	20
s	101	16201	409.0	-60.7	-77.7	9		
m	100	16260	410.2	-60.7	-77.7	9	300	19
w		16453					300	19
s	96.0	16513	413.1	-61.7	-78.7	9		
s	83.9	17345	427.6	-62.5	-81.5	6		
w		17977					345	15
s	74.6	18075	449.4	-59.1	-80.1	5		
m	70	18480	454.2	-60.7	-81.7	5	355	8
s	67.0	18752	458.2	-61.5	-82.5	5		
s	61.2	19317	476.9	-58.5	-80.5	4		
m	50	20580	501.9	-59.9	-82.9	3	40	9
w		21328					75	5
m	30	23800	588.9	-56.9	-80.9	3	65	7
m	20	26390	673.5	-52.9	-77.9	3	65	8
s	19.0	26721	683.5	-52.9	-77.9	3		
w		27422					95	5
s	16.3	27720	730.3	-47.9	-73.9	3		
m	10	30970	859.8	-42.5	-72.5	2	240	19
s	9.5	31328	875.5	-41.7	-71.7	2		

Station: 72469
Time: 97051500

Typ	Prs mb	Ht m	Theta K	Temp C	DewPt C	RH %	Dir deg	Spd kt

Station: 72469
Time: 97051600

Typ	Prs mb	Ht m	Theta K	Temp C	DewPt C	RH %	Dir deg	Spd kt
b	1000	127						
b	925	800						
b	850	1517						
G	841	1608	304.5	16.6	5.6	48	180	15
s	830	1720	306.2	17.2	4.2	42		
w		1828					195	12
s	799	2043	307.5	15.2	0.2	36		
w		2133					210	10
w		2438					270	9
s	737	2722	310.3	11.2	-0.8	43		
w		2742					330	25
m	700	3149	310.4	7.2	-0.8	57	45	22
w		3352					90	22
w		3656					330	5
w		3961					320	16
w		4266					315	21
s	600	4393	311.8	-3.7	-7.8	73		
w		4875					320	24
s	552	5046	313.6	-8.5	-12.1	75		
s	524	5448	315.0	-11.3	-19.3	52		
s	514	5596	315.5	-12.3	-17.1	67		
s	509	5671	316.4	-12.3	-18.3	61		
s	508	5686	316.6	-12.3	-22.3	43		
m	500	5810	316.8	-13.3	-22.3	47	310	31
s	496	5871	316.8	-13.9	-22.9	47		
s	492	5932	317.0	-14.3	-18.9	68		
s	483	6072	317.9	-14.9	-22.9	51		
w		6094					310	30
s	475	6198	318.2	-15.9	-18.3	82		
s	457	6488	319.8	-17.5	-21.8	69		
s	453	6554	320.3	-17.7	-28.7	38		
s	448	6637	320.6	-18.3	-33.3	26		
s	437	6822	321.1	-19.7	-29.7	41		
s	430	6942	321.3	-20.7	-35.7	25		
m	400	7470	322.6	-24.9	-40.9	21	315	30
w		7617					315	30
s	365	8128	323.4	-30.7	-43.7	27		
w		8531					310	32
s	326	8919	324.6	-37.5	-43.5	53		
w		9141					305	40
m	300	9490	325.9	-42.1	-48.1	52	305	43
w		10360					305	52
w		10664					310	52
m	250	10690	328.2	-52.3	-56.8	58	310	52
s	237	11033	328.4	-55.5	-59.9	58		
m	200	12100	334.3	-62.1	-69.1	39	315	51
w		13102					330	38
T	161	13416	342.8	-69.7	-76.7	35	320	34
m	150	13840	355.3	-66.5	-74.5	32	315	31
s	138	14348	369.2	-63.5	-73.5	25		
w		15235					310	26
s	115	15458	382.6	-66.9	-79.9	14		
s	109	15784	393.4	-64.3	-78.3	13		
w		16149					335	-18
m	100	16310	401.3	-65.3	-80.3	11	335	18

Table 3-3. Denver, Stapleton AP Upper Air Weather Data

3.2 Radar Tracking Data

Radar data from the ARTS IIIA[7] was obtained for the duration of the measurement program. The DIA Noise Abatement Office provided FAA ARTS IIIA radar system files in *.REL format. These data files consist of Beacon hits as well as interfacility messages. Interfacility messages contain one-time information relays such as:

- airline flight number
- aircraft beacon code
- arrival or departure
- destination airport and first fix
- scheduled arrival or departure time

Radar Beacon data contains aircraft location information assembled in radar sweep sequence. Radar receivers at DIA rotate at approximately 13 revolutions per minute (RPM), representing one radar hit every 4.5 seconds.

Table 3-4 contains an itemization of the raw radar data provided to Wyle Laboratories. During periods indicated, radar-tracking data was not available due to ARTS III interface system problems.

ARTS IIIA Radar Tracking Data Summary			
Date	**File Size (Bytes)**	**Date**	**File Size (Bytes)**
970513	23896716	970530	29572836
970514	26607552	970531	29081600
970515	30759528	970601	27231260
970516	28910088	970602	20346412
970517	23191700	970603	3284942
970518	24283532	970604	34341912
970519	22945616	970605	32577320
970520	26633636	970606	486932 *
970521	26597100	970607	Missing *
970522	19858528	970608	21373960
970523	28094792	970609	19347572
970524	26923196	970610	27526380
970525	18135972	970611	35307896
970526	16824096	970612	29116276
970527	22325084	970613	24155336
970528	28722224	970614	27898644
970529	8102708		

Note: *Incomplete due to problems at TRACON

Table 3-4

3.3 Noise Monitoring Data

As stated in Section 2.3 and shown in Figure 2-1, a total of 50 noise monitors were in operation during the measurement program. Each monitoring station recorded continuous, round-the-clock, one-second, slow response, A-weighted L_{eq}s with single-digit precision. Care was taken during the monitoring program to ensure that times were properly synchronized between the monitors and the radar tracking system. Figure 3-1 shows a sample time history for noise monitor #W02. Multiple peaks are visible as several aircraft pass overhead. The background noise level of approximately 43 dB is also apparent. The first, third, fourth, and fifth events are most likely departures from Runway 08, whereas the second noise event is likely a departure from Runway 17L as evidenced by the lower peak, longer duration, and unsteadiness caused by longer range propagation.

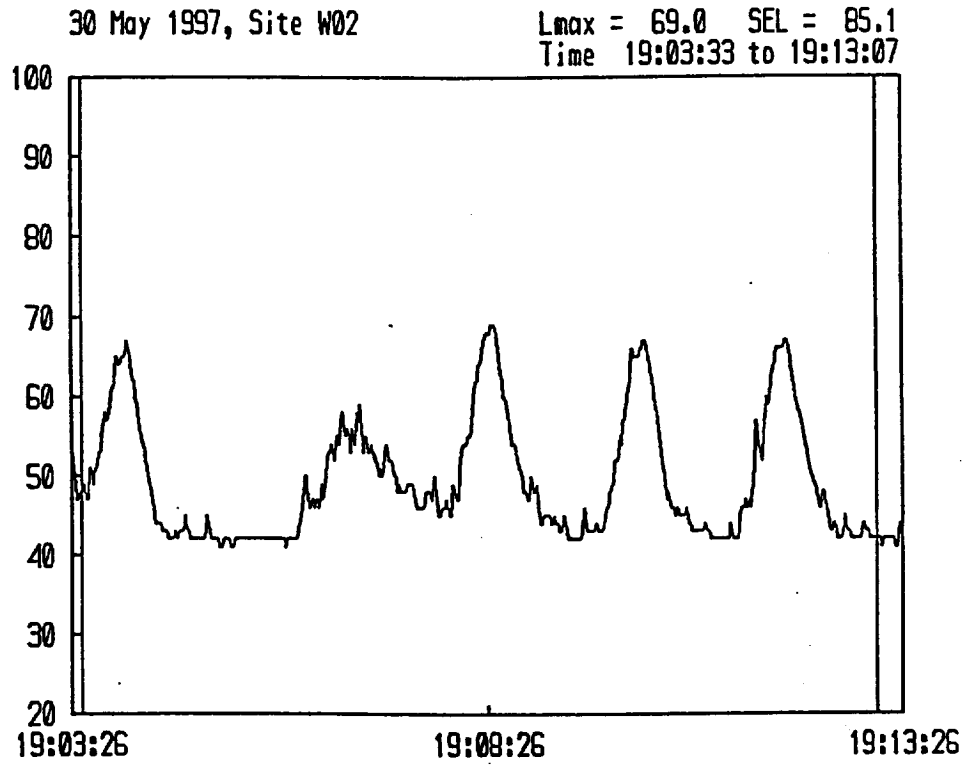

Figure 3-1. Time History for Monitoring Site W02

3.4 Airline Operational Information

Both United Airlines (UAL) and Delta Airlines (DL) cooperated by providing extensive data for all operations to and from Denver International Airport. Table 3-1 provides an overall view of the DIA operational traffic. UAL provided the following information for all 6,306 flights during the measurement period:

For Departures

- destination airport
- takeoff gross weight (TOGW)
- actual airframe/engine combination
- hush kit model, if applicable

For Arrivals

- actual airframe/engine combination
- hush kit model, if applicable

Table 3-5 gives a sample of the UAL data record for departures. Similarly, DL provided operational data for their 415 DIA operations. Table 3-6 contains a sampling of the DL operational data.

3.5 Aircraft and Engine Performance and Power Data

One of the key elements in this study is the prediction of thrust for all points along the flight trajectory. Integral to this thrust prediction process is the knowledge of detailed airframe and engine performance data, as well as pilot behavior and the effects of local atmospheric conditions on flight trajectories and throttle settings. In order to predict thrust, an understanding of pilot training techniques was required. To this end, UAL permitted full access to UAL flight training center personnel.

For the purpose of developing a performance prediction-based thrust methodology, UAL and DL provided the following information:

- Flight Manuals – takeoff sections for the numerous aircraft.[8–15]
- UAL Standard Performance Reference Handbook.[16]
- UAL fleet information – airframe/engine model noise number (Table 3-7).
- Performance Engineers Manual Fn/δ (net corrected installed thrust) numerical charts for the aircraft listed in Table 3-8.
- Maximum Allowable Takeoff Weight (MATW) data for all runways, and a range of atmospheric conditions at DIA for the airframe/engine combinations listed in Table 3-9.

United Airlines Operational Data								
UNITED AIRLINES TAKE=OFF WEIGHTS SORTED BY DATE AND TIME								
		T.O. DATE		FLIGHT		TAIL	T.O.	T.O. GROSS
ORIGIN	DEST	ACTUAL	SCHED.	NO.	FLEET	NO.	TIME	WEIGHT
DEN	SFO	970514	970514	1793	737		0	101,733
DEN	IAD	970514	970514	142	737	N316UA	6.2	110,050
DEN	SFO	970514	970514	1279	757	N541UA	6.23	172,252
DEN	DFW	970514	970514	216	737	N984UA	6.43	90,849
DEN	LAX	970514	970514	269	320	N412UA	6.45	130,869
DEN	MSP	970514	970514	1094	737	N910UA	6.46	95,013
DEN	PHX	970514	970514	2751	737	N943UA	6.58	0
DEN	ORD	970514	970514	610	727	N7462U	7.12	165,533
DEN	LAX	970514	970514	307	737	N986UA	7.15	96,713
DEN	LAX	970514	970514	1769	757	N555UA	7.55	182,787
DEN	LAS	970514	970514	2701	737	N377UA	8.18	115,956
DEN	MCI	970514	970514	484	737	N932UA	8.23	96,408
DEN	COS	970514	970514	1491	737	N395UA	8.23	87,482
DEN	SFO	970514	970514	1845	737	N951UA	8.23	114,368
DEN	DEN	970514	970514	1598	737	N983UA	8.24	99,278
DEN	MCO	970514	970514	1066	757	N586UA	8.25	190,724
DEN	IAH	970514	970514	1145	737	N991UA	8.25	99,372
DEN	EWR	970514	970514	1474	727	N7284U	8.26	158,280
DEN	SMF	970514	970514	759	727	N7276U	8.27	145,644
DEN	ABQ	970514	970514	467	737	N998UA	8.28	97,068
DEN	PHX	970514	970514	2753	737	N373UA	8.29	112,725
DEN	PHL	970514	970514	1660	737	N930UA	8.33	105,549
DEN	SAN	970514	970514	1091	727	N7265U	8.34	148,075
DEN	SNA	970514	970514	553	737	N352UA	8.35	105,189
DEN	DFW	970514	970514	1598	737	N983UA	8.35	0
DEN	LGA	970514	970514	1678	737	N340UA	8.35	114,635
DEN	MSP	970514	970514	204	737	N920UA	8.36	103,785
DEN	SLC	970514	970514	785	737	N322UA	8.37	109,827
DEN	ONT	970514	970514	1029	737	N923UA	8.39	100,151
DEN	LAX	970514	970514	817	727	N7445U	8.4	146,394
DEN	OAK	970514	970514	221	737	N312UA	8.41	106,831
DEN	SEA	970514	970514	293	D10	N1843U	8.43	347,972
DEN	LAX	970514	970514	193	D10	N1837U	8.44	343,531
DEN	SJC	970514	970514	279	737	N904UA	8.45	110,652
DEN	IAD	970514	970514	180	757	N562UA	8.46	187,779
DEN	SFO	970514	970514	835	D10	N1812U	8.48	363,628
DEN	BOS	970514	970514	1762	737	N363UA	9.03	116,779
DEN	ORD	970514	970514	240	777	N775UA	9.12	449,289
DEN	PDX	970514	970514	543	727	N7282U	9.14	161,529
DEN	BOI	970514	970514	729	737	N988UA	9.4	93,054
DEN	PHX	970514	970514	2755	737	N905UA	9.41	0
DEN	LAS	970514	970514	2703	737	N375UA	9.45	0
DEN	SLC	970514	970514	1111	737	N350UA	9.46	99,028
DEN	ORD	970514	970514	222	757	N594UA	9.47	194,939
DEN	SAN	970514	970514	1215	727	N7442U	9.5	152,740
DEN	SFO	970514	970514	207	737	N353UA	9.58	117,620
DEN	SEA	970514	970514	223	737	N355UA	10.02	122,349

Table 3-5

Delta Airlines Operational Data

DEN TAKEOFF ANALYSIS

Elev. 5,431 ft

DATE	FLIGHT	A/C TYPE	SHIP	DEP RWY	DEST	STAGE LENGTH (mi)	T/O WEIGHT (lb)	THRUST SETTING	T/O TEMP (F)	T/O TEMP (C)	V2 (kts)	EPR	EPR #2	THRUST (lbs)	#2 ENG THRUST (lbs)	# ENG	# ENG	TOTAL THRUST
19970609	DAL1488	B727	532HK	8	SLC	381	145240	ALTN/15	66	19	139	1.96	1.99	12750	12750	2	1	31322
19970604	DAL1488	B727	522	34	SLC	381	148792	ALTN/15	54	12	140	1.98	2.01	12975	12975	2	1	31874
19970522	DAL1488	B727	557	8	SLC	381	141465	ALTN/15	58	14	138	1.98	2.01	12975	12975	2	1	31874
19970519	DAL2120	B727	541HK	16	CVG	1081	170965	PKOF NORM/15	87	31	153	2.07	2.10	13950	13875	2	1	34208
19970610	DAL1488	B727	543	8	SLC	381	159245	NORM/15	82	28	145	2.09	2.12	14150	14100	2	1	34720
19970520	DAL1936	B727	405	8	SLC	381	163256	NORM/15	83	28	147	2.09	2.12	14150	14100	2	1	34720
19970601	DAL2120	B727	568	8	CVG	1081	169705	NORM/15	80	27	150	2.10	2.13	14250	14200	2	1	34966
19970519	DAL2120	B727	513	8	CVG	1081	165425	NORM/15	81	27	148	2.10	2.13	14250	14200	2	1	34966
19970604	DAL1936	B727	519	8	SLC	381	161229	NORM/15	81	27	146	2.10	2.13	14250	14200	2	1	34966
19970524	DAL1488	B727	546	8	SLC	381	151562	NORM/15	81	27	142	2.10	2.13	14250	14200	2	1	34966
19970608	DAL1488	B727	566	34	SLC	381	157601	NORM/15	81	27	144	2.10	2.13	14250	14200	2	1	34966
19970524	DAL317	B727	586	16	ATL	1208	174379	PKOF NORM/15	80	27	155	2.10	2.13	14250	14200	2	1	34966
19970522	DAL244	B727	469	8	ATL	1208	176485	PKOF NORM/15	75	24	156	2.11	2.14	14350	14275	2	1	35191
19970608	DAL244	B727	515	8	ATL	1208	166009	NORM/15	71	22	148	2.12	2.15	14450	14375	2	1	35437
19970519	DAL2120	B727	576	8	CVG	1081	162500	NORM/15	71	22	146	2.12	2.15	14450	14375	2	1	35437
19970610	DAL1488	B727	546	17L	SLC	381	150642	NORM/15	72	22	141	2.12	2.15	14450	14375	2	1	35437
19970522	DAL244	B727	568	8	ATL	1208	171193	NORM/15	74	23	150	2.12	2.15	14450	14375	2	1	35437
19970601	DAL1716	B727	528	8	JFK	1638	176720	PKOF NORM/15	74	23	156	2.12	2.15	14450	14375	2	1	35437
19970601	DAL804	B727	420	34	ATL	1208	155436	NORM/15	64	18	143	2.13	2.16	14550	14500	2	1	35703
19970610	DAL1936	B727	544	8	SLC	381	160675	NORM/15	64	18	145	2.13	2.16	14550	14500	2	1	35703
19970604	DAL2120	B727	557	8	CVG	1081	172795	NORM/15	64	18	151	2.13	2.16	14550	14500	2	1	35703
19970605	DAL1227	B727	407	34	SLC	381	161805	NORM/15	65	18	146	2.13	2.16	14550	14500	2	1	35703
19970601	DAL1936	B727	478	8	SLC	381	163950	NORM/15	65	18	147	2.13	2.16	14550	14500	2	1	35703
19970522	DAL1227	B727	566	8	SLC	381	160372	NORM/15	65	18	145	2.13	2.16	14550	14500	2	1	35703
19970608	DAL1488	B727	584	34	SLC	381	164452	NORM/15	65	18	147	2.13	2.16	14550	14500	2	1	35703
19970605	DAL1488	B727	586	8	SLC	381	155091	NORM/15	65	18	143	2.13	2.16	14550	14500	2	1	35703
19970604	DAL804	B727	537HK	8	ATL	1208	160711	NORM/15	65	18	145	2.13	2.16	14550	14500	2	1	35703
19970518	DAL1227	B727	523	17R	SLC	381	158599	NORM/15	66	19	144	2.13	2.16	14550	14500	2	1	35703
19970524	DAL1716	B727	524	8	JFK	1638	175303	NORM/15	67	19	152	2.13	2.16	14550	14500	2	1	35703
19970609	DAL1716	B727	563	8	JFK	1638	175487	NORM/15	67	19	152	2.13	2.16	14550	14500	2	1	35703
19970604	DAL1488	B727	483	8	SLC	381	153863	NORM/15	69	21	143	2.13	2.16	14550	14500	2	1	35703
19970520	DAL804	B727	518	17L	ATL	1208	170082	NORM/15	70	21	150	2.13	2.16	14550	14500	2	1	35703
19970520	DAL317	B727	560	8	ATL	1208	175633	PKOF NORM/15	70	21	152	2.13	2.16	14550	14500	2	1	35703
19970601	DAL1227	B727	445	8	SLC	381	160165	NORM/15	54	12	145	2.14	2.17	14650	14650	2	1	35989
19970605	DAL804	B727	565	34	ATL	1208	169592	NORM/15	54	12	150	2.14	2.17	14650	14650	2	1	35989
19970610	DAL244	B727	524	8	ATL	1208	163619	NORM/15	55	13	147	2.14	2.17	14650	14650	2	1	35989
19970524	DAL1227	B727	538HK	34	SLC	381	156727	NORM/15	55	13	144	2.14	2.17	14650	14650	2	1	35989

Table 3-6

United Airlines Fleet Data

UNITED AIRLINES

AIRPLANE IDENTIFICATION RECORD- "A.I.R." LIMITED DISTRIBUTION ISSUE

737-322 (CFM56-3-B1 or -3C-1)

N #	UA#	Ser.#
N395UA	9395	24670
N396UA	9396	24671
N397UA	9397	24672
N398UA	9398	24673
N399UA	9399	24674
N202UA	9002	24717
N203UA	9003	24718

737-322 (CFM56-3-B1 or -3C-1)

N #	UA#	Ser.#
N358UA	1358	24379
N366UA	1366	24535
N375UA	1375	24640
N376UA	1376	24641
N377UA	1377	24642
N381UA	1381	24656
N394UA	1394	24669

737-322 Fleet = 101
FAR 36 Stg 3

Note: the 13xx UA#'s represent the 737-322 Shuttle sub-fleet.

The 94xx and 99xx UA#'s indicate 22,000 lb. engine thrust rating; the 13xx, 93xx and 90xx UA#'s indicate 20,000 lb engine thrust rating.

737-522 (CFM56-3-B1 or -3C-1)

N #	UA#	Ser.#
N901UA	1701	25001
N902UA	1702	25002
N903UA	1703	25003
N904UA	1704	25004
N905UA	1705	25005
N906UA	1706	25006
N907UA	1707	25007
N908UA	1708	25008
N909UA	1709	25009
N910UA	1710	25254
N911UA	1711	25255
N912UA	1712	25290
N913UA	1713	25291
N914UA	1714	25381
N915UA	1715	25382
N916UA	1716	25383
N917UA	1717	25384
N918UA	1718	25385
N919UA	1719	25386
N920UA	1720	25387
N921UA	1721	25388
N922UA	1722	26642
N923UA	1723	26643
N924UA	1724	26645
N925UA	1725	26646
N926UA	1726	26648
N927UA	1727	26649
N928UA	1728	26651
N929UA	1729	26652
N930UA	1730	26655
N931UA	1731	26656
N932UA	1732	26658
N933UA	1733	26659
N934UA	1734	26662
N935UA	1735	26663
N936UA	1736	26667
N937UA	1737	26668
N938UA	1738	26671
N939UA	1739	26672
N940UA	1740	26675
N941UA	1741	26676
N942UA	1742	26679
N943UA	1743	26680
N944UA	1744	26683
N945UA	1745	26684
N946UA	1746	26687
N947UA	1747	26688

This A.I.R. is a part of the FAA-Approved UA Operations Specifications, Paragraph D-85.

CONTINUED
MAY 20/97
GN/MM 8-0-4-0
PAGE 4

GENERAL PROCESS MANUAL
TABLES AND CHARTS

Table 3-7

Available FN/δ Data Airframe/Engine Combinations
B727 Advanced JT8D-15 (pod and center engine)
B737-300 CFM-56-3-B1 (20,000 lbs. rated thrust)
B737-300 CFM-56-3-B2 (22,000 lbs. rated thrust)
B737-500 CFM-56-3-B1 (20,000 lbs. rated thrust)
B757-200 PW-2037
MD-80 JT8D-219

Table 3-8

Available Maximum Allowable Takeoff Weight Charts

Airframe	Engine
A319-100	V2522
A320-200	V2527
B727-Advanced	JT8D-15
B737-200	ADV-9A JT8D-9A
B737-200	ADV-17 JT8D-17
B737-222	STR-7 JT8D-7 & 7B
B737-300	(CFM 56-3 B1/C1-20K)
B737-300N	(CFM 56-3 B2-22K)
B737-500	(CFM 56-3 B1/C1-20K)
B757-200	PW2037
B767-200	JT9D-7R4D
B767-300ER	PW 4060
B777-200	PW4077
B777-200B	PW 4090
DC10-10	CF6-6D
DC10-30	CF6-50C2
DC10-30F	CF6-50C2

Table 3-9

For comparison with the Wyle thrust prediction model, the Climb and Throttle Scheduler (CATS code), UAL provided takeoff derated thrust predictions based on their in-house detailed performance code, accessible via their Unimatic system. Table 3-10 contains a sample printout from the Unimatic system for a B757-200 flight. Detailed derated thrust takeoff predictions such as that shown in Table 3-10 were provided for a total of 38 departures, representing six different airframe/engine combinations. DL provided additional takeoff derated thrust level data for a total of 197 departures representing six unique airframe/engine combinations.

On occasion, a pilot exercises his/her discretionary right and elects not to perform a noise abatement derated takeoff. Both UAL and DL record takeoff engine data via the ACARS engine monitoring system, available on newer commercial jet aircraft. For aircraft without the ACARS system, airlines conduct studies for accurately estimating the percentage of derated departure flights. Such historical data is recorded both by airframe nose number and by city-pairs. Table 3-11 contains a sample output from the UAL May historical derate records. In addition to the weight and destination information, DL also provided takeoff throttle settings (N1 or EPR as appropriate for the particular aircraft type) for the initial takeoff segment. DL calculated these takeoff levels using in-house performance codes in conjunction with available historical engine monitoring system data.

Unimatic Thrust Prediction Printout for a B757-200

```
GWTG  DEN  50  R8      G197945
RNWY  DATA-8
*F5  BLEED-NORMAL*
TOG  197.9P  ZFW  .OP
REDUCED  THRUST  OPTIONS
TW   EPR   N1  ATGW   ATEMP
0    1.40  86  200.1  102/38
5    1.40  86  200.1  102/38
10   1.40  86  199.3  100/37
MAX  EPR:  1.52  N1:  92
R250.0    P242.5   S230.0
T53(11)   ALTM 3006I
WIND 0000M
```

Table 3-10

United Airlines Historical Derate Data

City Pair	Flights ECM	Probable Flights	Reduced Flights	% Derate	ECM Reduced Thrust	% Reduction Derate Flights	Overall Reduction All Flights
DEN BIL	7	7	6	85.71	6	8.28	7.09
DEN BNA	1	2	2	100.00	1	4.30	4.30
DEN BOI	7	7	6	85.71	6	8.58	7.35
DEN BOS	73	127	98	77.17	16	3.70	0.81
DEN BUR	4	6	3	50.00	3	8.42	6.31
DEN BWI	28	41	27	65.85	5	3.41	0.61
DEN CLE	5	10	10	100.00	1	2.75	0.55
DEN CMH	23	36	34	94.44	2	1.15	0.10
DEN COS	70	0	0	100.00	70	11.51	11.51
DEN DEN	2	0	0	0.00	0	0.00	0.00
DEN DFW	61	49	6	83.61	51	9.24	7.72
DEN DSM	59	68	49	72.06	44	8.45	6.30
DEN DTW	10	12	11	91.67	6	4.16	2.50
DEN EUG	19	26	16	61.54	7	3.81	1.41
DEN EWR	46	69	50	72.46	23	4.43	2.22
DEN FSD	8	9	5	55.56	8	8.72	8.72
DEN GEG	4	7	7	100.00	0	0.00	0.00
DEN IAD	59	90	75	83.33	34	6.35	3.66
DEN IAH	31	44	35	79.55	29	7.50	7.02
DEN ICT	5	2	2	80.00	4	6.45	5.16
DEN IND	80	105	65	61.90	41	4.87	2.49
DEN LAS	268	229	201	83.96	225	5.32	4.46
DEN LAX	118	161	135	83.85	75	5.12	3.26
DEN LGA	122	120	83	38.52	47	5.77	2.22
DEN LNK	2	0	0	100.00	2	5.68	5.68
DEN MCI	60	73	54	73.97	48	7.97	6.37
DEN MIA	26	74	69	93.24	0	0.00	0.00
DEN MSP	4	7	6	85.71	4	9.96	9.96
DEN MSY	58	70	35	50.00	27	5.23	2.43
DEN OAK	45	75	63	84.00	30	5.50	3.67
DEN OKC	30	19	16	83.33	25	9.32	7.76
DEN OMA	16	7	3	87.50	14	9.75	8.53
DEN ONT	32	55	46	83.64	21	3.78	2.48

Table 3-11

3.6 Lateral Array

Between 12 June and 13 June, a lateral array was set up approximately 25 miles east of the Runway 08/26 eastbound departure threshold. For a period of 24 hours, noise monitors, spaced approximately two miles apart, recorded one-second, slow- response, A-weighted sound level data for 24 hours. Measurements were augmented at sites #3, #5, and #11 with digital tape recordings. Approximately 213 departure flights from Runway 08 occurred during this 24-hour interval.

A sample of noise monitor data for one particular departure is shown for each of the lateral array monitors in Figure 3-2. It is interesting to note that visual inspection of the time history at monitor W19 would not normally indicate the presence of an aircraft; however, when viewed in sequence with sites W14–W18 an ever-so-slight rise above background noise levels is indicative of the present and audible aircraft noise.

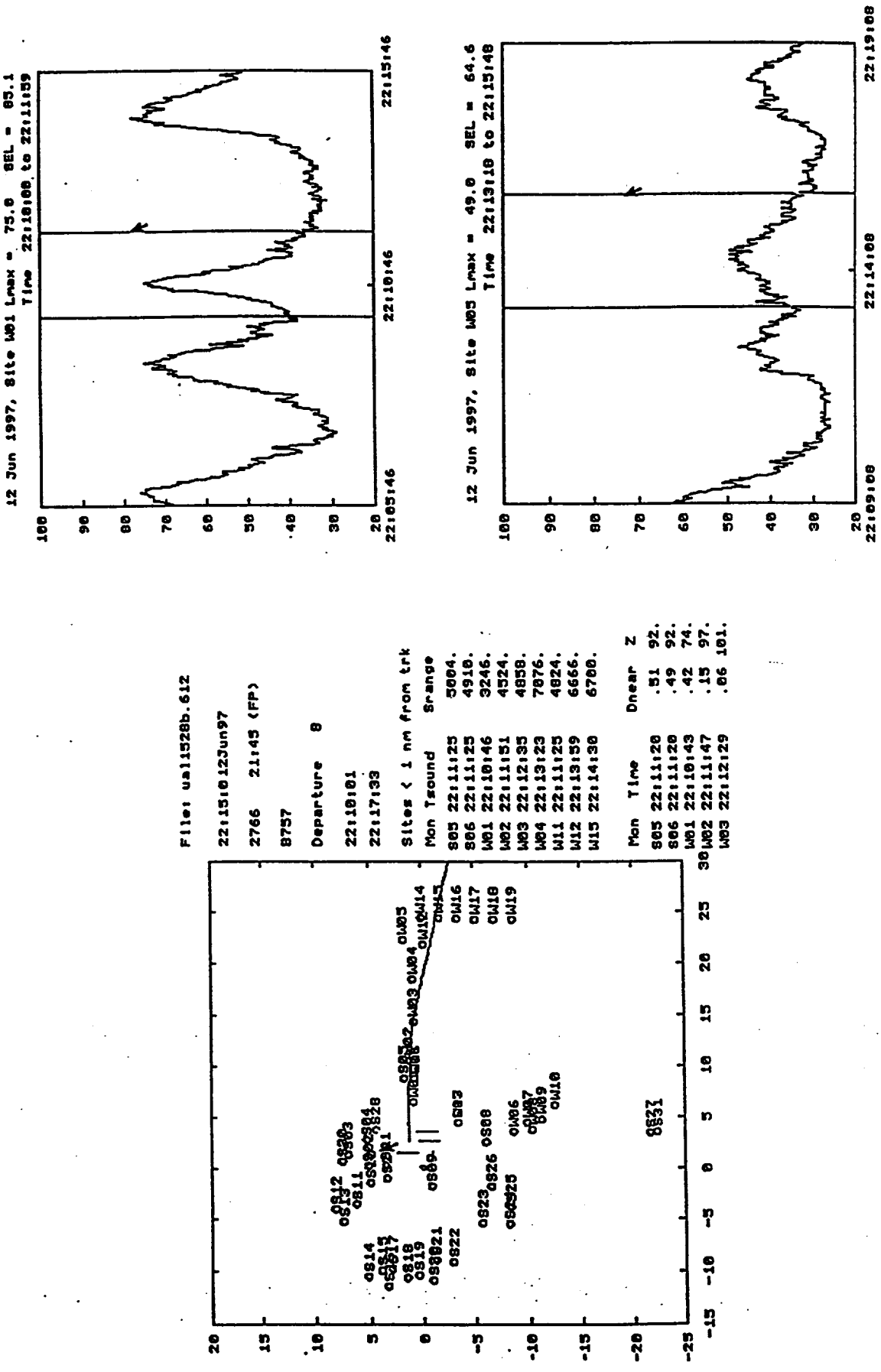

Figure 3-2. Lateral Array Noise Measurements

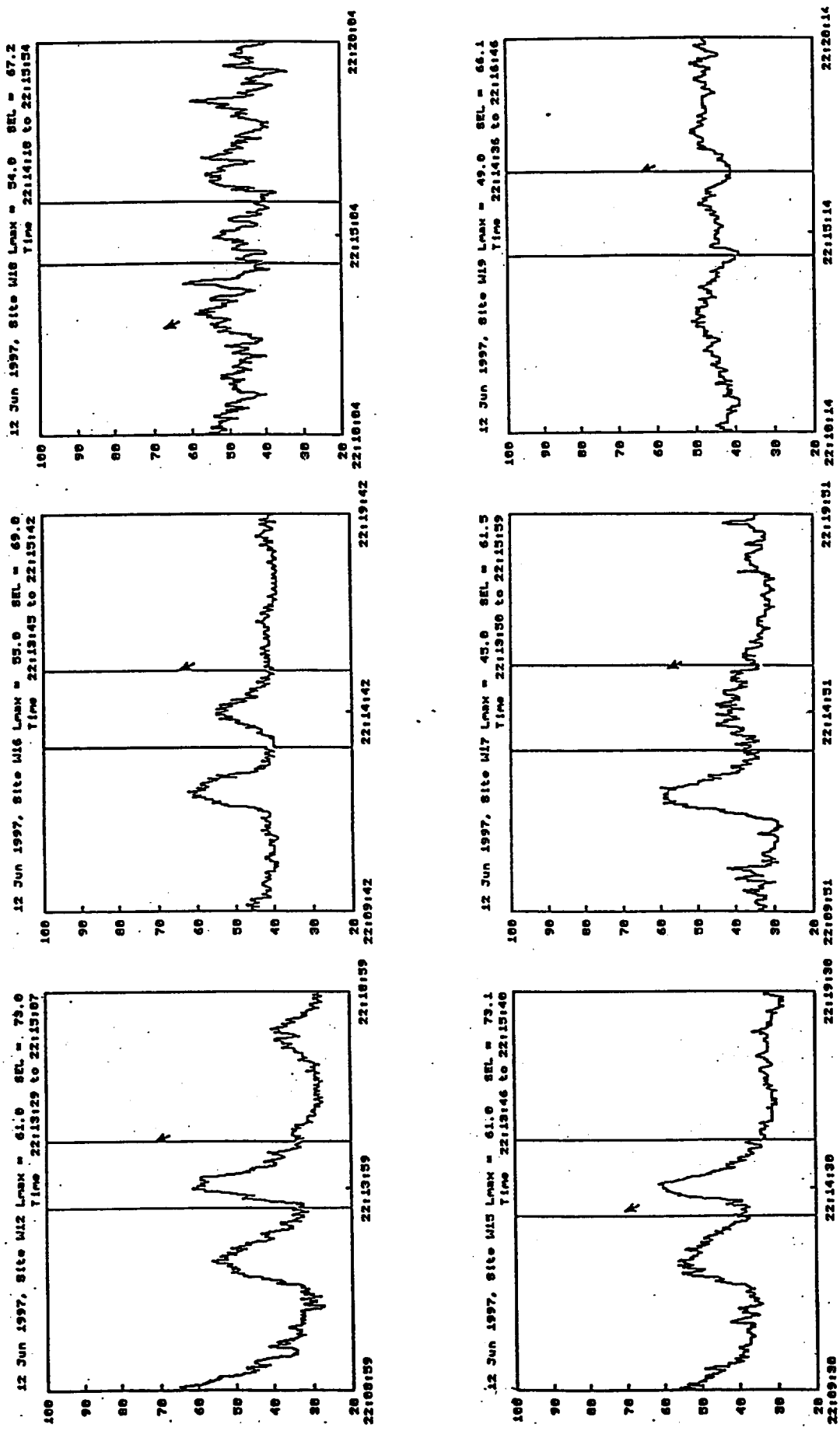

Figure 3-2. (Continued)

4 Data Analysis

As with any large noise measurement study, significant effort is expended in reducing the available data into a useful format for inspection and analysis. Given the huge volume of data acquired during this study, a program scope decision was made that only May flight tracks and noise events would be correlated and considered in any subsequent analysis. Analysis of the data consisted of six major steps:

1. Radar Data Processing
2. Extraction of Noise Events
3. Prediction of Thrust
4. INM Analysis
5. Flight Track and Noise Event Correlation
6. Sensitivity Analyses

The following sections document each of these steps.

4.1 Radar Data Processing

During the course of the project, DIA provided radar-tracking data from the FAA's ARTS[17] system at the airport. Data were supplied in the form of files from the Dimensions International system[18], which is a PC-based system that collects a subset of ARTS data, and forwards this to the noise monitoring system. The data in this file contains the following information:

- Flight Plan records, which contain the aircraft flight number, type of aircraft (nominal four-character code), assigned beacon code, scheduled arrival or departure time, and initial/final routing information.
- Departure Messages, which mark the time when departing flights reach an altitude of 300 feet above field level and are under air traffic control.
- Terminate Beacon records, which indicate that the aircraft is no longer being tracked. This corresponds to the hand-off to en-route control for departing flights, and landing for arrivals.
- Target Report records, which contain the raw information returned from the radar and transponder. This consists of the range and bearing to the aircraft, and the beacon code and altitude MSL reported by the transponder.
- Tracking Report records, in which the target report data has been converted to local X, Y Cartesian coordinates.

Records in the Dimensions file appear in the real-time order that they occur. Each record is marked with a time corresponding to when the record was written onto the PC. This time is generally within a few seconds of real time.

Processing consisted of the following steps:

- Arriving and departing flights at DIA were identified from Flight Plan records.
- For each flight, all Tracking Report records were collected, beginning with the Flight Plan and ending with either the Terminate Beacon or loss of Tracking Reports.
- Aircraft speed was computed using a local polynomial spline fit to the raw data.
- Runway assignment was obtained by matching the early (departure) or final (arrival) tracking points and heading with proximity to the runway ends and the runway headings.

Tracking data for each flight, which included position and speed, were written to individual ASCII files for use in the noise analysis. Figure 4-1 contains a sampling of one day of departure data radar flight tracks and flight profiles.

4.2 Noise Event Extraction

Several schools of thought exist on how to identify aircraft noise events within a time-history record. The traditional method employed by most noise monitoring systems uses a pattern recognition approach. Events meeting the aircraft pattern criteria are tagged as aircraft noise events and included in subsequent L_{dn} analyses. Wyle Laboratories has developed and implemented an alternate approach, which performs a "track first" direct correlation between flight tracks and noise events. This methodology begins with a radar flight track and, based on synchronized monitor and radar times and the geometric point of closest approach, predicts sound event arrival time at the noise monitor. This 'track first' approach serves two purposes:

1. It accurately identifies noise events as aircraft noise events.
2. It associates such events with actual flight tracks.

During the processing of data, flight track and noise correlations were performed for both departures and arrivals. A graphical program was developed, which allowed rapid semi-automated track correlation while keeping the human in the loop for verification and record creation. Figure 4-2 shows a sample flight track and correlated noise event for monitor #S05.

During the data analysis phase, the noise-flight track correlations shown in Table 4-1 were created. These data records were recorded for both arrivals and departures and represent all airline operations. Flight tracks were pre-screened using weather criteria developed in the Dulles study, namely winds under 10 knots and no appreciable amounts of precipitation. The final subset of data analyzed in INM considered only departures, and UAL and DL operations, and represented only the airframe and engine combinations for which accurate thrust predictions could be made.

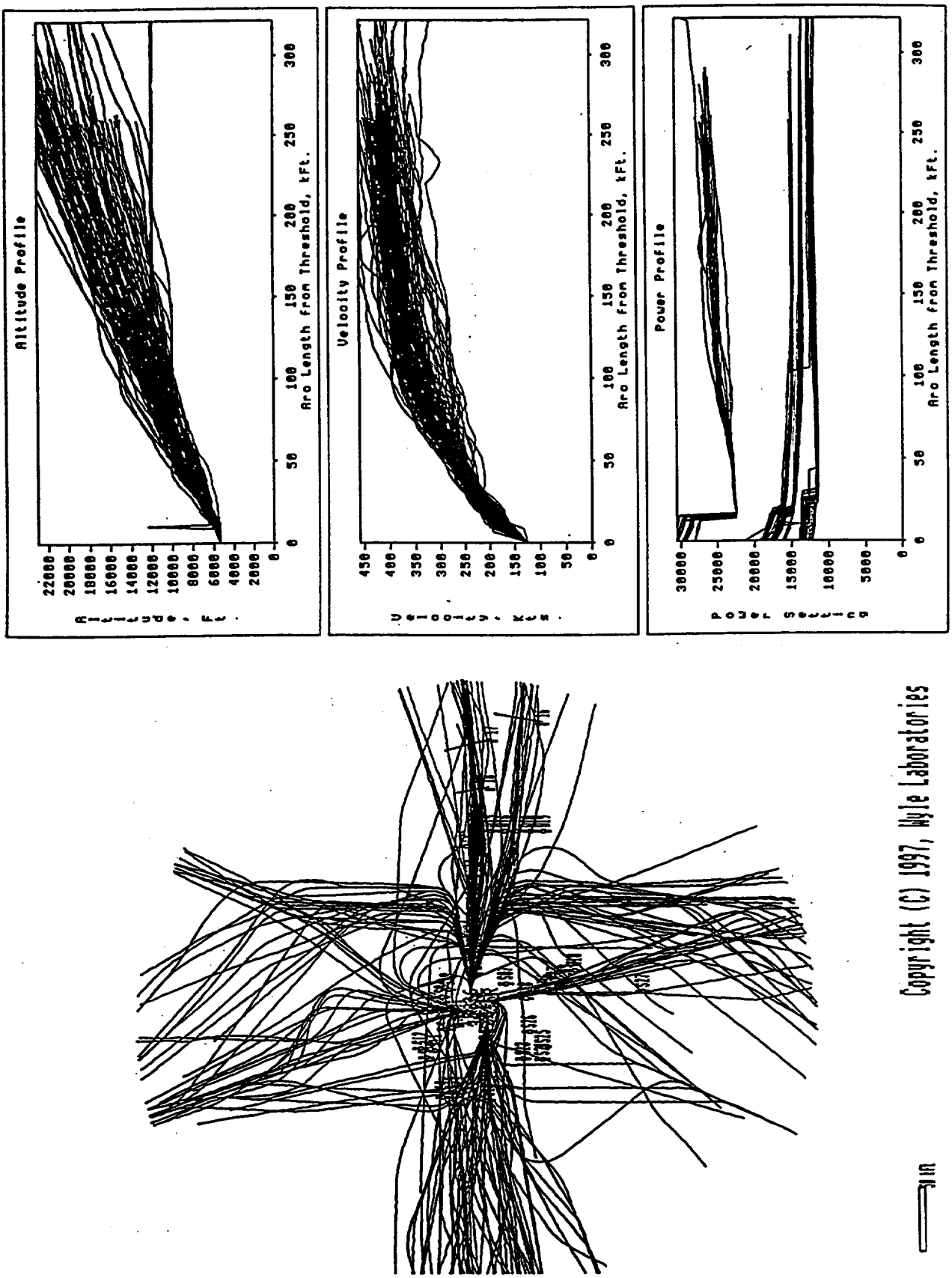

Figure 4-1. One Day of Departure Flight Tracks and Profiles (Power Mode 6)

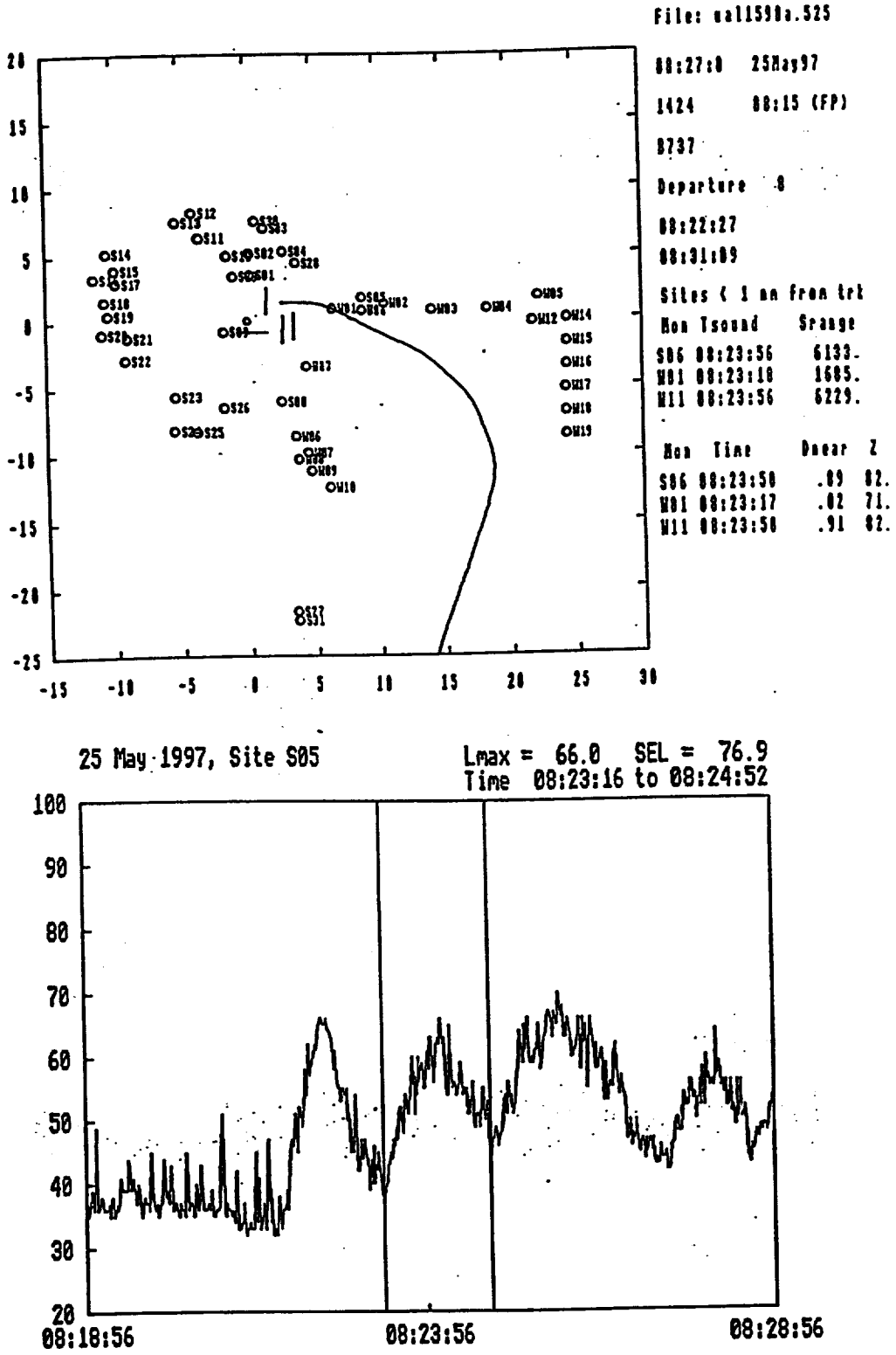

Figure 4-2. Sample Flight Track and Correlated Noise Event for S05

Extracted Noise Correlations		
Date	**No. of Flight Tracks**	**No. of Noise Events**
5/21/97	235	1,597
5/22/97	585	2,824
5/23/97	575	3,381
5/24/97	321	1,641
5/25/97	285	1,246
5/26/97	248	921
5/27/97	343	1,858
5/28/97	415	1,984
5/29/97	134	573
5/30/97	544	1,170
TOTALS	3,685	17,135

Table 4-1

Table 4-2 illustrates a sample noise correlation record. The point of closest approach is determined by calculating the shortest distance to individual flight segments. This will be either the length of a perpendicular between the monitor and the flight segment calculated via a dot product, or the shortest distance to either segment endpoint as required by the track curvature and monitor geometry. Vital data written in the noise correlation record includes the following:

Global Data

- flight number
- date
- operation type
- runway assignment
- aircraft type (based on ARTS information)

At the Point of Closest Approach to a Given Monitor

- time
- altitude
- track distance from threshold
- speed
- slant range
- elevation angle
- sound arrival time

Based on the Noise Time-History Data

- L_{max}
- SEL
- limits of integration for SEL calculation

Sample Noise Correlation Record

Flight/file	Date	AC Time	Op	Rwy	AC	Alt	TrkDist	Speed	Mon	Slant	Tarr	Lmax	SEL	From	To	Angle	
UAL1086A.525	25 May 1997	08:56:54.88	Arr	35L	B73S	6900.	-27312.	180.4	S08	1491.	08:56:56	75.0	83.9	08:56:07	08:57:30	60.39	199801261025
UAL1086A.525	25 May 1997	08:56:18.06	Arr	35L	B73S	7400.	-38704.	189.3	W06	9690.	08:56:27	56.0	68.5	08:55:57	08:57:24	10.04	199801261025
UAL1086A.525	25 May 1997	08:56:08.89	Arr	35L	B73S	7500.	-41645.	193.1	W07	18442.	08:56:26	47.0	57.4	08:55:56	08:56:56	5.38	199801261025
UAL1086A.525	25 May 1997	08:56:04.20	Arr	35L	B73S	7600.	-43012.	193.9	W08	17076.	08:56:20	56.0	66.2	08:55:28	08:56:50	6.02	199801261025
UAL1086A.525	25 May 1997	08:54:36.99	Arr	35L	B73S	9300.	-74540.	224.8	S25	7694.	08:54:44	60.0	74.2	08:54:14	08:55:14	30.02	199801261026
UAL1086A.525	25 May 1997	08:52:46.93	Arr	35L	B73S	11000.	-116720.	235.3	S09	11531.	08:52:57	74.0	83.2	08:51:48	08:53:27	29.67	199801261026
UAL1035A.525	25 May 1997	11:09:59.32	Arr	35L	B73S	6968.	-27580.	174.8	S08	1913.	11:10:01	72.0	81.3	11:09:21	11:10:31	45.45	199801261026
UAL1035A.525	25 May 1997	11:09:59.32	Arr	35L	B73S	6968.	-27580.	174.8	S08	1913.	11:10:01	72.0	81.3	11:09:21	11:10:31	45.45	199801261026
UAL1035A.525	25 May 1997	11:03:11.29	Arr	35L	B73S	12991.	-180519.	323.4	W04	9972.	11:03:20	62.0	74.7	11:02:50	11:04:17	51.94	199801261027
UAL1043A.525	25 May 1997	10:37:39.41	Arr	35R	B727	6200.	-12596.	161.9	S07	5617.	10:37:45	64.0	75.8	10:37:15	10:38:15	7.95	199801261027
UAL1043A.525	25 May 1997	10:36:39.75	Arr	35R	B727	7400.	-30909.	189.1	S08	5953.	10:36:45	70.0	79.3	10:35:45	10:36:30	17.56	199801261027
UAL1043A.525	25 May 1997	10:35:57.27	Arr	35R	B727	7820.	-44560.	191.0	W06	2257.	10:35:59	73.0	82.7	10:35:29	10:36:44	69.15	199801261027
UAL1043A.525	25 May 1997	10:29:07.03	Arr	35R	B727	13000.	-201345.	317.7	W04	8700.	10:29:15	63.0	74.6	10:28:25	10:29:45	64.61	199801261027
UAL1066A.525	25 May 1997	08:15:30.52	Dep	08	B757	7437.	24015.	220.7	W01	2456.	08:15:33	74.0	85.1	08:15:03	08:16:35	56.89	199801261027
UAL1066A.525	25 May 1997	08:16:03.99	Dep	08	B757	8683.	37486.	253.7	S06	6626.	08:16:10	67.0	76.2	08:15:40	08:16:58	30.71	199801261027
UAL1066A.525	25 May 1997	08:16:03.94	Dep	08	B757	8681.	37468.	253.7	W11	6721.	08:16:10	65.0	76.7	08:15:40	08:17:18	30.14	199801261027
UAL1066A.525	25 May 1997	08:15:59.36	Dep	08	B757	8485.	35576.	250.0	S05	11666.	08:16:10	58.0	69.4	08:15:09	08:17:25	16.02	199801261027
UAL1066A.525	25 May 1997	08:17:13.36	Dep	08	B757	11288.	71524.	333.8	W03	16106.	08:17:28	53.0	66.2	08:16:39	08:18:07	22.08	199801261028
UAL1066A.525	25 May 1997	08:17:50.54	Dep	08	B757	12200.	93813.	379.2	W04	22755.	08:18:11	46.0	59.7	08:17:41	08:18:36	18.07	199801261028
UAL1066A.525	25 May 1997	08:18:18.19	Dep	08	B757	13600.	112114.	392.4	W12	22834.	08:18:39	48.0	62.1	08:18:09	08:19:21	21.83	199801261028
UAL1066A.525	25 May 1997	08:18:18.19	Dep	08	B757	13600.	112114.	392.4	W05	33969.	08:18:49	71.0	81.7	08:18:19	08:19:19	14.50	199801261028
UAL1078A.525	25 May 1997	10:29:01.94	Dep	08	B727	6600.	23897.	191.5	W01	2718.	10:29:04	88.0	96.6	10:28:34	10:30:06	26.67	199801261028
UAL1078A.525	25 May 1997	10:29:39.74	Dep	08	B727	7217.	37778.	237.6	S06	3517.	10:29:43	86.0	96.1	10:29:13	10:30:51	33.06	199801261028
UAL1078A.525	25 May 1997	10:29:39.74	Dep	08	B727	7217.	37776.	237.6	W11	3400.	10:29:43	86.0	96.4	10:28:35	10:31:02	34.21	199801261028
UAL1078A.525	25 May 1997	10:29:39.76	Dep	08	B727	7218.	37785.	237.6	S05	3628.	10:29:43	83.0	92.8	10:29:13	10:30:47	32.54	199801261028
UAL1078A.525	25 May 1997	10:30:53.02	Dep	08	B727	9511.	70984.	296.7	W03	4321.	10:30:57	81.0	94.0	10:30:27	10:32:04	81.91	199801261028
UAL1078A.525	25 May 1997	10:31:39.70	Dep	08	B727	10718.	96029.	340.2	W04	5671.	10:31:45	79.0	91.5	10:31:15	10:32:58	79.60	199801261028
UAL1078A.525	25 May 1997	10:32:15.66	Dep	08	B727	11790.	117387.	365.4	W12	8117.	10:32:23	80.0	90.7	10:31:53	10:33:50	55.39	199801261028
UAL1078A.525	25 May 1997	10:32:19.82	Dep	08	B727	11972.	120147.	368.6	W05	9903.	10:32:29	74.0	86.5	10:31:59	10:33:45	43.98	199801261028
UAL1080A.525	25 May 1997	11:10:47.19	Dep	08	B73S	8478.	38409.	251.8	S06	5197.	11:10:52	69.0	78.9	11:10:22	11:11:29	37.71	199801261028
UAL1080A.525	25 May 1997	11:10:47.16	Dep	08	B73S	8477.	38396.	251.8	W11	5293.	11:10:52	68.0	79.3	11:10:22	11:11:29	36.80	199801261029
UAL1080A.525	25 May 1997	11:10:38.52	Dep	08	B73S	8104.	34824.	247.8	S05	10276.	11:10:48	63.0	73.8	11:10:18	11:11:38	16.03	199801261029
UAL1080A.525	25 May 1997	11:11:56.93	Dep	08	B73S	10498.	71123.	317.5	W03	14753.	11:12:10	56.0	68.6	11:11:40	11:12:40	20.91	199801261029
UAL1080A.525	25 May 1997	11:12:43.13	Dep	08	B73S	12200.	97459.	348.4	W04	19860.	11:13:01	60.0	71.3	11:12:31	11:13:47	20.82	199801261029
UAL1080A.525	25 May 1997	11:13:15.32	Dep	08	B73S	13892.	116798.	358.6	W12	18559.	11:13:32	51.0	65.7	11:13:02	11:14:28	28.24	199801261029
UAL1082A.525	25 May 1997	19:07:58.15	Dep	17L	B727	6800.	25643.	222.6	S07	3433.	19:08:01	85.0	96.0	19:07:31	19:08:55	23.65	199801261029
UAL1082A.525	25 May 1997	19:08:30.60	Dep	17L	B727	7598.	39097.	270.1	S08	11489.	19:08:41	77.0	84.3	19:08:11	19:09:46	10.00	199801261029
UAL1084A.525	25 May 1997	11:43:01.34	Arr	35L	B757	7112.	-27592.	175.3	S08	1656.	11:43:03	76.0	86.0	11:42:33	11:43:48	65.55	199801261029

Table 4-2

4.3 Thrust Prediction

A critical factor in this study, required for the elimination of all unknowns other than atmospheric propagation and noise source level effects, is the accurate prediction of aircraft thrust at all points on the radar trajectory. A new operational procedure-based methodology was developed for prediction of the throttle state. Detailed performance Fn/δ charts are then used to convert engine state to net corrected installed thrust in pounds, as required by the INM. Section 4.3.1 gives a presentation of the methodology and applicability of this method. Section 4.3.2 describes five alternate thrust prediction techniques, which were examined in considerable detail. Section 4.3.3 gives a comparison of these thrust prediction methods.

4.3.1 Departure Thrust Prediction Based on Operational Procedures

A performance prediction method was used for evaluating the departure throttle settings. This methodology is based heavily on pilot training procedures developed by UAL. In order to predict throttle settings, additional data is required for each flight, including exact airframe/engine equipment usage, takeoff gross weight, and atmospheric data. Sample data from various sources is itemized in Chapter 3. For this project, only commercial flight departure operations from UAL and DL were considered. Table 4-3 contains a flowchart of the performance prediction process.

Takeoff Thrust Prediction Methodology Flowchart

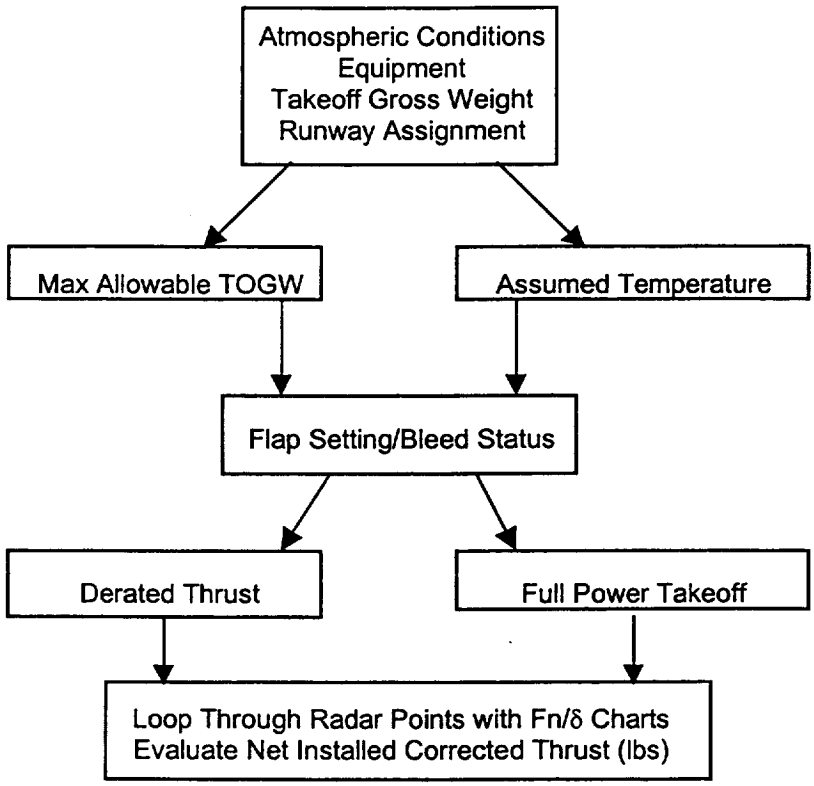

Table 4-3

The prediction of thrust for a given commercial aircraft departure requires knowledge of local airfield atmospheric conditions. The pilot decisions regarding details of the departure procedures is based on local weather reporting station information, updated at least hourly or as required by changing local conditions. (See Section 3.1 for weather data details.) Key information from an aircraft performance perspective is Outside Air Temperature (OAT) and atmospheric pressure. Engine performance is affected significantly by changes in both airfield temperature and pressure. These effects are even more critical for operations from a high-altitude airport such as DIA. Data from the weather services were interpolated linearly to the departure time for the thrust prediction process.

Actual equipment usage, such as the exact airframe and engine models used for the flight, are also required. This data, obtained directly from the airlines, allowed a more exact knowledge of performance capabilities of the particular aircraft. The radar interfacility message stream contains only four character descriptors for the aircraft type. As such, the particular model and engine type are not identified. In addition, airlines occasionally make equipment substitutions after the initial automatic flight plan has been logged into the ARTS system. The airline information obtained for this study contains factual historical information from the maintenance records.

Another key parameter required for takeoff thrust prediction is the takeoff gross weight (TOGW) of the aircraft. As with the equipment usage, FAA mandates require all airlines to log such information. This database was also received for the measurement period for UAL and DL departures (see Section 3.4).

Runway assignment was based on the actual radar track, as variable wind and traffic conditions often dictate last-minute departure changes. Assignments considered the direction and location of the departing flight and the available runways. This information, evaluated in the radar-processing phase (Section 4.1), was stored in the output powered flight track and profile RAT file.

Assessment of the Maximum Allowable TOGW (MATOGW) was based on the tables provided by the airlines for each airframe/engine combination on all available runways. Detailed performance analyses completed in-house at the airlines considered such variables as headwinds, runway gradients, airframe aerodynamic performance including a range of flap settings, and detailed engine efficiencies over a range of TOGW and atmospheric conditions. The resulting matrix of cases was built into tables such as the one shown in Table 4-4, the MATOGW for the B737-500 CFM-56-3-B1 for 5-degree flaps and bleeds ON. This chart contains temperatures along the leftmost column, with various runways across the top. The last column reflects the performance-limited case. Performance Limit Weight is defined as the maximum weight at which the airplane can achieve the minimum FAR-specified climb gradient, usually limited at the beginning of second-segment climb. The climb gradient required depends on the number of engines installed. Contained within each chart element is the MATOGW in thousands of pounds for the particular airframe/engine combination on the given runway at the selected temperature for the specified flap and bleed setting. These data tables were created in the flap sequence as specified in the airframe manufacturer performance manuals and the UAL pilot training procedure documentation, and contained within the UAL aircraft flight manual. The sequence

Maximum Allowable Takeoff Weight Chart
For the B737-500, Flaps 5, Bleeds ON

PART 07 OF 16 PARTS

B-737-500 CFM56-3-B1
DENVER, CO DENVER INTERNATIONAL
DEN/KDEN - ELEV 5431
TAKEOFF - BLEEDS ON
FLAP 5

RWY	7	8	8E	16	17L	17LF	17R	17RG	PERF
LENGTH	12000	12000	11700	12000	12000	11690	12000	11670	LIMIT
NOTES	.	.	E	T1	T1	FT1	T1	GT1	.
DEG F									
-20	119.7	124.6	124.6	124.6	124.6	124.6	124.6	124.6	118.0
-10	119.4	124.5	124.5	124.5	124.5	124.5	124.5	124.5	117.9
0	119.2	124.4	124.4	124.4	124.4	124.4	124.4	124.4	117.8
10	118.9	124.2	124.2	124.2	124.2	124.2	124.2	124.2	117.7
20	118.7	124.1	124.1	124.1	124.1	124.1	124.1	124.1	117.6
30	118.5	124.0	124.0	124.0	124.0	124.0	124.0	124.0	117.5
40	118.2	123.8	123.8	123.8	123.8	123.8	123.8	123.8	117.4
50	117.9	123.5	123.5	123.5	123.5	123.5	123.5	123.5	117.2
60	117.5	123.1	123.1	123.1	123.1	123.1	123.1	123.1	117.0
70	117.2	122.6	122.6	122.6	122.6	122.6	122.6	122.6	116.8
79	116.9	121.9	121.9	121.9	121.9	121.9	121.9	121.9	116.6
80	116.7	121.7	121.7	121.7	121.7	121.7	121.7	121.7	116.4
90	112.0	117.0	117.0	117.0	117.0	117.0	117.0	117.0	111.4
100	107.0	111.1	111.1	111.1	111.1	111.1	111.1	111.1	106.1
102	105.7	109.4	109.4	109.4	109.4	109.4	109.4	109.4	104.7
110	102.2	104.7	104.7	104.7	104.7	104.7	104.7	104.7	100.6
LB/KT	60	0	0	0	0	0	0	0	0F
HEAD	60	0	0	0	0	0	0	0	100F
LB/KT	380	0	0	0	0	0	0	0	0F
TAIL	380	0	0	0	0	0	0	0	100F

-E-
RWY 8 TKOF FM TWY R9 W/ E 11700FT AVBL (RWY 8E).

-F-
RWY 17L TKOF FM TWY P9 W/ S 11690FT AVBL (RWY 17LF).

-G-
RWY 17R TKOF FM TWY M9 W/ S 11670FT AVBL (RWY 17RG).

-T1-
IN CASE OF ENGINE FAILURE ON TAKEOFF FROM RUNWAYS 16-17L/R, BEGIN LEFT TURN TO 080 DEG MAG AT D4.0 S OF DEN DME.
END OF PART 07 OF 16 PARTS
_08011559 108362 0803

Table 4-4

of flap schedules is airframe/engine and airline specific; however, much commonality occurs among airframes and airlines. These MATOGW charts are screened in the appropriate sequence to determine the flap setting. The chart is entered with the actual OAT for the particular runway, and the MATOGW linearly interpolated. This value is then compared with the Actual TOGW (ATOG) and the flaps increased if necessary. If the ATOG exceeds the MATOGW for all flap settings and Bleeds ON, then the analysis proceeds through the Bleeds OFF data.

These charts and specified flap sequences are runway specific and contain the various aerodynamic and performance tradeoffs between extra runway length and TOGW. At high altitudes such as DIA, a simple increase in flap setting utilizing the minimum defined field length does not always allow for a gain in TOGW, since the engines are usually operating at their maximum thrust rated limit. Instead the "Improved" flap settings, such as the 1I setting for the B737-200, make use of the extra runway length at DIA for achieving higher V2 speeds. Procedural requirements by the airframe manufacturer and/or airline operator may prohibit the use of derated thrust for these improved flap schedules for higher ATOGs.

During this interpolation process for evaluating the flap setting based on MATOGW and Actual OAT, the ATOG is also considered. If an interpolation at the final flap setting based on ATOG indicates that a higher temperature departure is possible, this higher temperature becomes the basis for derated thrusts. Physically, the difference between this higher Assumed Temperature (ATEMP) and the actual OAT represents excess departure performance. According to the UAL *Standard Performance Reference Handbook*, the "... rule of thumb, an average thrust reduction of 1% provides a 5% reduction in operating cost, with a like effect on engine failure rate ..." quantifies the benefits of using reduced thrust for takeoff. Note, however, that the interpolation procedure and evaluation of the ATEMP varies from one airline to the next. For example, UAL allows the ATEMP to be determined as a floating value driven by performance margins. DL, on the other hand, prescribes a standard ATEMP threshold for derated thrusts. The individual airline departure procedures must therefore be considered when predicting derated takeoff thrust levels.

Once the ATOG has been evaluated, Table 4-5 is utilized to obtain the required takeoff N_1 throttle setting. This table is entered with the ATOG and interpolated linearly to the pressure altitude at the airport. For various airframe/engine combinations, a Bleed Correction and an N_1 adjustment must be applied. Table 4-6 is a sample N_1 Adjustment as a function of OAT and ATOG for the B737-300(B1) aircraft.

MAXIMUM TAKEOFF THRUST - PMC ON 737-300 (B1/C1-20K)

NOTE
The heavy line in the table is used for the Reduced Thrust calculation.

Assumed Temp or OAT (°F)	Pressure Altitude (1000 Feet)									
	-1000	SL	1	2	3	4	5	6	7	8
130	90.0	90.6	91.2	91.9	NA	NA	NA	NA	NA	NA
120	90.7	91.1	91.7	92.3	93.7	94.7	NA	NA	NA	NA
110	91.3	91.7	92.2	92.7	94.0	95.0	95.0	95.0	NA	NA
102	91.8	92.2	92.6	93.0	94.2	95.4	95.4	95.4	95.1	94.7
100	91.9	92.3	92.7	93.1	94.3	95.6	95.6	95.5	95.1	94.6
94	92.0	92.5	93.0	93.4	94.7	96.0	96.0	95.9	95.2	94.4
90	92.1	92.6	93.1	93.5	95.0	96.3	96.2	96.1	95.4	94.6
88	91.9	92.7	93.2	93.6	95.1	96.4	96.3	96.2	95.5	94.8
86	91.8	92.8	93.2	93.6	95.0	96.5	96.4	96.3	95.6	94.9
85	91.7	92.7	93.2	93.6	94.9	96.5	96.5	96.4	95.7	94.9
82	91.4	92.4	93.3	93.7	94.7	96.3	96.4	96.5	95.9	95.2
80	91.3	92.3	93.1	93.7	94.6	96.1	96.4	96.7	96.0	95.3
79	91.2	92.2	93.0	93.7	94.6	96.0	96.4	96.7	96.1	95.4
78	91.1	92.1	92.9	93.6	94.5	95.9	96.4	96.8	96.2	95.5
76	90.9	91.9	92.8	93.5	94.4	95.7	96.2	96.7	96.2	95.6
70	90.4	91.4	92.2	92.9	93.9	95.2	95.7	96.1	96.1	96.0
60	89.6	90.5	91.4	92.1	93.1	94.3	94.8	95.2	95.3	95.4
56	89.3	90.2	91.0	91.7	92.7	93.9	94.4	94.9	95.1	95.2
50	88.7	89.7	90.5	91.2	92.1	93.4	93.8	94.2	94.4	94.5
40	87.8	88.8	89.6	90.2	91.2	92.5	92.9	93.3	93.5	93.6
30	87.0	87.9	88.7	89.3	90.3	91.6	92.0	92.4	92.6	92.7
20	86.1	87.0	87.7	88.4	89.4	90.6	91.0	91.4	91.6	91.7
10	85.2	86.1	86.8	87.5	88.4	89.6	90.1	90.5	90.6	90.7
0	84.3	85.1	85.9	86.6	87.5	88.7	89.1	89.5	89.7	89.8
-10	83.3	84.2	85.0	85.6	86.5	87.7	88.1	88.5	88.7	88.8
-20	82.4	83.3	84.0	84.7	85.6	86.7	87.1	87.5	87.7	87.8
-40	80.5	81.5	82.1	82.7	83.6	84.7	85.2	85.6	85.7	85.8

Bleed Correction
Engine Bleeds off: + .8% N_1
No correction required for engine anti-ice on.

Table 4-5

Reduced Takeoff Thrust – 737-300 (B1)										
Assumed Temp (°F)	%N_1 Adjustment									
	OAT (°F)									
	-40	0	40	50	60	70	80	90	100	110
120	0	0	-6.7	-5.8	-5.0	-4.0	-3.1	-2.3	-1.6	-.8
110	0	0	-5.9	-5.1	-4.2	-3.3	-2.4	-1.6	-.8	0
100	-12.5	-8.8	-5.1	-4.3	-3.4	-2.6	-1.7	-.8	0	0
90	-11.9	-8.0	-4.4	-3.5	-2.6	-1.7	-.8	0	0	0
80	-11.2	-7.3	-3.5	-2.7	-1.7	-.8	0	0	0	0
70	-10.5	-6.4	-2.6	-1.8	-.8	0	0	0	0	0
60	-9.7	-5.6	-1.8	-.7	0	0	0	0	0	0

Table 4-6

The second segment of the departure profile is the Climb segment. The process by which this throttle setting is determined is considerably easier than for takeoff. The Maximum Climb Thrust table, provided by the airlines, Table 4-7, contains Total Air Temperature down the left column and pressure altitude across the top row. A linear interpolation in two dimensions is used to determine the climb N1 or EPR. As before, these charts are a function of the exact airframe/engine combination.

FAA regulations do not permit takeoff segment derated thrust levels that are lower than the climb segment thrust level. After the climb thrust has been calculated for derated takeoffs, the thrust must be increased to the climb thrust if necessary. This requirement applies only to the actual N1 or EPR setting. The net corrected installed thrust-in-pounds may in fact be less for second segment when considering altitude and Mach effects, even though the throttle setting is identical.

In the cockpit the pilot sets the throttle level, either N1 or EPR, depending on the engine type. The onboard control system for virtually all modern commercial aircraft holds the engines at the prescribed throttle position until a command control change is input. Other than subtle differences between rolling starts and maximum throttle brake release starts, which primarily affect noise near the start of the roll, the throttle setting can be assumed to be constant. A further refinement to this assumption might be made in the future via speed and rotation point data analysis. However, due to the radar system resolution limitations, these details were not available at DIA for this particular measurement program. Additional measurements, such as videotape triangulation technologies, would be required for such a study.

Climb Thrust Table

MAXIMUM CLIMB THRUST (N_1)
737-300 (B1/C1-20K)

TAT	Pressure Altitude (1000 Feet)								
°C	SL	5	10	15	20	25	30	35	37
50	88.9	89.0	89.2	NA	NA	NA	NA	NA	NA
40	89.8	90.0	90.2	90.7	NA	NA	NA	NA	NA
30	89.9	90.4	91.1	91.6	91.9	92.1	NA	NA	NA
20	88.4	90.5	91.8	92.5	92.8	93.0	93.2	NA	NA
10	86.8	88.9	91.0	92.7	93.5	93.8	94.0	94.0	94.0
0	85.3	87.4	89.4	91.1	93.1	94.4	94.6	94.6	94.6
-10	83.7	85.7	87.7	89.4	91.3	93.1	94.6	95.2	95.2
-20	82.1	84.1	86.0	87.7	89.6	91.3	92.8	95.7	96.0
-30	80.5	82.4	84.3	85.9	87.8	89.5	90.9	93.8	94.5
-40	78.8	80.7	82.6	84.1	86.0	87.6	89.0	91.9	92.5

Bleed Correction ($\%N_1$)

Engine Bleeds off:	+.7	Engine anti-ice on:	-.9
Packs high:	-.5	Wing anti-ice on:	-1.6

Table 4-7

With this fixed-throttle setting, the manufacturer's Installed Engine Decks (Fn/δ) are used to determine the net corrected installed thrust. Thrust in lbs. was calculated as a function of Mach number and altitude, and N1 or EPR as appropriate. These Fn/δ charts are considered manufacturer-proprietary property and as such are not published in this document.

At this stage of the analysis, each point in the radar track in the initial takeoff segment is analyzed in sequence. Based on the local atmospheric conditions, Mach number, and N1/EPR, the Fn/δ is determined for input into the INM. The atmospheric variations with altitude were based on interpolation of atmospheric weather balloon data to the flight departure time. The local velocity as reported by the ARTS system was converted to calibrated airspeed and the temperature converted to Total Temperature as required by the particular prediction method and Fn/δ charts.

Standard departure procedures in place at DIA require climb at takeoff thrust to 1,000 feet above ground level (AGL). A scan of the departure profiles and an evaluation of the altitude where the "knee in the curve" occurs, indicated that the majority of departures were adhering to this guideline.

As required by INM, a thrust level needs to be assigned to each flight profile point. In this study both tracks and profiles were treated simultaneously with individual node points determined by radar returns. As such, the thrust is required at each radar return. At this point in the analysis process the two N1/EPR settings (takeoff and climb segments) are known. These must then be converted into net corrected installed thrust-in-lbs. as required by INM. While the N1/EPR settings remain constant across the flight segments, the Mach number, altitude, and outside air temperatures are varying at each radar point along the profile. Because of this, the thrust levels vary at each profile point.

The transition between the takeoff and climb was made at the radar point closest to or above 1000 feet AGL. Future refinements to this methodology may include a pattern recognition method for determining the transition point between takeoff and climb throttle settings, as well as a gradual rather than an instantaneous change between settings. Discussions with UAL flight training personnel indicated that the throttle and flap cleanup technique was highly pilot-dependent and could not be reliably predicted. Guidelines such as X seconds per flap degree of retraction for acceleration before changing throttles, despite detailed airline studies, were not available. It might be possible to determine the extent of the transition from flaps to clean and acceleration with change to climb segment thrust based on radar data; however, such methods were not employed in this study.

4.3.2 Alternate Thrust Prediction Techniques

Several other thrust prediction techniques have been presented in other documents. For example, SAE AIR 1845[19] and the INM 5.1 Technical Manual[20] describe the following procedures:

- thrust as a function of Velocity (Equation A1)
- thrust as a function of EPR (Equation A2)
- thrust as a function of N1 (Equation A3)
- thrust as a function of Flight Path Angle (Equation A8)

In addition, Dr. John-Paul Clarke, from the Charles Stark Draper Labs at the Massachusetts Institute of Technology, has developed an improved physical equation for the prediction of thrust as a function of N1/EPR.[21] These methods may be categorized based on the physics and particular formulation of the techniques:

A. thrust as a function of velocity

B. thrust as a function of throttle setting (N1 or EPR)

C. thrust as a function of Flight Path Angle

Each of these methods, and their particular implementation in this project, are described below.

A. Thrust as a Function of Velocity. Equation (A1) in SAE-AIR-1845 and expanded with higher order terms in INM states that:

$$\frac{F_n}{\delta_{am}} = E + FV_c + G_a h + G_b h^2 + HT_{am}$$

(SAE Eqn. A1)

where the individual airframe/engine coefficients are given for sea level conditions in the Bishop & Mills report.[22] Note that there are two sets of coefficients, one each for Takeoff and Climb conditions. These coefficients, unadjusted, were applied directly to the DIA radar velocity points yielding net-corrected installed thrust-in-lbs.

A second set of coefficients was derived for DIA conditions (5431 ft. MSL, 64°F) for the airframe/ engine types listed in Table 4-8.

Updated DIA Performance Coefficients	
• Boeing 737-300 / CFM 56-3/B1-20K • Boeing 737-300 / CFM 56-3/B2-22K • Boeing 737-500 / CFM 56-3/B1-20K	
Takeoff Thrust	**Climb Thrust**
E = 22000.0	E = 18360.0
F = -27.3	F = -16.1211
Ga = 0.165517	Ga = 0.14
Gb = 0.0	Gb = 0.0
H = 0.0	H = 0.0

Table 4-8

B. Thrust as a Function of EPR or N1. The second performance prediction method as defined in SAE AIR 1845 describes thrust as a function of N1 or EPR as:

$$\frac{F_n}{\delta_{am}} = E + FV_c + Gh + HT_{am} + K_1(EPR)$$

(SAE Eqn. A2)

$$\frac{F_n}{\delta_{am}} = E + FV_c + Gh + HT_{am} + K_2\left(\frac{N_1}{\sqrt{\theta_t}}\right) + K_3\left(\frac{N_1}{\sqrt{\theta_t}}\right)^2$$

(SAE Eqn. A3)

Again, coefficients are itemized in Bishop & Mills for sea level standard day conditions. Unfortunately, improved coefficients for DIA were not available. As before, the actual radar data was examined to produce the total temperature and pressure altitude. The throttle was switched instantaneously from takeoff to climb at the radar point at or above the 1,000-foot AGL altitude.

An improved thrust prediction method based on physical parameters such as local Mach number, with higher order terms, was developed by J.P.Clarke.[21] The following equation details this technique:

$$\frac{F_n}{\partial_{am}} = \left[E + K_2(N_1c) + K_3(N_{1C})^2\right]\exp\left[\left(\frac{260 + N_{1c}}{2 * N_{1c}}\right) * M\right]$$

Where

$$N_{1c} = \frac{N_1}{\sqrt{\theta_t}}$$

and M is the Mach number

This method utilizes the same performance coefficients as for Method #3, and is currently only available for the following aircraft:

- B737-300 CFM 56-3B1 (20K)
- B737-500 CFM 56-3B1 (20K)
- B737-300 CFM 56-3B2 (22K)

C. Thrust as a Function of Flight Path Angle. The third physical throttle prediction method itemized in SAE-AIR-1845 utilizes flight path angle as its driving parameter.

$$\gamma = \arcsin\left(1.01\left\{\frac{N\left(\frac{F_n}{\delta_{am}}\right)_{avg}}{\left(\frac{W}{\delta_{am}}\right)_{avg}} - R\right\}\right)$$

(SAE Eqn. A8)

This prediction method was dropped from the current study when proprietary Fn/δ data became available.

4.3.3 Comparison of Thrust Prediction Techniques

As discussed in Section 4.3.2, several thrust prediction techniques were implemented with the available radar data. Figures 4-3 and 4-4 show a single B737-300/CFM 56-3B1 aircraft departure from Runway 08. The climb and velocity profile, as given in the ARTS IIIA radar data is shown in Figure 4-3. Figure 4-4 compares five of the power prediction methods. Table 4-9 itemizes the power modes and identifies the power prediction method.

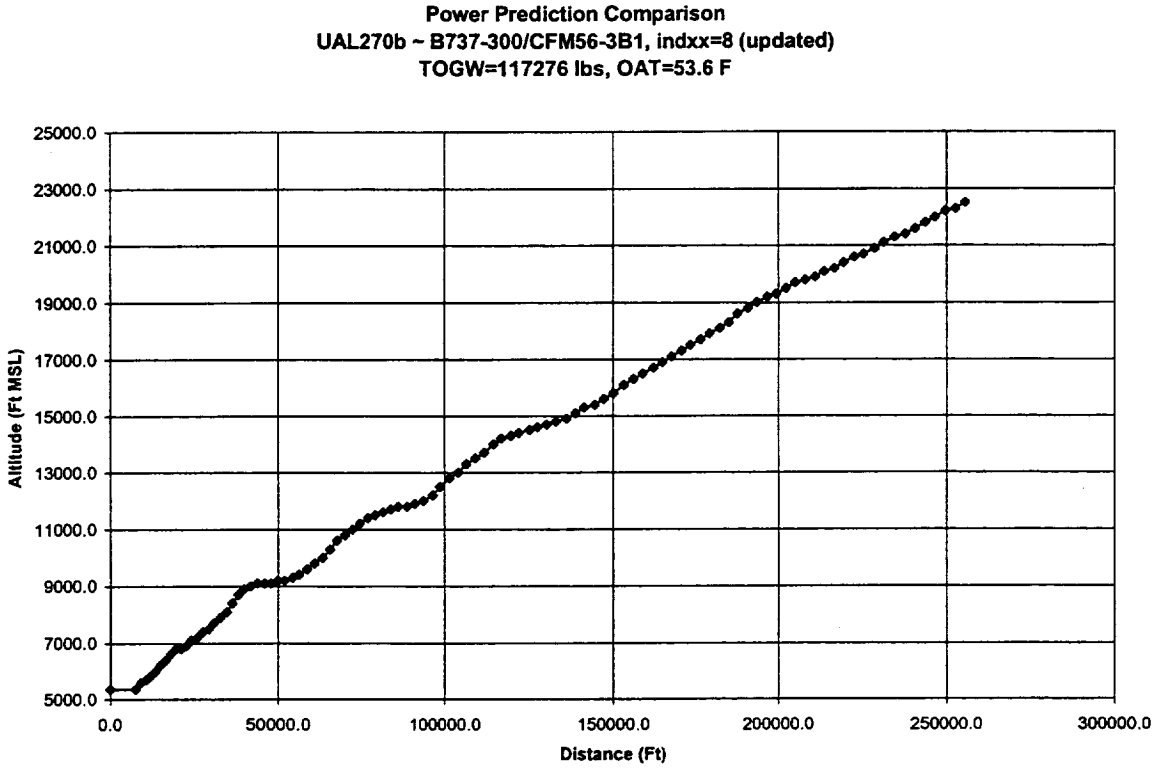

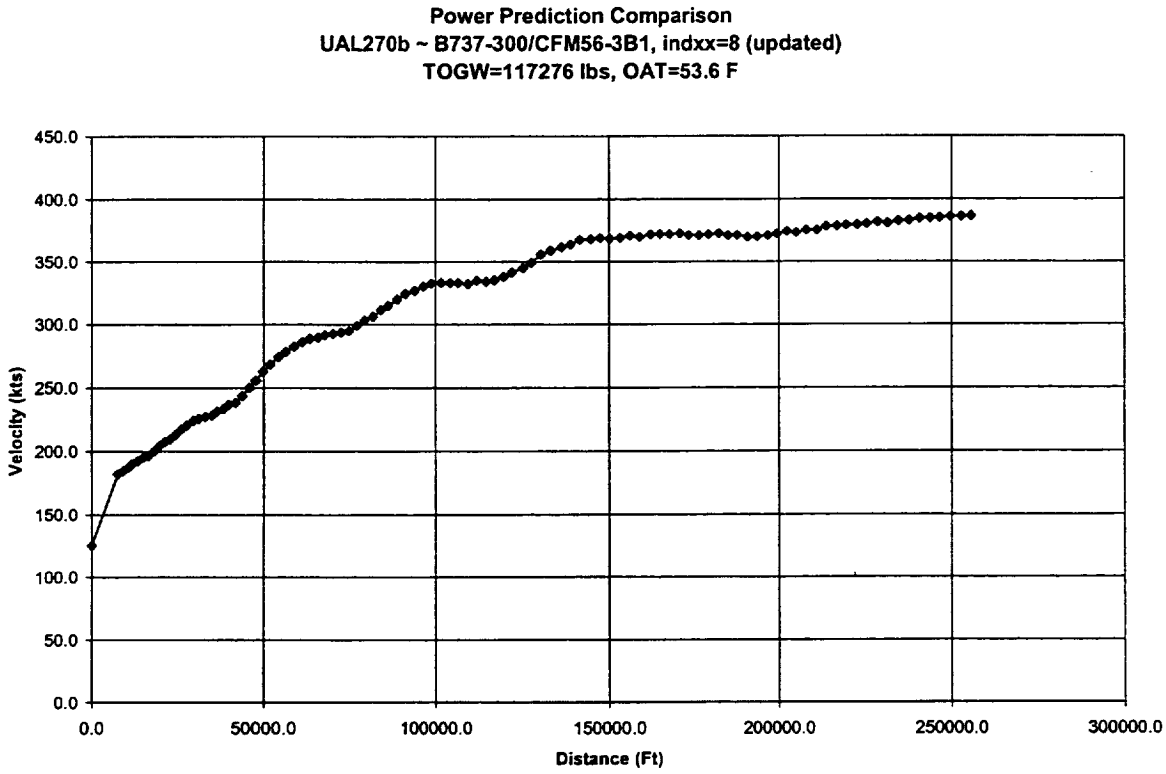

Figure 4-3. Selected Departure Altitude and Velocity Profiles From Runway 08

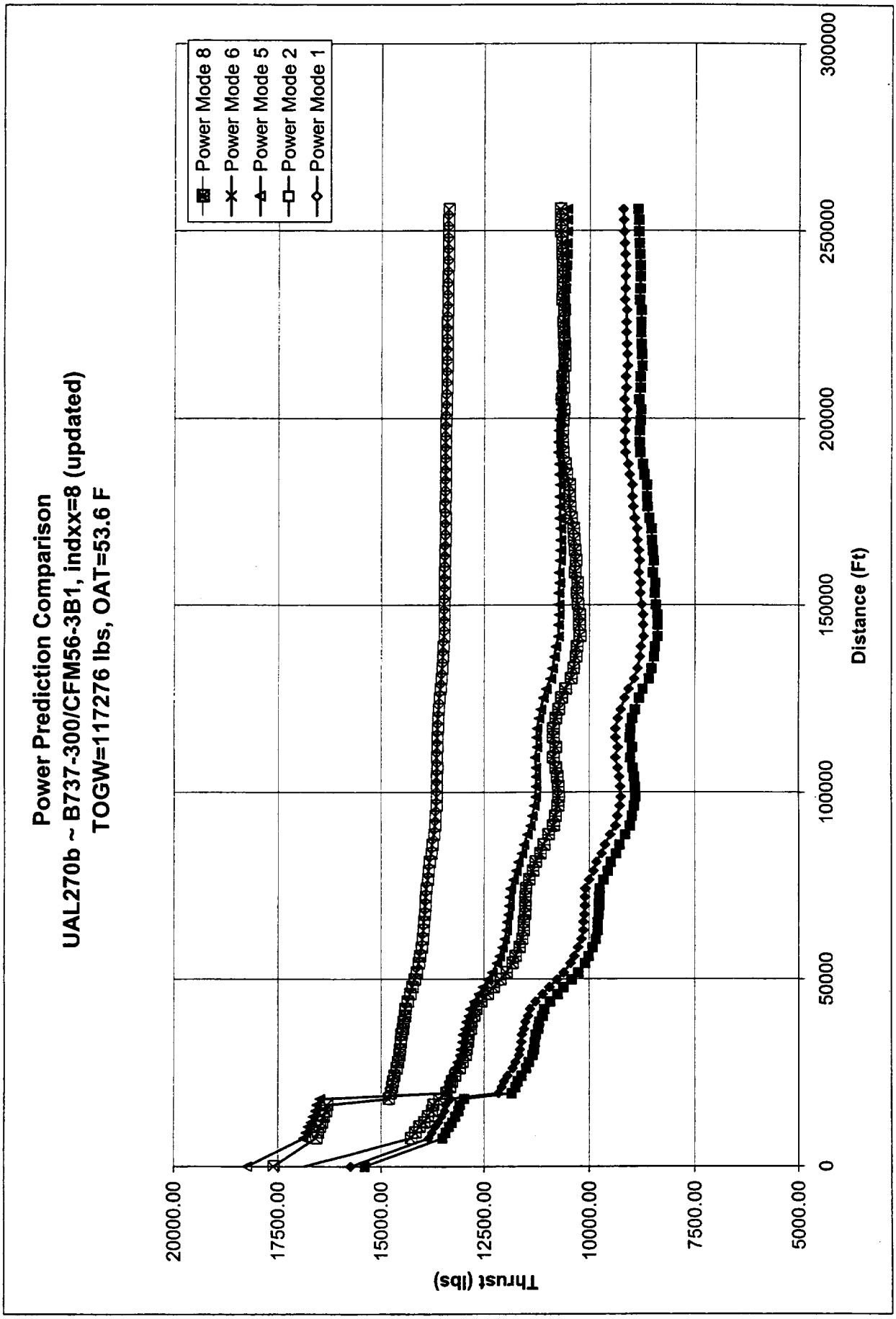

Figure 4-4. Power Profiles for Selected Departure from Runway 08

Thrust Prediction Methods	
Power Mode	
6	Thrust from Manufacturers' Fn/d charts
1	Thrust from Velocity (SAE-Air-1845, Equation A1)
2	Thrust from N1 and EPR (SAE-AIR-1845, Equations A2 and A3)
5	Thrust from J.P. Clarke Mach Equations
8	Thrust from Velocity (SAE-AIR-1845 Equation A1) with coefficients adjusted for DIA conditions

Table 4-9

Comparing Power Modes 1 and 8 highlights the effect of updating the performance coefficients for DIA flight conditions. It is apparent that there is a slight difference in the takeoff and climb thrust levels, and a continuing difference of about 1,000 lbs across the remainder of the flight trajectory.

Power Mode 2, thrust from N1 or EPR based on SAE-AIR-1845, is an approximation to the exact actual installed engine performance from the manufacturer's Fn/δ charts, or Power Mode 6. Figure 4-4 illustrates that the takeoff thrust is underpredicted. All power prediction methods show a drastic underprediction of thrust as compared with the manufacturer's Fn/δ curves (power mode 6) for second segment climb. This is most likely due to the high DIA departure altitude, and hence significantly higher operating altitudes than the methods can handle.

This is most likely a manifestation of using sea level coefficients rather than DIA-specific performance data, but also that the trend with increasing distance, Mach number, and altitude is to underpredict the thrust. This is possibly an effect due to neglecting compressibility effects and applying the SAE-AIR-1845 equation beyond its original range of intent. Power Mode 5, the improved thrust equation developed by J.P. Clarke, does include higher-order terms and Mach compressibility effects, and one can see from Figure 4-4 that while it more closely approximates the behavior of the actual Fn/δ installed performance curves at takeoff, at higher Mach numbers the thrust is still underpredicted. As noise studies and impact analyses extend farther away from the airports, into regions where aircraft are traveling at higher Mach numbers and entering into compressibility regions, these Mach number and compressibility effects predicted by the detailed engine installation Fn/δ charts effects cannot be neglected.

4.4 INM Analysis

The INM Version 5.1a[1,20] was an integral part of the data analysis. The INM was used to analyze individual flight tracks singly and predict the Sound Exposure Level at the noise monitoring sites. Tools were developed which allowed automated processing of the radar data and direct creation of DBF files. The following information was provided to INM for its use in noise prediction:

- Flight Track
- Flight Profile
- Velocity Profile
- Power Profile
- Aircraft Information:
  - Noise Power Distance Tables
  - Takeoff Gross Weight
  - Flight identifier
- Airport Information
  - Operating Conditions
  - Terrain Characteristics

The Thrust data was calculated via the CATS code in any one of the five implemented power prediction methods and was fed directly into the INM. Each of the individual track analyses considered the actual atmospheric and climatalogical data when determining thrust levels; however, since INM restricts a given study to one atmosphere and temperature, some data fidelity was lost. A separate study was created for each day, with individual flight tracks being represented by individual aircraft with individual profiles. A special console application, which generated a new study.INM file, was used with the new aircraft types. The front-end graphical user interface of INM 5.1 was then used simply to load the case and study and run the analysis. Output was obtained via the detailed grid analysis, where one single-point-detailed grid was created for each noise monitoring location. The detailed grid output file was then saved in ASCII format for future Prediction versus Measurement correlation processing. A sample detailed INM grid output is shown in Table 4-10.

INM has the ability to incorporate terrain effects, in terms of ground altitude offsets (no shielding, or reflective terrain effects) into the noise predictions. The terrain east of DIA gradually slopes downhill, while terrain south of DIA slopes upward (Table 2-3). These changes from flat terrain manifest themselves as different effective above-ground altitudes when terrain considerations are included in the analysis. INM was executed both with terrain calculations included (terrain ON) and terrain calculations ignored (terrain OFF). Subsequent sections of the report compare the effects of terrain on the analysis for DIA.

Sample INM Detailed Grid Output

METRIC	GRD	I	J	ACFT	OP	PF	S	RWY	TRK	SDISTANCE	ALT	ANG	SPEED	THRUST	EQUIV	ONE	ALL	PERCENT
SEL	S10	1	1	UA1495	D	U	1	34	1495	0 11735.4	1669	0.0	215.7	11795.97	1.0000	73.1	73.1	14.535
SEL	S10	1	1	UA1566	D	U	1	34	1566	0 12237.3	1071	0.0	218.8	11776.91	1.0000	72.0	72.0	11.531
SEL	S10	1	1	UA451	D	U	1	34	451	0 14286.5	1269	5.5	229.3	11745.97	1.0000	71.2	71.2	9.420
SEL	S10	1	1	UA295	D	U	1	34	295	0 13658.8	1265	5.6	217.0	11804.15	1.0000	71.2	71.2	9.377
SEL	S10	1	1	UA1157	D	U	1	34	1157	0 13762.3	1270	5.7	218.7	11777.94	1.0000	70.8	70.8	8.699
SEL	S10	1	1	UA543	D	U	1	34	543	0 13825.9	1251	5.5	216.6	11768.29	1.0000	70.3	70.3	7.630
SEL	S10	1	1	UA1629	D	U	1	34	1629	0 13975.0	1270	5.6	219.8	11766.94	1.0000	69.4	69.4	6.244
SEL	S10	1	1	UA522	D	U	1	34	522	0 13374.8	1171	5.1	208.3	11797.91	1.0000	68.7	68.7	5.378
SEL	S10	1	1	UA1496	D	U	1	34	1496	0 13157.1	1249	5.5	231.4	11781.79	1.0000	68.7	68.7	5.349
SEL	S10	1	1	UA1750	D	U	1	34	1750	0 19109.5	769	0.0	183.8	13703.00	1.0000	66.4	66.4	3.174
SEL	S10	1	1	UA759	D	U	1	34	759	0 18156.8	1293	4.0	214.6	11770.80	1.0000	65.3	65.3	2.456
SEL	S10	1	1	UA1561	D	U	1	34	1561	0 18590.9	1534	4.7	194.4	11831.63	1.0000	65.1	65.1	2.321
SEL	S10	1	1	UA740	D	U	1	34	740	0 21667.2	697	1.5	172.1	13461.58	1.0000	64.5	64.5	2.044
SEL	S10	1	1	UA704	D	U	1	34	704	0 19053.9	869	2.4	177.8	12455.00	1.0000	63.9	63.9	1.770
SEL	S10	1	1	UA1154	D	U	1	34	1154	0 21275.2	576	1.2	181.1	13122.84	1.0000	63.8	63.8	1.721
SEL	S10	1	1	UA780	D	U	1	34	780	0 22138.9	671	0.0	180.6	13572.62	1.0000	63.4	63.4	1.578
SEL	S10	1	1	UA436	D	U	1	34	436	0 22220.3	700	1.4	174.9	12656.11	1.0000	61.8	61.8	1.080
SEL	S10	1	1	UA1260	D	U	1	34	1260	0 23305.4	471	0.0	174.0	13494.45	1.0000	61.6	61.6	1.035
SEL	S10	1	1	UA1236	D	U	1	08	1236	0 33175.7	-80	0.0	24.0	14725.00	1.0000	56.2	56.2	0.298
SEL	S10	1	1	UA1802	D	U	1	08	1802	0 33175.7	-80	0.0	125.0	14005.00	1.0000	55.7	55.7	0.265

Table 4-10

4.5 Noise Measurement and INM Prediction Data Correlation

A series of post-processors was developed, which linked together noise measurement records, INM predictions, and atmospheric information at the point of closest approach.

These processors interrogated the correlated noise event records (Section 4.2) and the INM noise prediction results (Section 4.4) with the atmospheric conditions (Section 3.1). Although INM does not allow for user-defined atmospheres, for the purposes of data correlation and sensitivity studies, and in order to determine any possible atmospheric effects, this additional step was taken. Once the three data sources were linked by date and flight number and operational state (Arrival/Departure), the resulting unique combination of data was input to a database program for post-processing. Table 4-11 shows a sampling of the final correlated output data. Each of the available independent variables in Table 4-11 is defined below in Table 4-12.

The sources for data contained in Table 4-12 are as follows:

Columns 1 to 16: Noise Correlation Database and Radar Track Data

Columns 17 to 34: INM Output Detailed Grid Report

Columns 35 to 48: Power Calculation Analysis

Columns 49 to 54: Atmospheric weather analysis for the point of closest approach

Independent Variables for Correlation Analyses

Flight/file	Date			AC Time	Op	Rwy	AC	Alt	TrkDist	Speed	Mon	Slant	Tarr	Lmax	SEL	From	To
UAL785B.521	21	May	1997	0.354903935	Dep	25	B73S	6847	20034	212.4	S09	3494	0.35494213	77	84.7	0.354594907	0.355289352
UAL785B.521	21	May	1997	0.356407755	Dep	25	B73S	11184	77170	330.5	S18	7853	0.356493056	63	74.9	0.356145833	0.356724537
UAL785B.521	21	May	1997	0.356353588	Dep	25	B73S	11082	74532	325.9	S17	7507	0.356435185	66	76.9	0.356087963	0.356701389
UAL785B.521	21	May	1997	0.356526273	Dep	25	B73S	11507	82741	338.6	S16	7818	0.356608796	71	80.7	0.356134259	0.356956019
UAL759A.521	21	May	1997	0.356744907	Dep	34	B727	6200	20964	192.6	S01	5687	0.356805556	73	83.6	0.356342593	0.357291667
UAL759A.521	21	May	1997	0.357058333	Dep	34	B727	6581	30232	219.8	S02	3399	0.357094907	83	92.6	0.35662037	0.357789352

Angle		METRIC	GRD	I	J	ACFT	OP	PF	S	RWY	TRK	S	DISTANCE	ALT	ANG	SPEED	THRUST	EQUIV	ONE	ALL	PERCENT
26.42	1.99801E+11	SEL	S09	1	1	UA785	D	U	1	25	785	0	3416.7	1371	23.9	211.5	14858.06	1	77	77	1.543
49.09	1.99801E+11	SEL	S18	1	1	UA785	D	U	1	25	785	0	7721.8	5733	49.2	329.7	13832.35	1	68.1	68.1	39.687
51.55	1.99801E+11	SEL	S17	1	1	UA785	D	U	1	25	785	0	7369.1	5624	51.1	324.4	13868.93	1	68.8	68.8	11.692
52.25	1.99801E+11	SEL	S16	1	1	UA785	D	U	1	25	785	0	7770.8	6097	51.8	339.6	13770.26	1	66.6	66.6	17.646
9.69	1.99801E+11	SEL	S01	1	1	UA759	D	U	1	34	759	0	5658.8	769	7.1	191.1	11819.31	1	82.8	82.8	47.789
24.75	1.99801E+11	SEL	S02	1	1	UA759	D	U	1	34	759	0	3337.8	1122	22.5	218.5	11618.38	1	91.4	91.4	92.659

Operation		date	Indxx	T(1)	P(1)	DerateN1	ClimbN1	weight	MATOGW	OAT	AsmTemp	flap	bleed
UAL785B	SCH0815	19970521	8	30636.77	19235.97	90.36	89.76	108182	119000	55.4	37.58	1	ON
UAL785B	SCH0815	19970521	8	30636.77	19235.97	90.36	89.76	108182	119000	55.4	37.58	1	ON
UAL785B	SCH0815	19970521	8	30636.77	19235.97	90.36	89.76	108182	119000	55.4	37.58	1	ON
UAL785B	SCH0815	19970521	8	30636.77	19235.97	90.36	89.76	108182	119000	55.4	37.58	1	ON
UAL759A	SCH0820	19970521	5	30782.07	12170.57	1.96	1.95	147916	172198	55.4	42.78	5	NORMAL
UAL759A	SCH0820	19970521	5	30782.07	12170.57	1.96	1.95	147916	172198	55.4	42.78	5	NORMAL

PressFE	dThrAlt	OATAlt	PAlt	DewPt	RHum	WindDAlt	WindSAlt	aMach
2810.6	6600	52.92	2670.47	41.59	66.69	265.27	7.02	0.191211
2810.6	6600	40.17	2284.48	26.58	58.94	294.11	9.19	0.301107
2810.6	6600	40.61	2292.73	26.84	58.51	294.98	9.42	0.296792
2810.6	6600	38.77	2258.34	25.76	60.27	291.36	8.47	0.308912
2810.6	6500	52.81	2733.91	45.33	78.74	262.68	6.91	0.173426
2810.6	6500	52.86	2696.55	43.14	71.72	264.21	6.98	0.197875

Table 4-11

Independent Variables for Correlation Analyses		
No.	**Row Header**	**Definition**
1	Flight/File	Airline flight number. Letter following the flight number indicates the occurrence of that flight. A is usually arrival; B is generally departure.
2	Date	Local date.
3	AC Time	Local time for the first radar tracking point.
4	Op	Operation type – Arrival or Departure.
5	Alt	Altitude of the aircraft (feet) at the point of closest approach.
6	TrkDist	Ground track distance (feet) traveled to the point of closest approach.
7	Speed	Aircraft Speed (knots) at the point of closest approach.
8	Mon	Monitor Identifier.
9	Slant	Slant range between the monitor and point of closest approach (feet)
10	Tarr	Arrival time (local DIA time) of the sound generated by the aircraft at the point of closest approach.
11	Lmax	Maximum A-weighted sound level for the event.
12	SEL	Integrated A-weighted Sound Exposure Level for the event.
13	From	Limits of integration for SEL calculation.
14	To	Limits of integration for SEL calculation.
15	Angle	Elevation Angle between aircraft at point of closest approach and noise monitor, 90° = overhead
16	Un-identified	Internal time stamp record locator
17	Metric	INM output metric for detailed grid
18	GRD	Noise monitor identifier
19	I	Output detailed grid index
20	J	Output detailed grid index
21	OP	Operation Type
22	PF	Profile Group Identifier
23	S	Profile Stage # (not used)
24	Rwy	Runway assignment
25	TRK	Identifying Track Label
26	S	Sub-Track Number
27	Distance	Slant Range from the grid to the point of closest approach (feet).
28	Alt	Aircraft Altitude (AFE) at point of closest approach (feet).
29	ANG	Elevation angle (degrees) from the grid point to the aircraft at point of closest approach.
30	SPEED	Speed (TAS–Knots) of the aircraft at the point of closest approach.
31	THRUST	Thrust Setting (pounds) of the aircraft at the point of closest approach.
32	EQUIV	Equivalent # operations
33	ONE	Metric value for a single operation
34	ALL	Metric value for all operations
35	PERCENT	Percent of the total Metric Value that is caused by the flight operation.
36	Operation	Flight number and scheduled time.
37	Date	Operation date (local).
38	Index	Internal unique airframe/engine index assignment.
39	T(1)	First data point time in the radar track (seconds after midnight, local time).
40	P(1)	Takeoff power setting (lbs)
41	Derate N1	Takeoff N1 or EPR Setting.

Table 4-12

→

Independent Variables for Correlation Analysis (Continued)		
No.	**Row Header**	**Definition**
42	Climb N1	Climb Segment N1 or EPR Setting
43	Weight	Takeoff gross weight (lbs).
44	MATOGW	Maximum Allowable Takeoff Gross Weight
45	OAT	Outside air temperature at the airport at the departure time (°F).
46	AsmTemp	Assumed Temperature (°C) for derated thrust calculations.
47	Flap	Flap setting used for takeoff.
48	Bleed	Takeoff Bleed status
49	Press FE	Atmospheric pressure at the airport at the departure time (in Hg).
50	DTHRALT	Radar altitude where thrust transition from takeoff to climb throttle occurs.
51	PAlt	Atmospheric pressure at the point of closest approach (in Hg).
52	DewPt	Dew Point at the point of closest approach (°F).
53	RHum	Relative Humidity at the point of closest approach (%).
54	Wind D Alt	Wind Direction at the point of closest approach.
55	Wind S Alt	Wind Speed (knots) at the point of closest approach.
56	Mach	Aircraft Mach number based on local atmospheric conditions at the point of closest approach.

Table 4-22 (Continued)

5 Results

A total of 14,992 flight tracks were screened for air carrier, weather conditions (Section 5.2) and departure tracks, and analyzed. UAL and DL provided critical takeoff gross weight and historical equipment records (Section 5.3). Noise levels were predicted for 50 monitors based on five power calculation methods. In Section 4.3, the five power prediction methods were compared. Based on the results of these comparisons given in Table 5-1, only power mode 6 with terrain turned ON was used for further detailed sensitivity analysis.

Figures 5-1 through 5-5 illustrate the overall prediction accuracy for the five power modes. Because of the vast number of data points and the semi-automated correlation process, the occasional large predicted-measured SEL appears below the trend line in Figures 5-1 through 5-5. Due to the massive scope of effort that would have been involved in performing a detailed analysis on each and every data point, only significant anomalous discrepancies were eliminated from the database. Perhaps the focus of a future study might involve more detailed analyses of a few selected flight tracks, specifically a revisit to the measurement correlation records and acoustic one-second noise event time-history data. Section 4.3 documents the thrust prediction process and highlights the assumption that when available, a derated thrust takeoff analysis was performed.

Given pilot discretionary options, and a vast number of operators for which ACARS engine monitoring data was not available, the following approach was developed for estimating which flights performed derated thrust departures, and which flights did not. The ultimate decision whether or not a derated thrust takeoff is performed lies with the pilot. UAL provided the overall fleet data presented in Table 5-2.

The overall percentage of UAL flights, which executed derated departures from DIA in May 1997, was 5173. This represents a 75.4% derate level. Correspondingly, 24.6% of departures were made at full throttle. Based on the derated thrust methodology, only 10.9% of flights were deemed incapable of performing derated departures based on the performance and atmospheric criteria. This means that an additional 13.7% of the UAL May 1997 flights performed full throttle departures. Since we have no direct means for applying this percentage to the thrust prediction analysis, a post-analysis update technique was utilized. Overall, there was an average of 4.4 noise events per flight. This means that the 13.7% (76 flights) with 4.4 events per flight, representing 334 noise events, were predicted based on derated thrust instead of full throttle. After the noise predictions were correlated with the measurements, they were sorted by predicted-measured levels. Data was sorted in correlation order, and the 334 maximum INM-measured differential correlation records were deleted from the analysis on the grounds of over-approximated thrust derate level. This analysis logic allows us to apply the UAL historical derate information globally to the noise correlation study.

Future analysis could possibly develop a feedback loop whereby those tagged flights could be re-analyzed without a thrust derate, hence remaining in the final statistical analysis. Similarly, the derate breakdown by individual aircraft in combination with the overall city-pair derates could be combined to develop a statistical probability of derate for each individual flight track.

Available information from UAL included percentages of operations, which used derated thrust takeoffs with breakdown by equipment for all city pairs, and by city pairs for all equipment types. This data was screened to determine the overall UAL-DIA departure fleet average thrust derate percentiles. Based on the May 1997 data, Table 5-2 was developed.

Predicted-Measured SEL for All Power Modes							
Power Mode	Terrain Status	Mean Prediction Error	Std. Dev	No. Original Points	Mean Prediction Error	Std. Dev	No. Final Analysis Points
1	ON	-8.29	5.68	2,270			
1	OFF	-7.47	5.48	2,947			
2	ON	-6.78	6.50	2,780			
2	OFF	-6.03	6.44	2,627			
5	ON	-10.65	6.40	2,297			
5	OFF	-9.65	6.17	2,281			
6	ON	-6.11	5.01	2,437	-4.44	3.33	2,013
6	OFF	-5.17	4.92	2,461	-3.51	3.46	2040
8	ON	-11.77	6.44	2,279			
8	OFF	-10.78	6.23	2,267			

Table 5-1

Overall UAL Fleet Data Based on May 1997 Data		
	Terrain ON	Terrain OFF
Total UAL DIA Departures in May 1997	6,854	
Total UAL Derated Takeoffs in May 1997	5,173	
Percent of Flights Derated	75.4%	
Percent of Flights Not Derated	24.6%	
Percent of Flights Not Derated in the Thrust Prediction	10.9%	
Additional Percent That Should Not Have Been Derated But Were	13.7%	
Total Number of Flights in the Analysis	703	698
Number that Should Not Have Been Derated But Were	96	96
Number of Noise Events Per Flight	4.4	
Number of Noise Events to be Filtered Out	424	421

Table 5-2

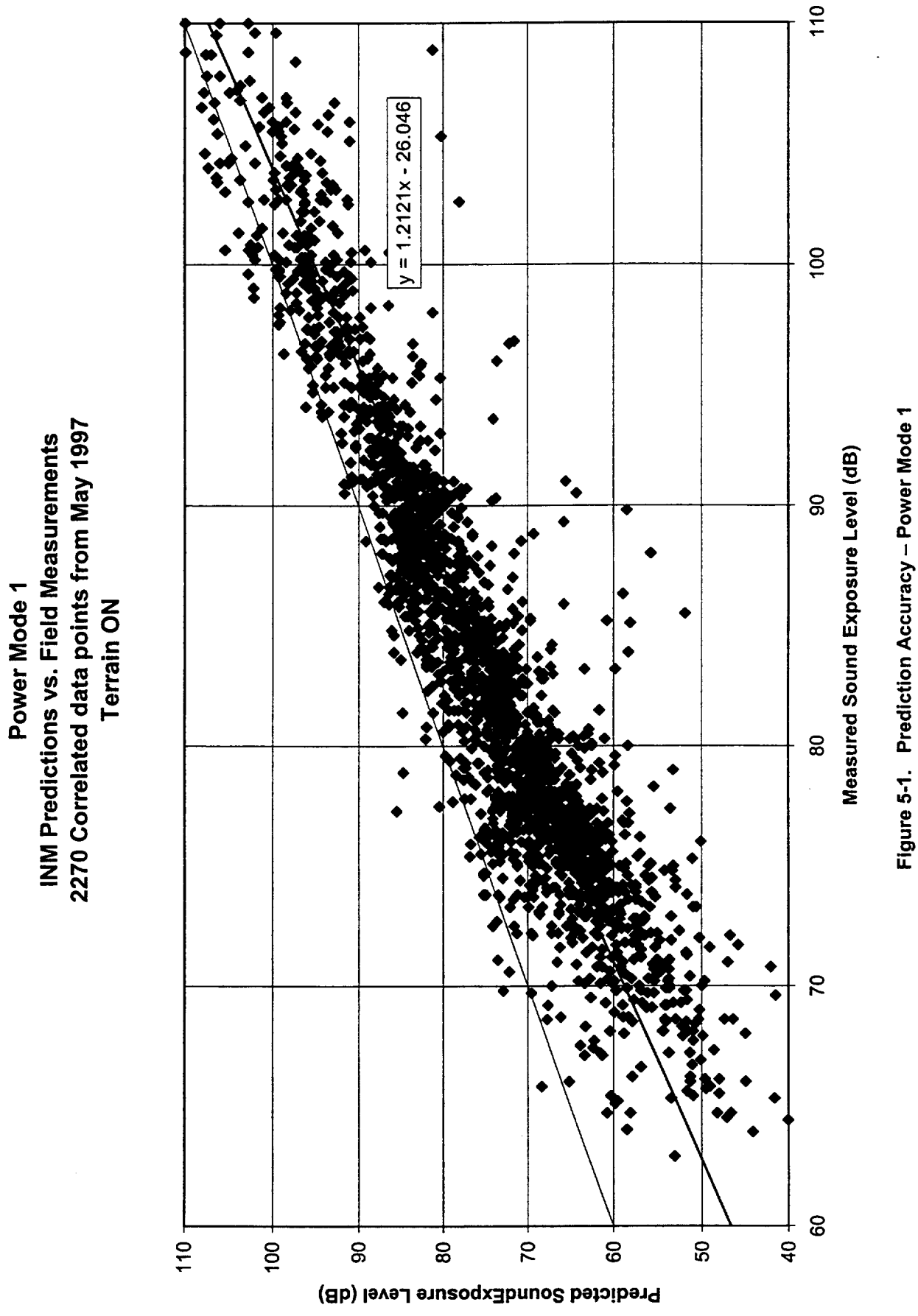

Figure 5-1. Prediction Accuracy – Power Mode 1

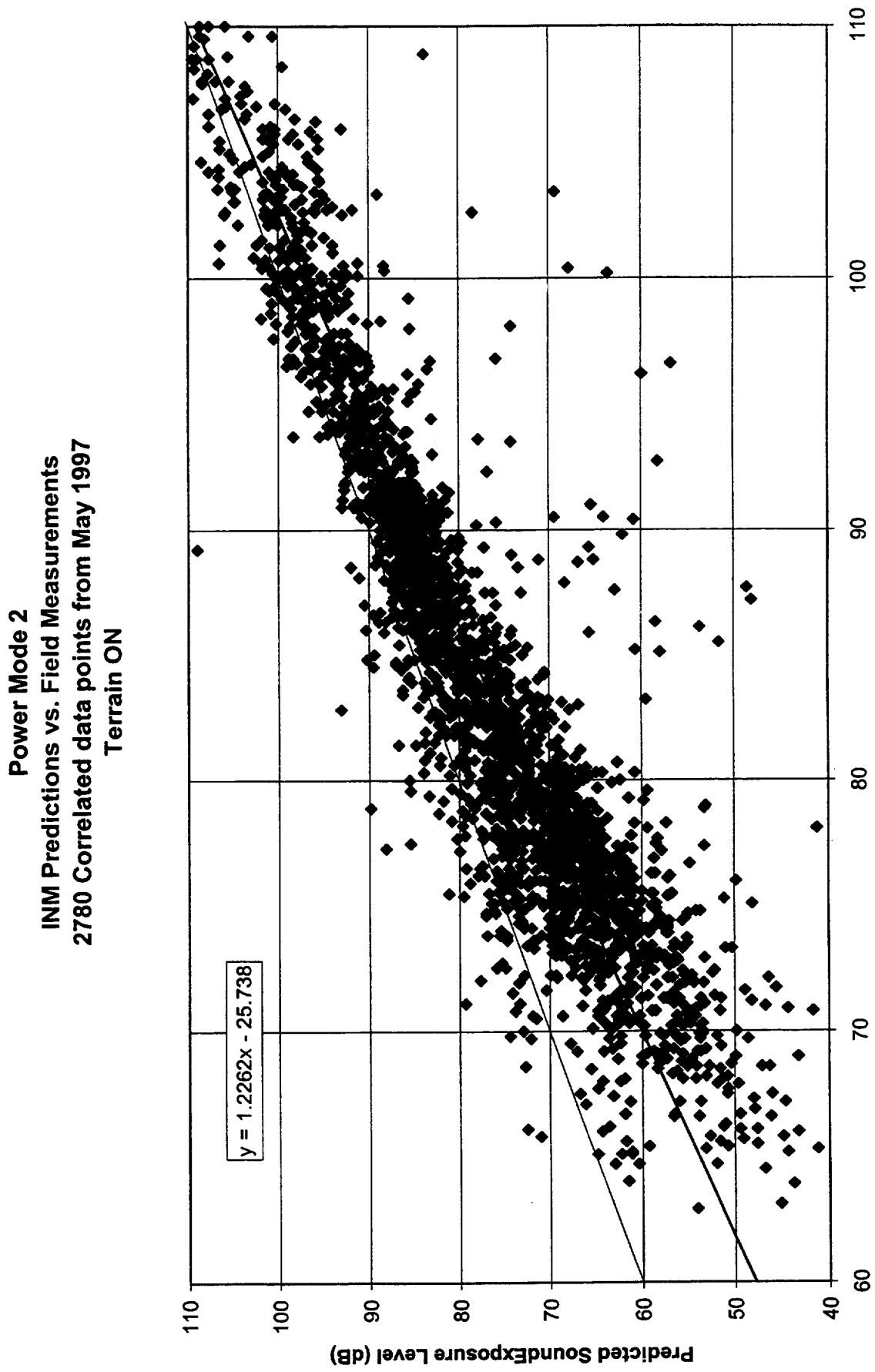

Figure 5-2. Prediction Accuracy – Power Mode 2

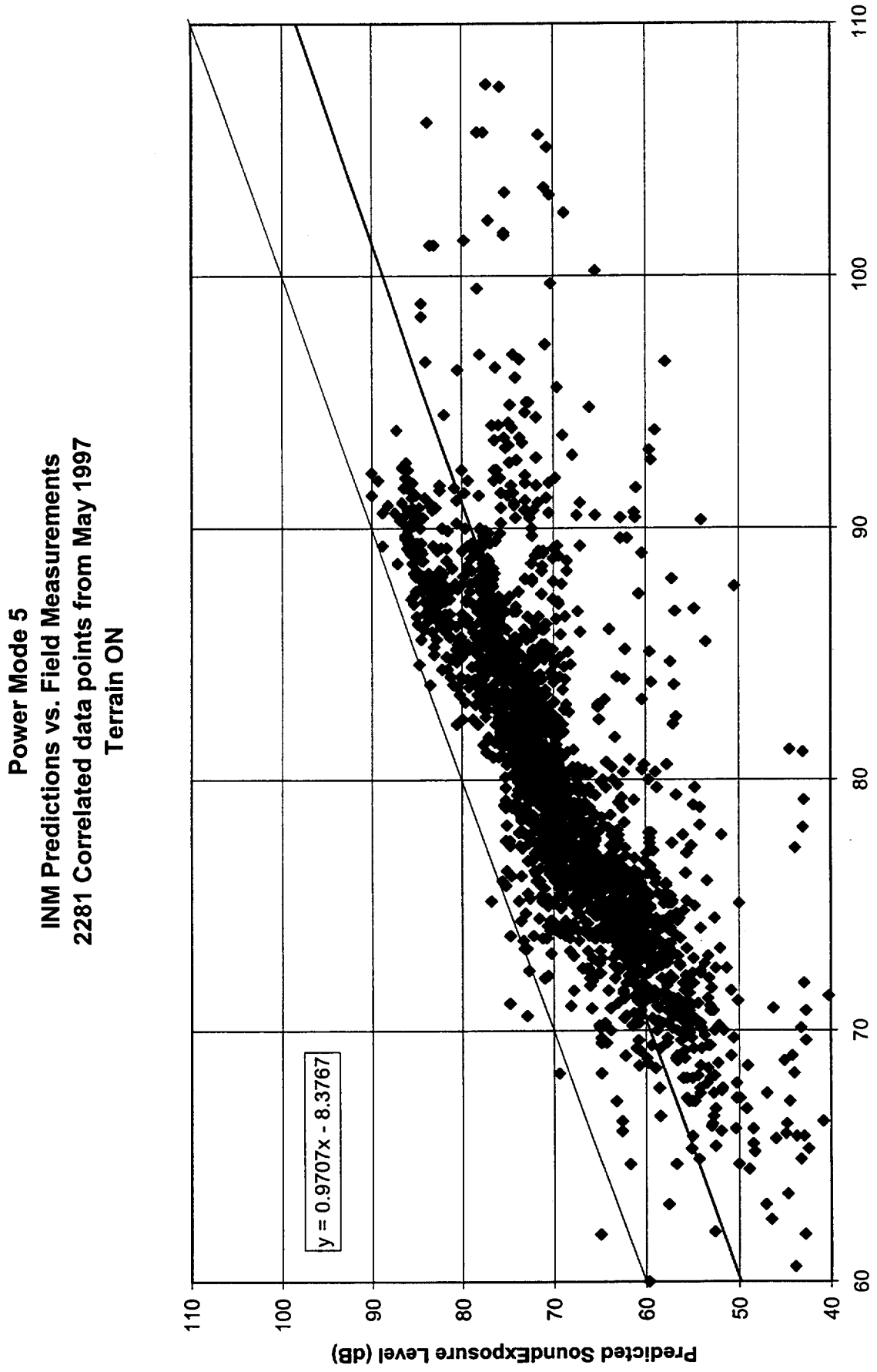

Figure 5-3. Prediction Accuracy – Power Mode 5

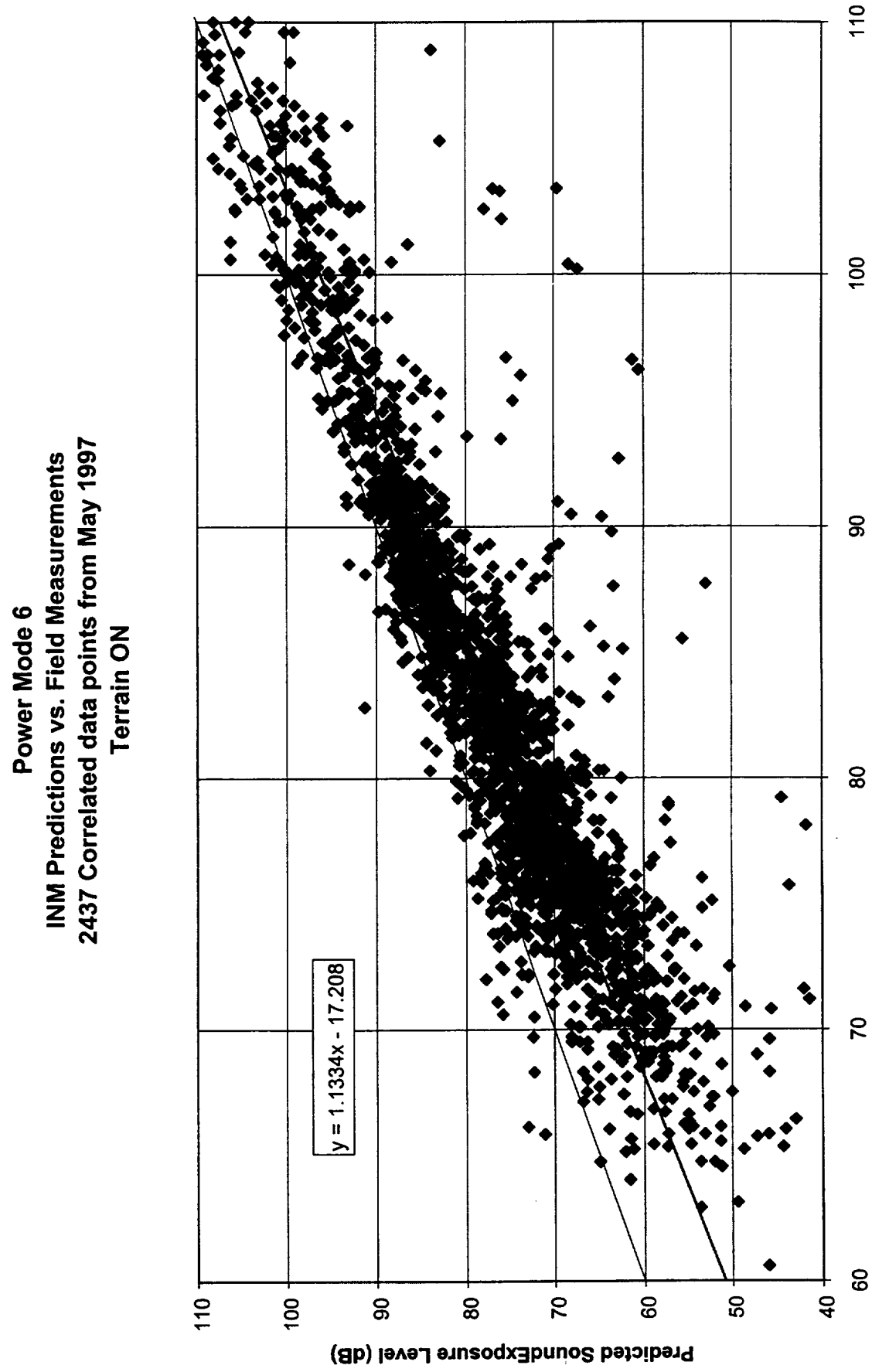

Figure 5-4. Prediction Accuracy – Power Mode 6

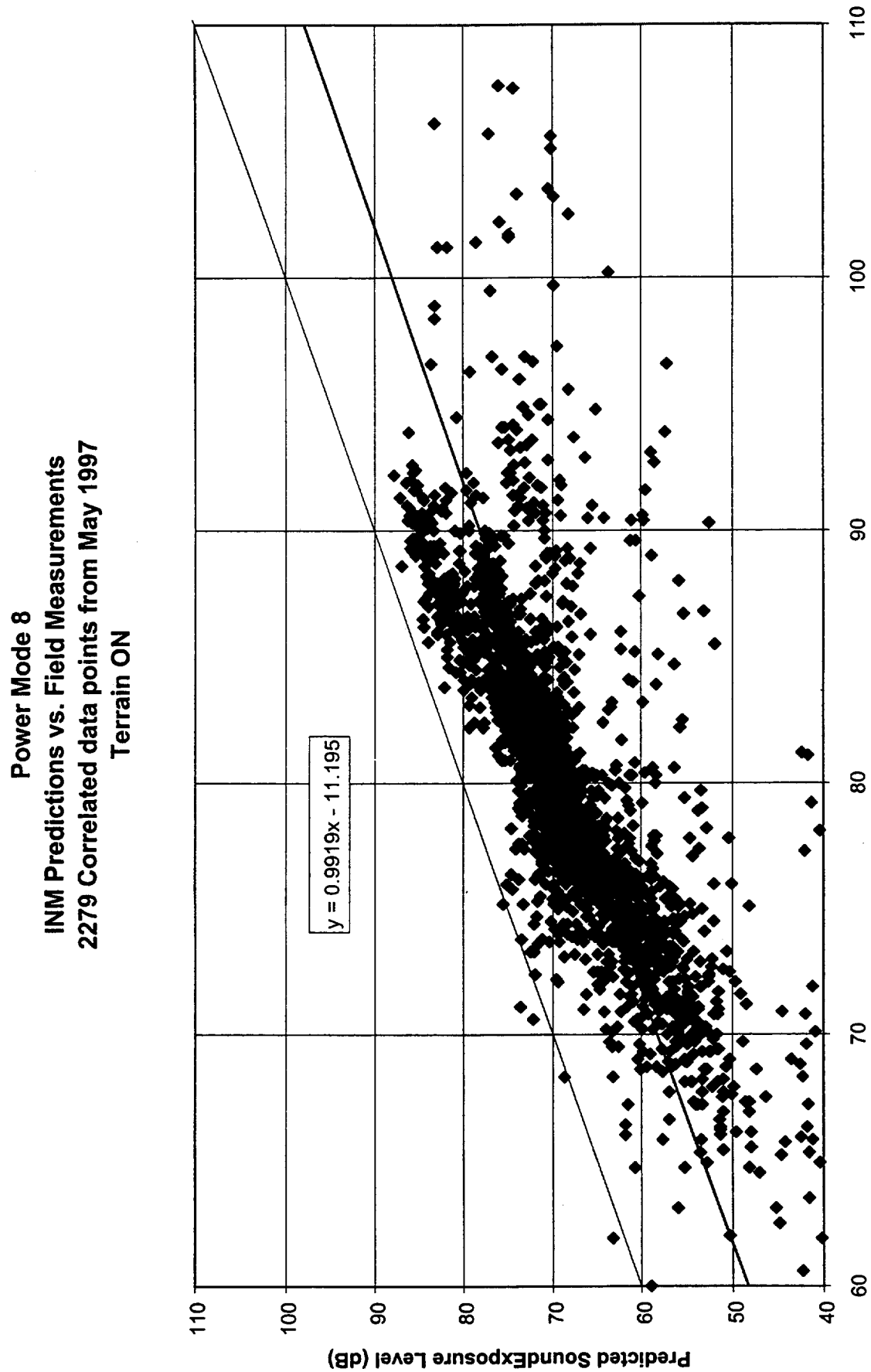

Figure 5-5. Prediction Accuracy – Power Mode 8

Within INM there is an algorithm that determines whether or not sound levels at a particular detailed grid location will be calculated. This noise-significant[20] algorithm, which the INM user is unable to control directly, did not yield a detailed grid output noise prediction for all flight tracks at all monitors. Furthermore, when comparing terrain effects, the noise-significant criteria yielded different results, and hence changed exactly at which receiver locations noise levels were predicted. Subsequent correlations yielded a different number of output analysis points, as can be seen in the No. Original Points column in Table 5-1. From a research point of view, the ability to control the noise-significant testing algorithms in INM would be most desirable. Even though the same flight tracks were analyzed for Terrain ON and Terrain OFF, this feature in INM caused the correlated events to change.

Each of the different power prediction methods shown in Table 5-1 contains a different number of flight tracks. These varied because weights and performance data were not available for detailed power predictions for all airframe/engine combinations. Chapter 4 explains in more detail the particular equipment considered for each of the power modes.

Analysis of noise correlation data (monitor measurements subtracted from INM-predicted values) was divided into three general areas:

1. Geometrical Parameters
2. Atmospheric Conditions at the Noise Source
3. Operational Statistics
4. Aircraft Maneuver Parameters

5.1 Geometrical Parameter Results

Geometrical Parameters at the point of closest approach such as aircraft altitude, elevation angle, and slant range are addressed in the analyses via the direct input of radar tracking data to INM. Parameters at the receiver stations were treated by defining receiver locations and performing a detailed grid analysis, both accounting for terrain elevations (Terrain ON) and by simplifying the predictions using a flat earth approximation (Terrain OFF).

Upon comparison of the Terrain ON and Terrain OFF Columns in Table 5-1, a mean prediction error difference on the order of one dB is apparent. Further study of the correlated data indicates that more than 60% of the analysis points were from monitors east of Runway 08/26. Table 5-3 lists the breakdown of correlated events by site, and by quadrant. Considering the gently downhill sloping terrain to the east and looking at the ground elevation levels found in Table 2-3, those correlated events in the east quadrant will drive the overall results. Initially, with the reduced ground altitudes and correspondingly increased slant ranges, it could be expected that the predicted noise levels would decrease when accounting for the true terrain. This was indeed the case, and manifests itself as more negative mean prediction error on Table 5-1 for cases with Terrain ON. There was very little change in the standard deviation between the flat earth and Terrain ON analysis.

Radar data was used to determine the relationship between the difference between modeled and measured SEL and various geometric parameters at the point of closest

Summary of Correlated Events by Site and by Quadrant

Number of Hits/Site for Power 6 Terrain OFF/ON		
Site	Terrain OFF	Terrain ON
S01	66	70
S02	32	32
S03	44	46
S04	40	40
S05	214	199
S06	163	151
S07	27	28
S08	26	26
S09	134	136
S10	29	27
S11	12	12
S12	10	9
S13	5	5
S14	8	8
S15	8	8
S16	12	10
S17	18	18
S18	19	22
S19	40	39
S20	51	50
S21	46	48
S22	44	49
S23	5	4
S24	1	2
S25	1	1
S26	0	0
W01	138	143
W02	170	172
W03	153	148
W04	148	149
W05	107	88
W06	18	19
W07	13	12
W08	15	15
W09	7	7
W10	10	10
W11	123	131
W12	83	80
Sum	2040	2014

Overall Hits/Site by Quadrant				
	Terrain OFF		Terrain ON	
	No. Events	% Events	No. Events	% Events
East	1299	63.67	1261	62.61
South	123	6.02	124	6.15
West	380	18.62	388	19.26
North	238	11.66	241	11.96
Total	2040		2014	

Table 5-3

approach of the aircraft to the measurement position. Figures 5-6, 5-7, and 5-8 show the least-squares linear relationship for [SEL(INM)-SEL(Measured)] for power mode 6 and aircraft altitude, aircraft elevation, and aircraft slant range, respectively.

In each case, the average difference between modeled and measured SEL increases with the independent parameter. By comparing the t-value for the slope parameter with the critical t-value of 2.576, it is found that this increase is statistically significant at the 99 percent level of confidence. The rate of change in the modeled-measured difference is greatest for the altitude parameter, for which it is 0.61 dB per 1,000 feet, resulting in an 8.5 dB increase over the measurement range from about 6,000 feet to 20,000 feet. For the elevation angle measurement, the rate of change of modeled-measured difference is 0.01 dB per degree, resulting in a .9 dB increase over the measurement from about 2 to 90 degrees. Finally, for the slant range measurement, the rate of change in the modeled-measurement difference is 0.18 dB per 1,000 ft, resulting in a 6-dB increase over the measurement range from about 2,000 to 38,000 ft.

Note, however, a marked decrease in elevation sensitivity over previous studies.[5] This is most likely due to significantly improved flight track – noise event correlation methodology and more accurate track and profile modeling. It does raise some concerns however, regarding long-range elevation angle effects on noise propagation, specifically lateral attenuation. Statistically, it has been shown that the correlative linear trend line does indeed conclusively indicate a reduction in prediction accuracy with increasing elevation angle.

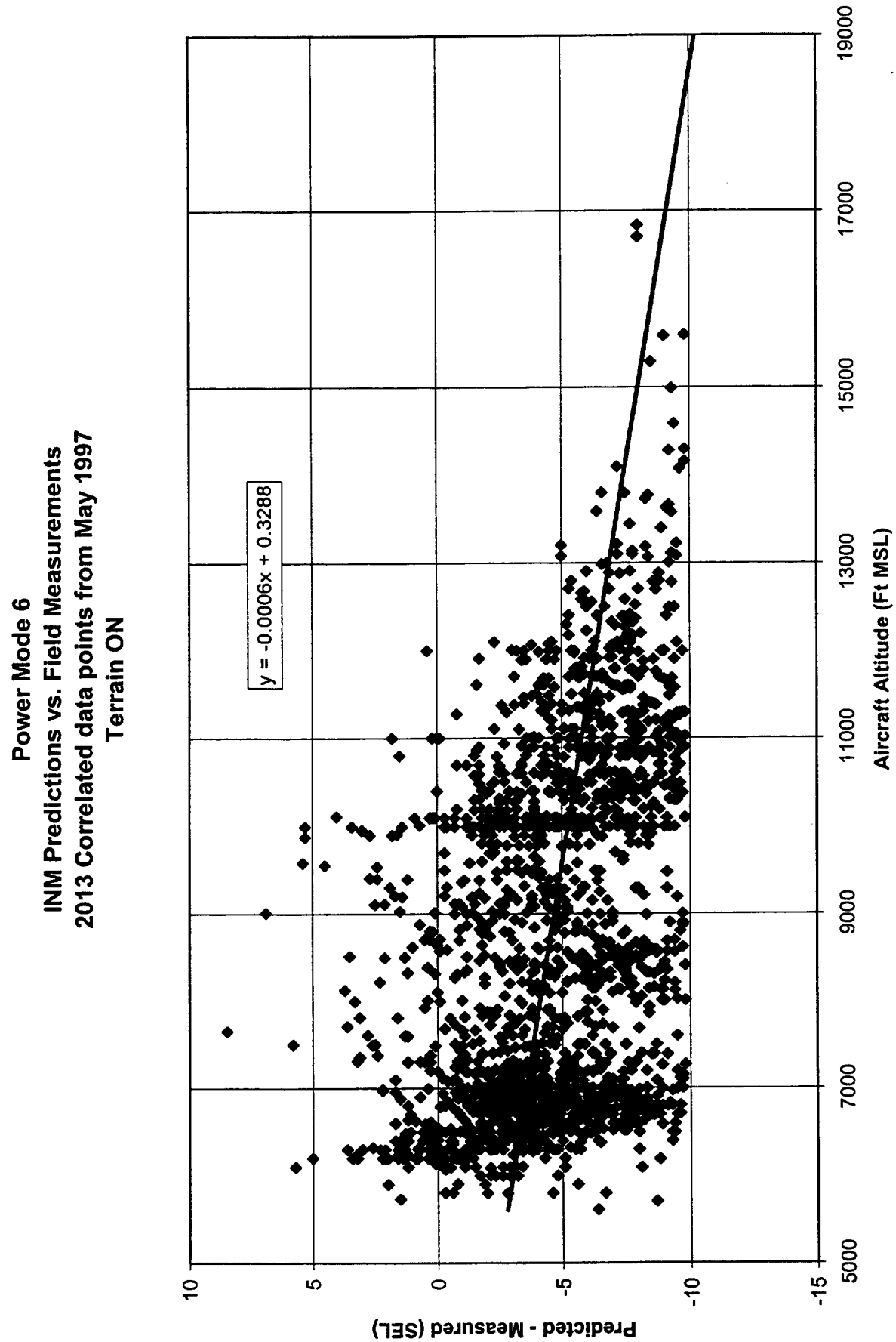

Figure 5-6. Altitude Sensitivity – Power Mode 6

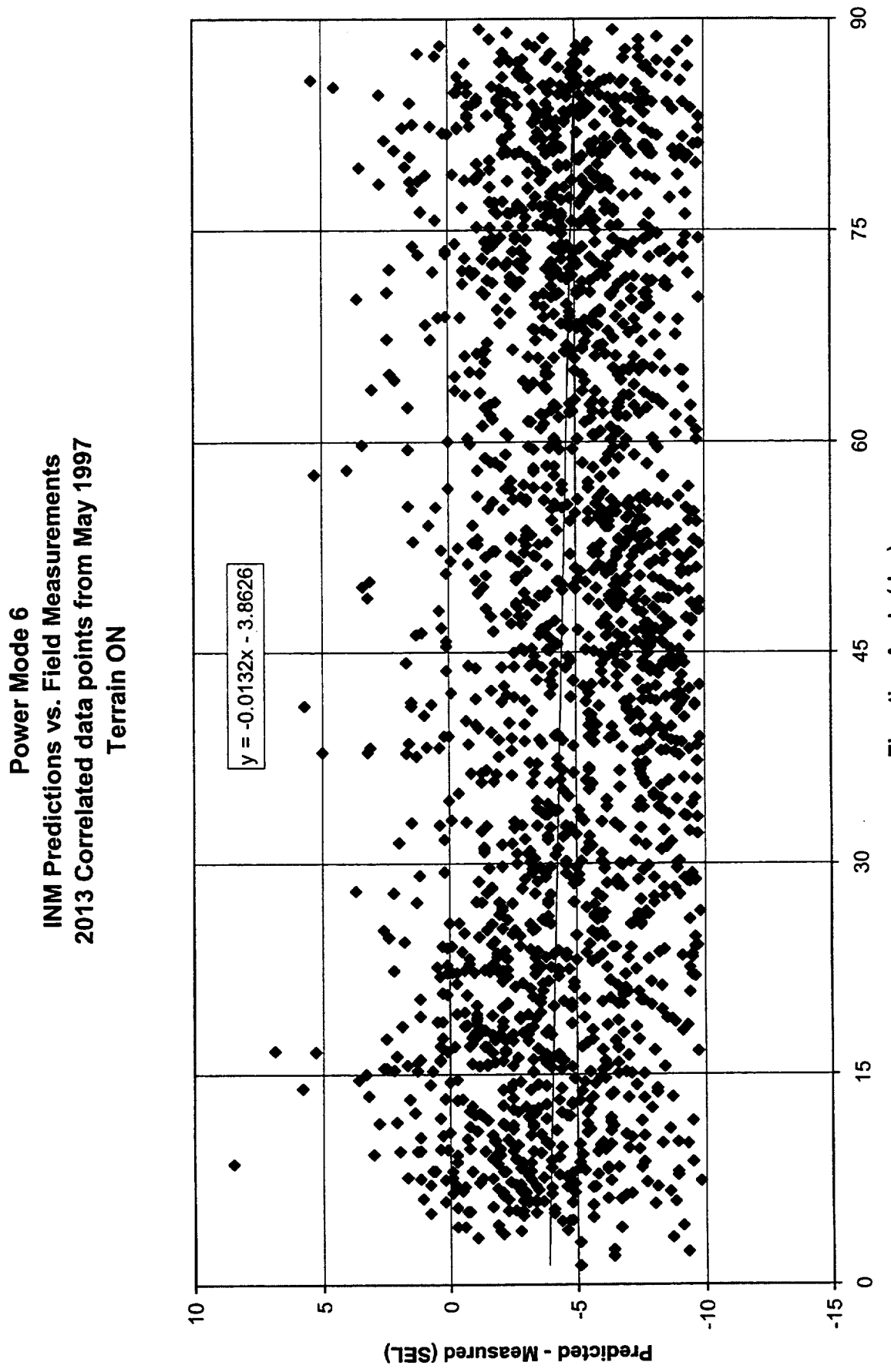

Figure 5-7. Elevation Angle Sensitivity – Power Mode 6

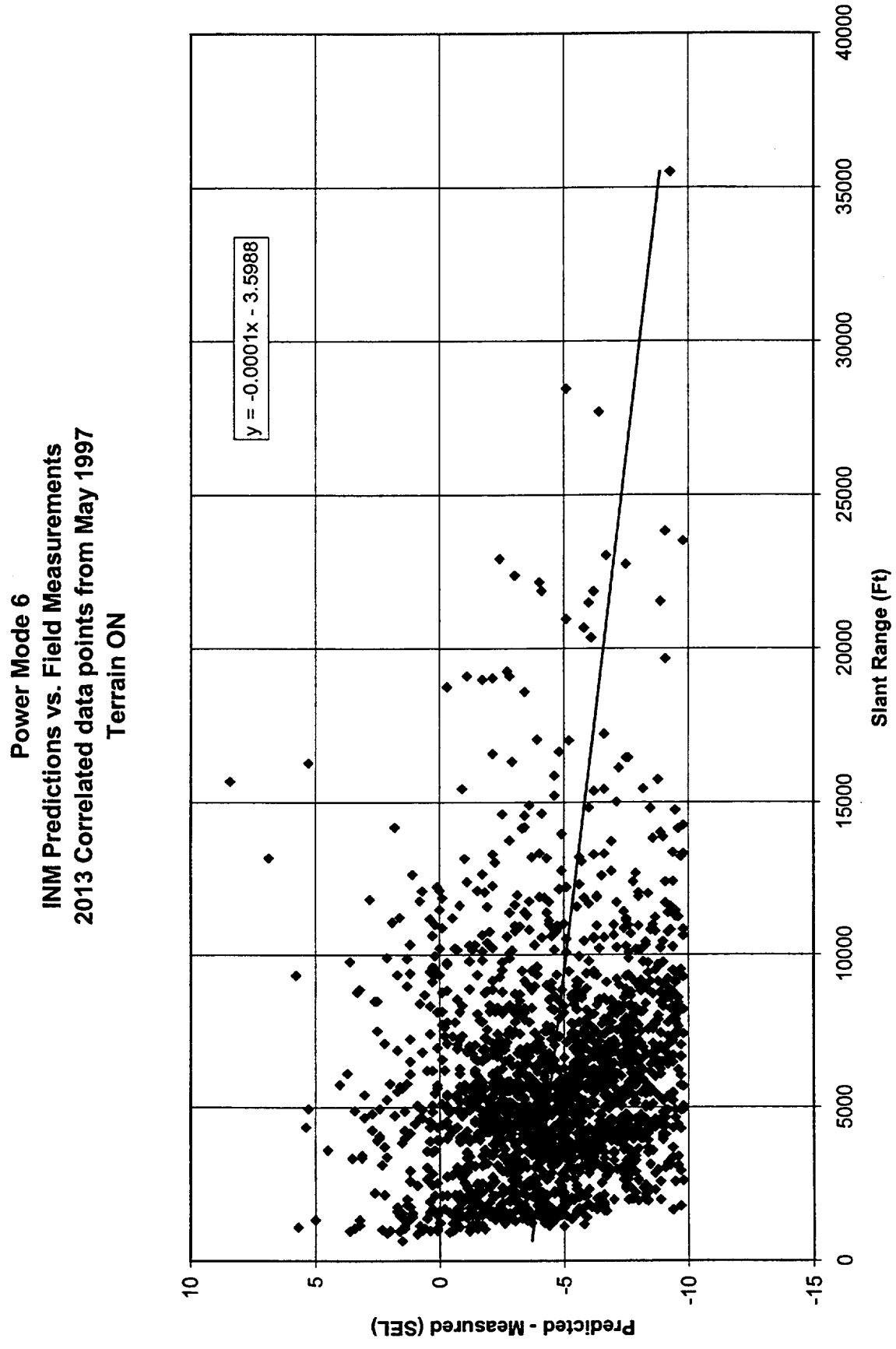

Figure 5-8. Slant Range Sensitivity – Power Mode 6

All three of these geometric parameters, obviously related, suggest three potential sources for noise prediction improvements:

1. Possible improvement to the NPD database for large distances.
2. Possible improvements should be made to the acoustical algorithms, which extrapolate beyond the 25,000-foot maximum distance contained in the INM database.
3. Additional research should be undertaken to address the lateral attenuation discrepancies for long propagation distances.

Data analysis revealed a stronger relationship between altitude and prediction accuracy (predicted SEL – measured SEL) than between slant range and prediction accuracy. This result seems to imply that the source levels are being improperly reduced as the aircraft gains altitude. Item 1 will involve extending the INM NPD database to include higher altitudes and distances. Item 2 focuses on improving the existing INM methodology for extrapolation beyond the maximum distance contained within the database. Assessment of the relative magnitude of error due to incorrect noise source levels for aircraft at high altitudes versus discrepancies due to incorrect noise source levels for aircraft at lower altitudes yet longer slant ranges should be investigated. One possible approach is to calculate new NPD data for various combinations of altitude, elevation angle and slant range, accounting for noise source impedance effects due to varying aircraft altitude. These user-defined NPD curves could then be incorporated into the INM analysis on a track-by-track and receiver-by-receiver basis. Item 3 will require a more in-depth look at those data points with low elevation angles and low slant ranges, and perhaps make use of the lateral array DAT recordings.[23]

5.2 Atmospheric Conditions

Atmospheric conditions affect both the sound generation at the source and its propagation through the atmosphere. Figures 5-9 and 5-10 show the sensitivity of Predicted – Measured SEL with airport air temperature and airport atmospheric pressure. As indicated in these figures, one would not expect a very strong sensitivity to airport flight conditions since care was taken in the data processing phase to use the best available atmospheric data for the creation of INM inputs, namely the power setting at the point of closest approach. Given the number of monitors at a great distance from the airport, it could be expected that local atmospheric conditions at the point of closest approach would be a stronger driver on the parametric analysis. This was indeed the case.

At the point of closest approach, from Figures 5-11 and 5-12 a clear trend towards noise level underprediction is apparent with decreasing outside air temperatures and decreasing atmospheric pressure. It is important to note that temperature and pressure at the aircraft (at the point of closest approach) are related to each other and to altitude. It is unclear to what degree variations in temperature or pressure from standard day conditions affect the results. Similarly, a tendency to underpredict noise levels with increasing wind speed at altitude is apparent (Figure 5-13). The upper air data used on these correlation analyses was obtained via linear interpolation of nearby twice-daily NOAA balloon launches at Stapleton Airport, and may not reflect the exact atmospheric conditions present at the point of closest approach. Nonetheless, these rough atmospheric correlations suggest that a more detailed upper air atmospheric sensitivity study should be implemented.

Within INM, flexibility for user-defined atmospheres and use of actual upper air temperature, pressure, and wind direction is not currently permitted. The atmosphere used within INM is a Non-International Standard Atmosphere. Although actual power data was input directly to INM, the non-ISA atmosphere manifests itself in the acoustic impedance algorithms.[20] This adjustment is purely a ground adjustment accounting for non sea-level level airports and their surrounding terrain. It is not a function of atmospheric conditions at the point of closest approach.

Noise source effects due to winds present at the aircraft at the point of closest approach were analyzed. Figure 5-13, a sensitivity of noise correlation, shows a slight effect of wind speed on prediction accuracy. A future analysis should include a comparison of wind direction (relative to the flight path) effects on noise source modifications and atmospheric propagation. Given the available upper air data and scope of the current study, detailed noise source generation and effects were not considered.

A statistical analysis of two atmospheric parameters revealed a definite dependence of noise correlation on both outside air temperature at the point of closest approach and on the barometric pressure at the point of closest approach. Similarly, as evidenced by the t-value of -9.00, a dependence on wind speed at altitude was also determined.

Atmospheric absorption is not treated as an independent parameter within INM. It is indirectly accounted for using the SAE ARP 866A lateral attenuation algorithms[24] in the NPD database source noise levels.

These atmospheric sensitivity studies suggest several areas for future analysis and possible improvements:

1. Evaluate the sensitivity of prediction errors to atmospheric conditions at the point of closest approach using more accurate weather data in order to develop an acoustic impedance correction, which properly accounts for conditions present at the noise source.
2. Develop alternate atmospheric models or possibly user-definable atmospheres for incorporation into INM.

Develop a methodology that accurately accounts for wind effects, both magnitude and direction, on noise source generation.

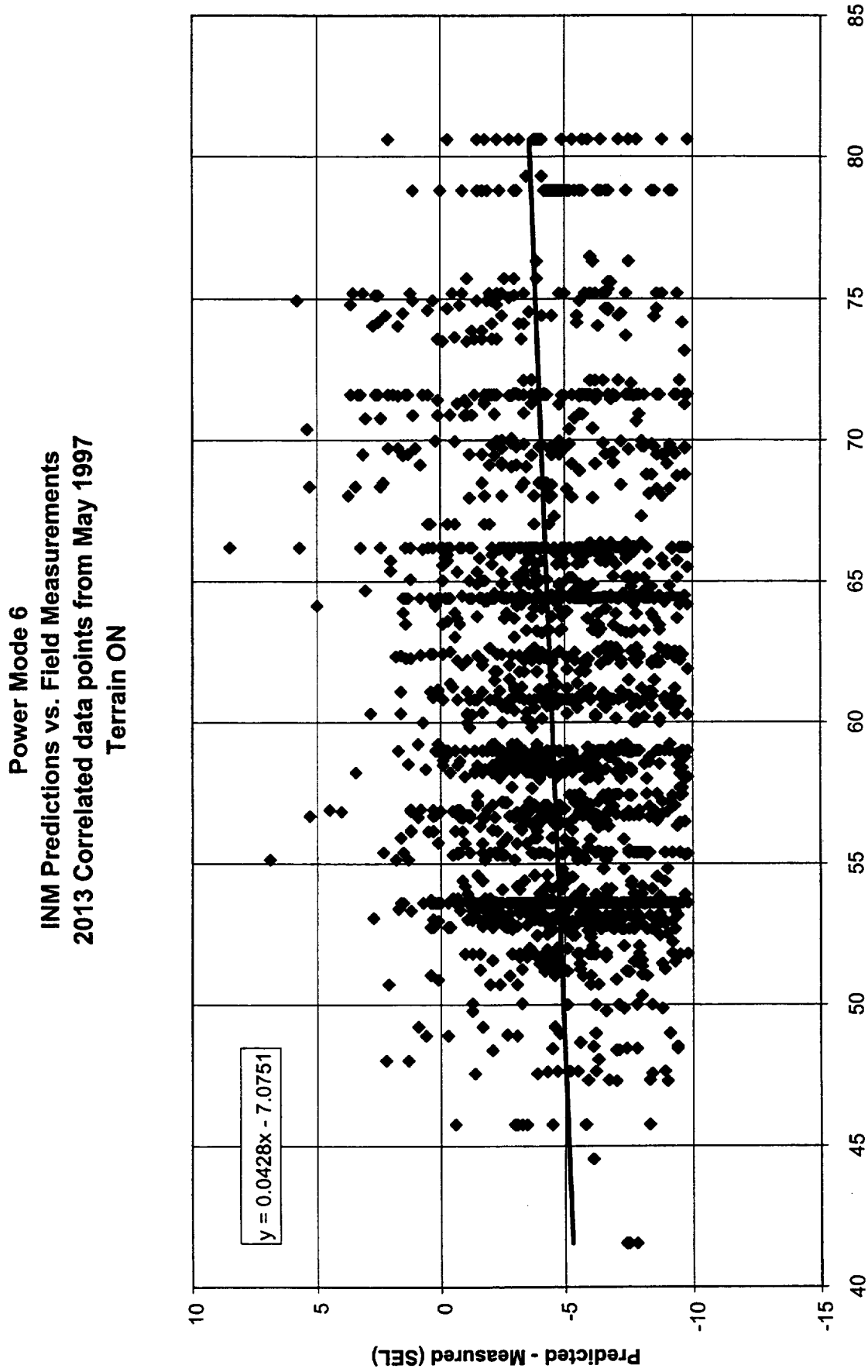

Figure 5-9. Airport Temperature Sensitivity – Power Mode 6

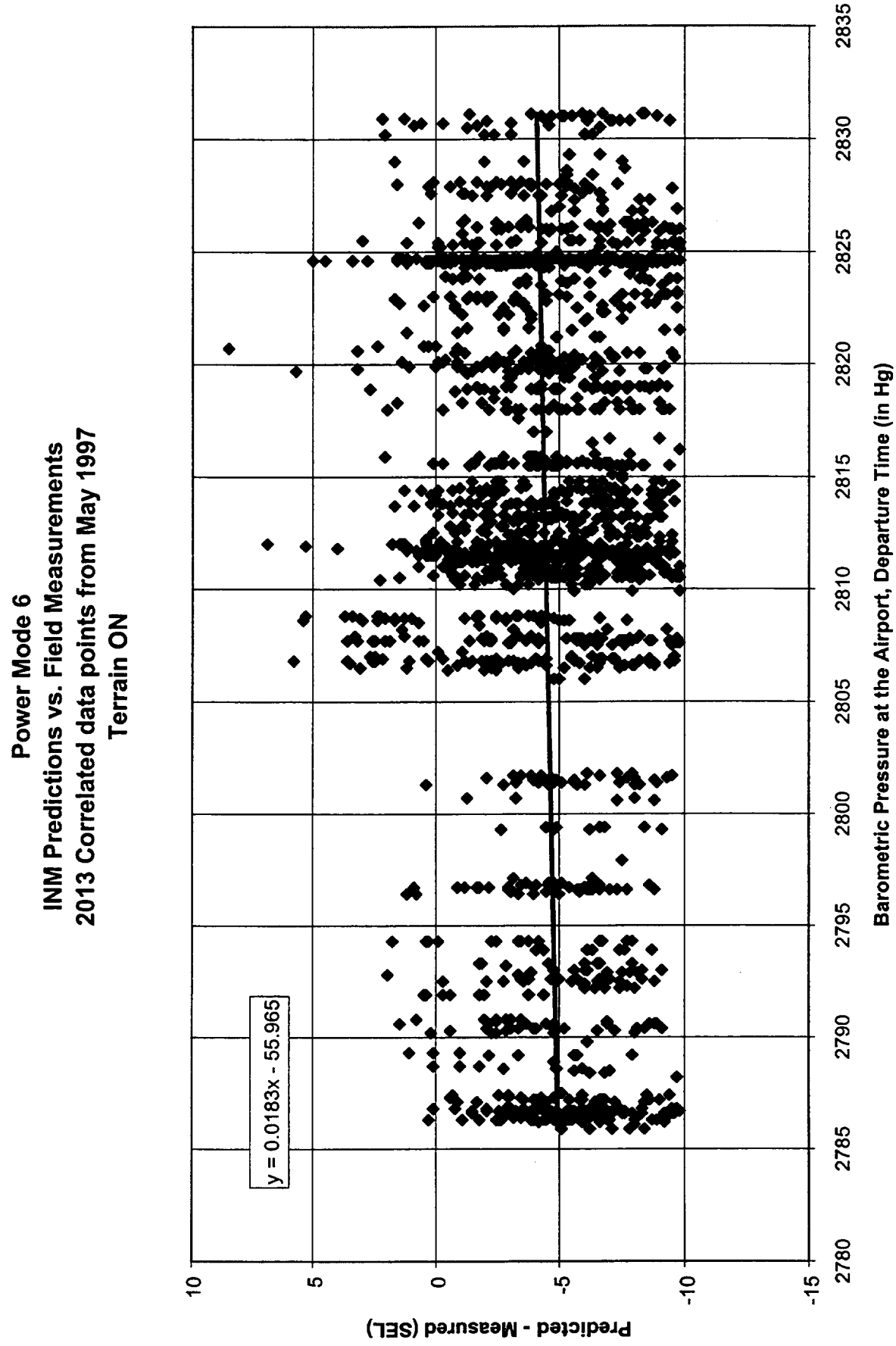

Figure 5-10. Airport Atmospheric Pressure Sensitivity – Power Mode 6

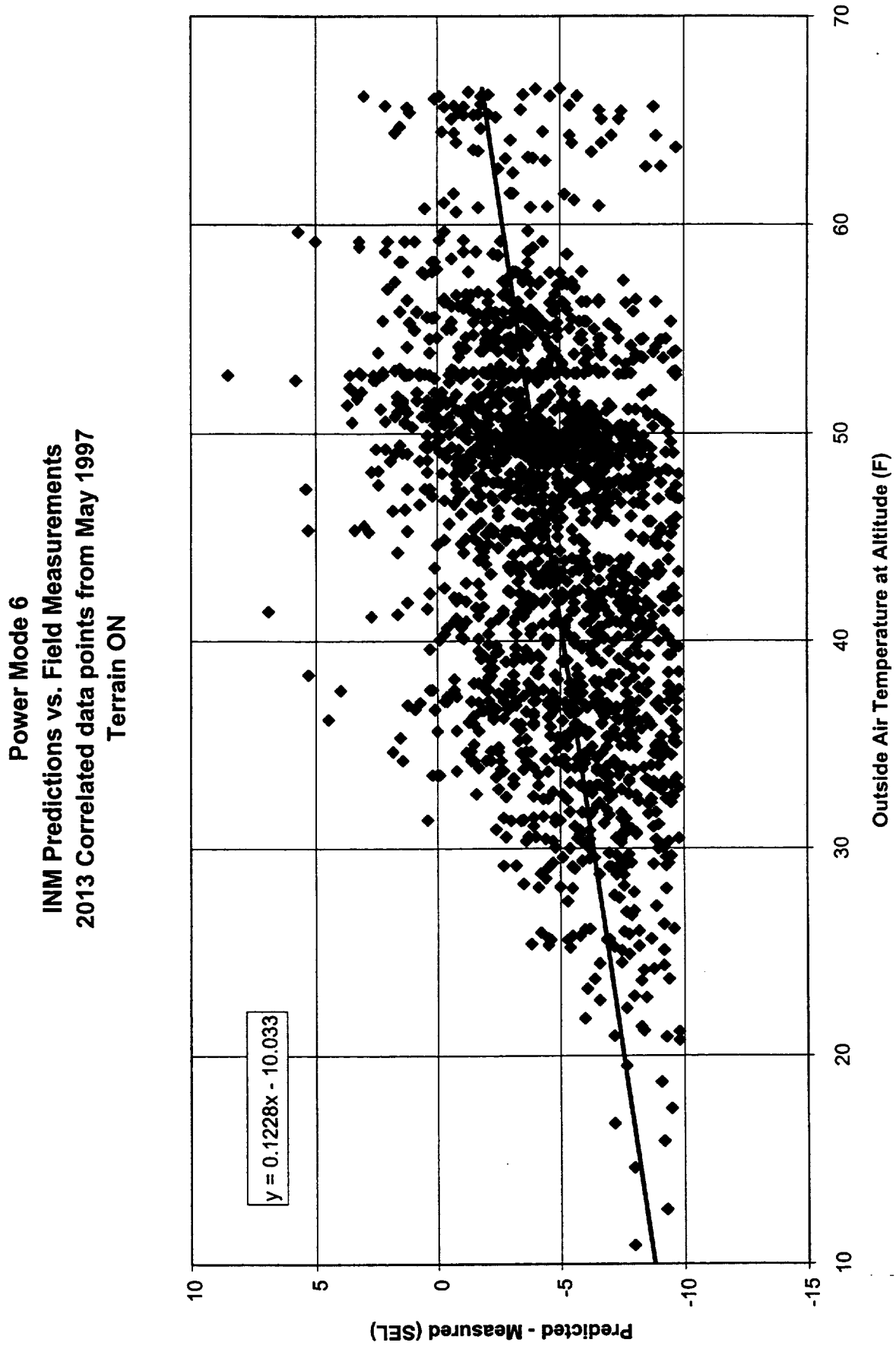

Figure 5-11. Point of Closest Approach Outside Air Temperature Sensitivity – Power Mode 6

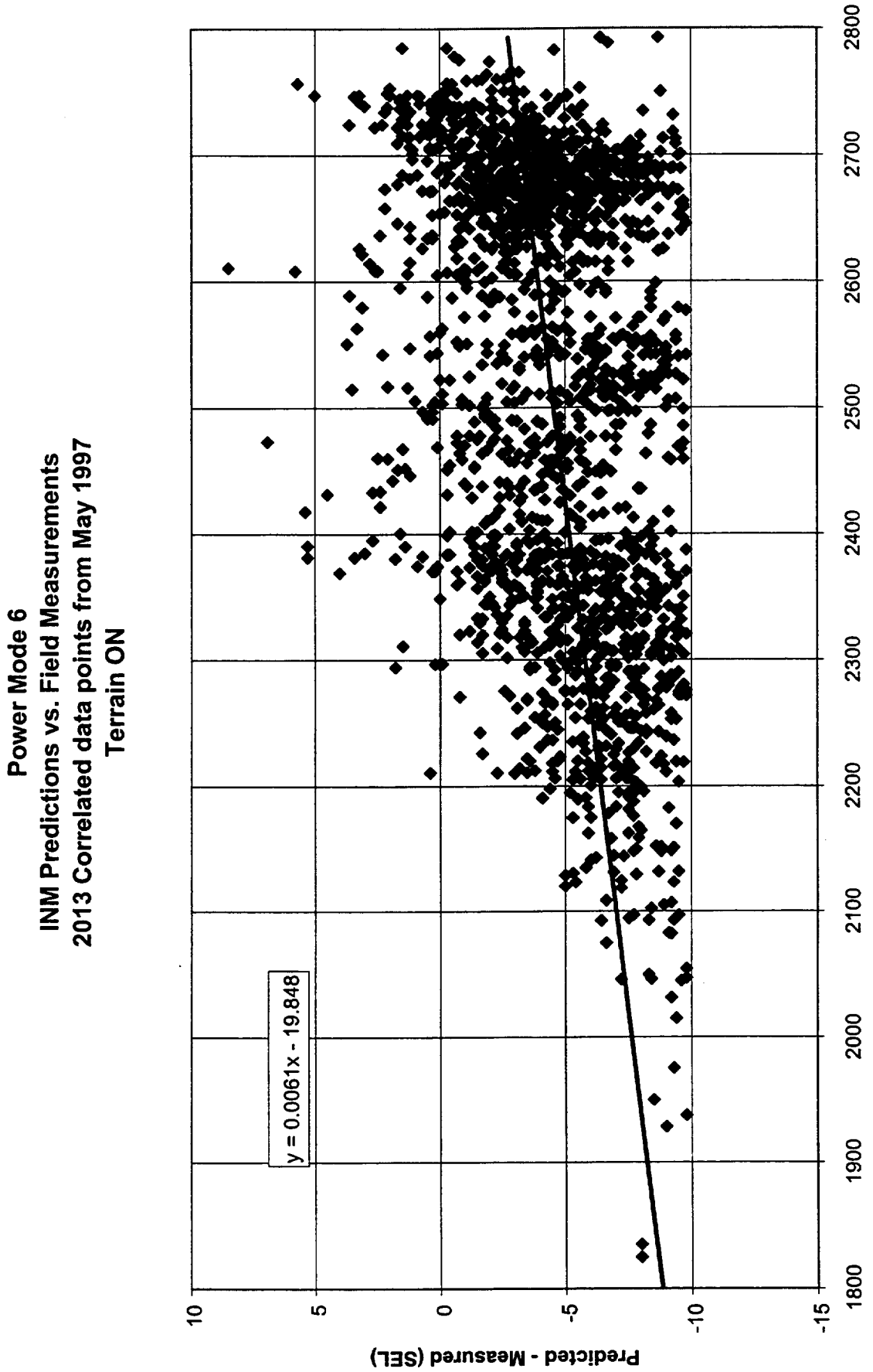

Figure 5-12. Point of Closest Approach Atmospheric Pressure Sensitivity – Power Mode 6

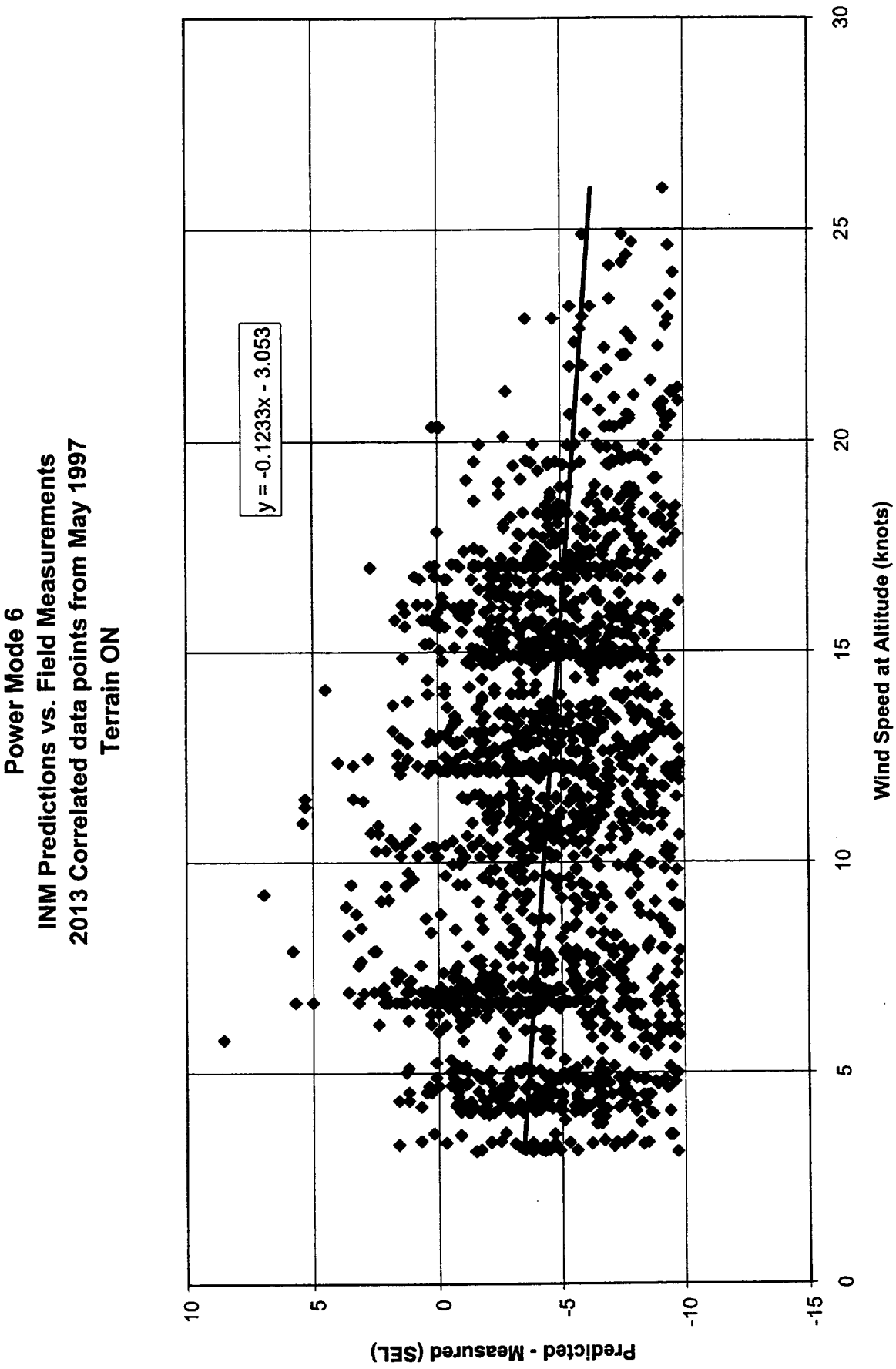

Figure 5-13. Point of Closest Approach Wind Speed (knots) Sensitivity – Power Mode 6

5.3 Operational Statistic Results

Operational parameters possibly affecting noise predictions can be placed into two categories, departure state and maneuver state. Since the majority of noise monitors were located beyond the transition to second segment climb location, operational parameters are only indirectly related to the prediction accuracy. Maneuver-state parameters are those operational parameters present at the point of closest approach (i.e., the noise source characteristics). The following parameters are within the departure-state category:

- Takeoff Gross Weight (Figure 5-14)
- Takeoff Thrust Level (Figure 5-15)
- Maximum Allowable Weight Factor (Figure 5-16)
- Derated Thrust Assumed Temperature (Figure 5-17)
- Thrust Derate Temperature Differential (Figure 5-18)

As expected, for Power Mode 6, calculation of thrust directly from the installed Fn/δ engine performance curves resulted in little sensitivity to derated thrust parameters. INM was input the profiles directly. These profiles were obtained from the radar data. Had the procedure step calculations of departure profiles been used instead, an additional source of error would have been introduced. Since one of the inputs to the procedure steps calculations is TOGW, additional prediction accuracy sensitivity with TOGW might have been introduced. Figures 5-14 through 5-18 document the various departure operational parameters. The differences between aircraft types are visible in the clustering of datapoints for charts with dimensional engine parameters on the ordinate. Normalized variables are presented below. Noise monitors focused on areas farther away from the airport, where any detailed departure operational procedures performed on and near the runways are not expected to influence noise predictions. For studies where noise within an area near the initial departure segment is of concern, this conclusion should not be drawn.

Normalized takeoff derate thrust, which put the various aircraft types on equal footing with one another used the following independent variables:

- Maximum Allowable Weight Factor (%) = $\frac{\text{MATOGW} - \text{TOGW}}{\text{TOGW}}$ (Figure 5-16)
- Derate Assumed Temperature (°F) (Figure 5-17)
- Thrust Derate Temperature Differential (Figure 5-18)

Analysis of the various departure derate parameters did not indicate whether the strong sensitivity was due to atmospheric conditions (Thrust Derate Temperature Differential [Figure 5-18]), or lower takeoff weights (Maximum Allowable Weight Margin [Figure 5-16]).

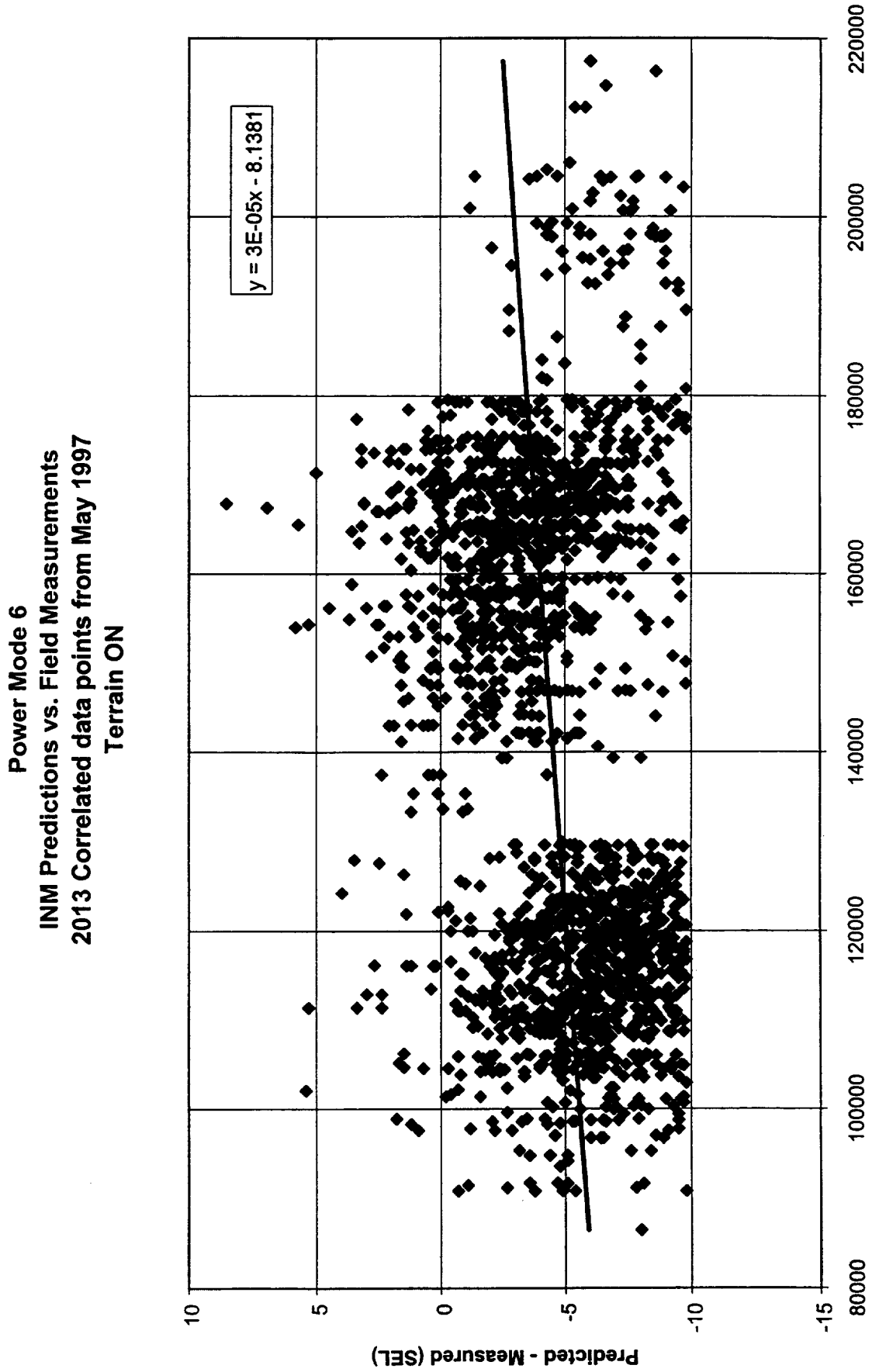

Figure 5-14. Takeoff Gross Weight Sensitivity – Power Mode 6

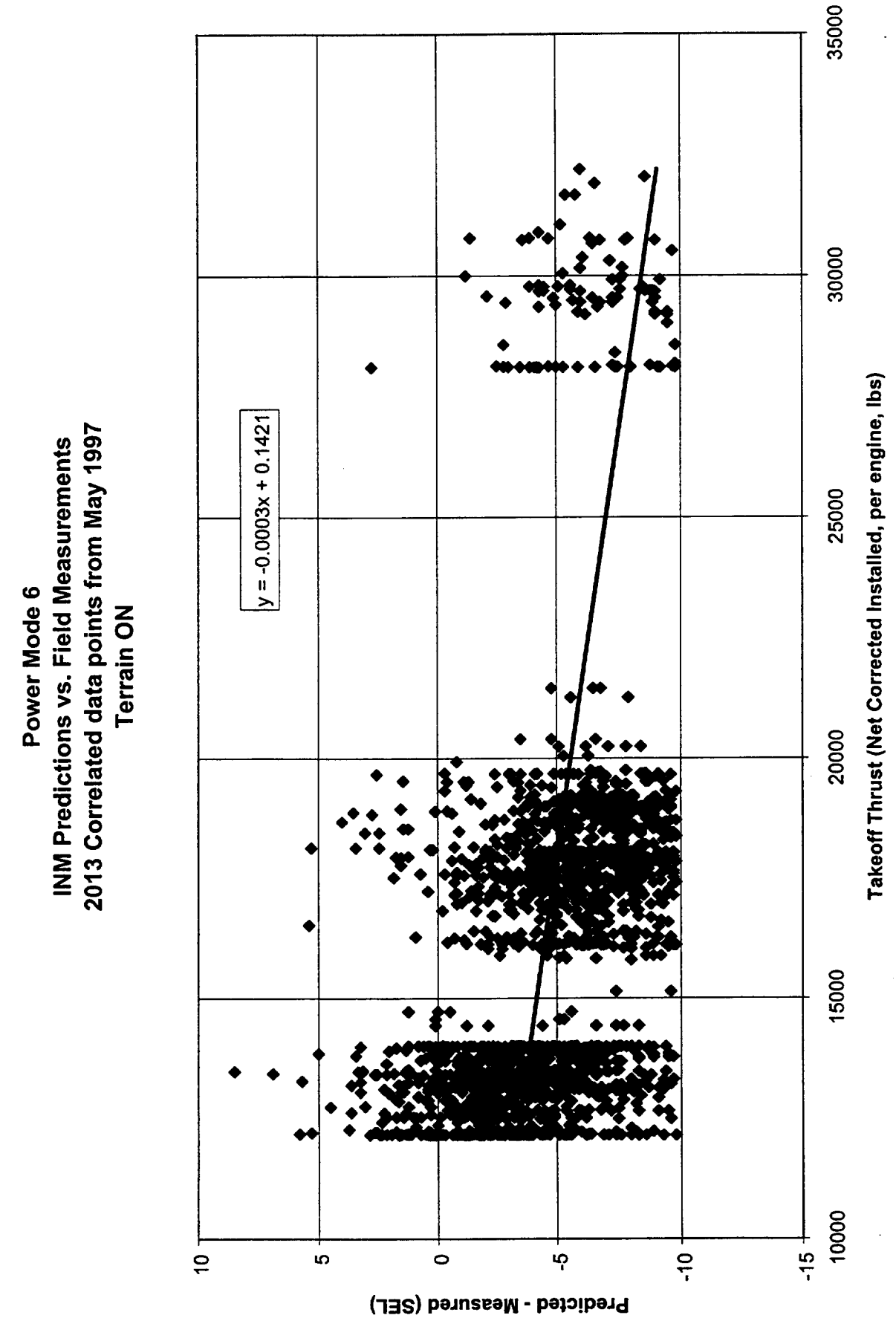

Figure 5-15. Takeoff Thrust Level (lbs) – Power Mode 6

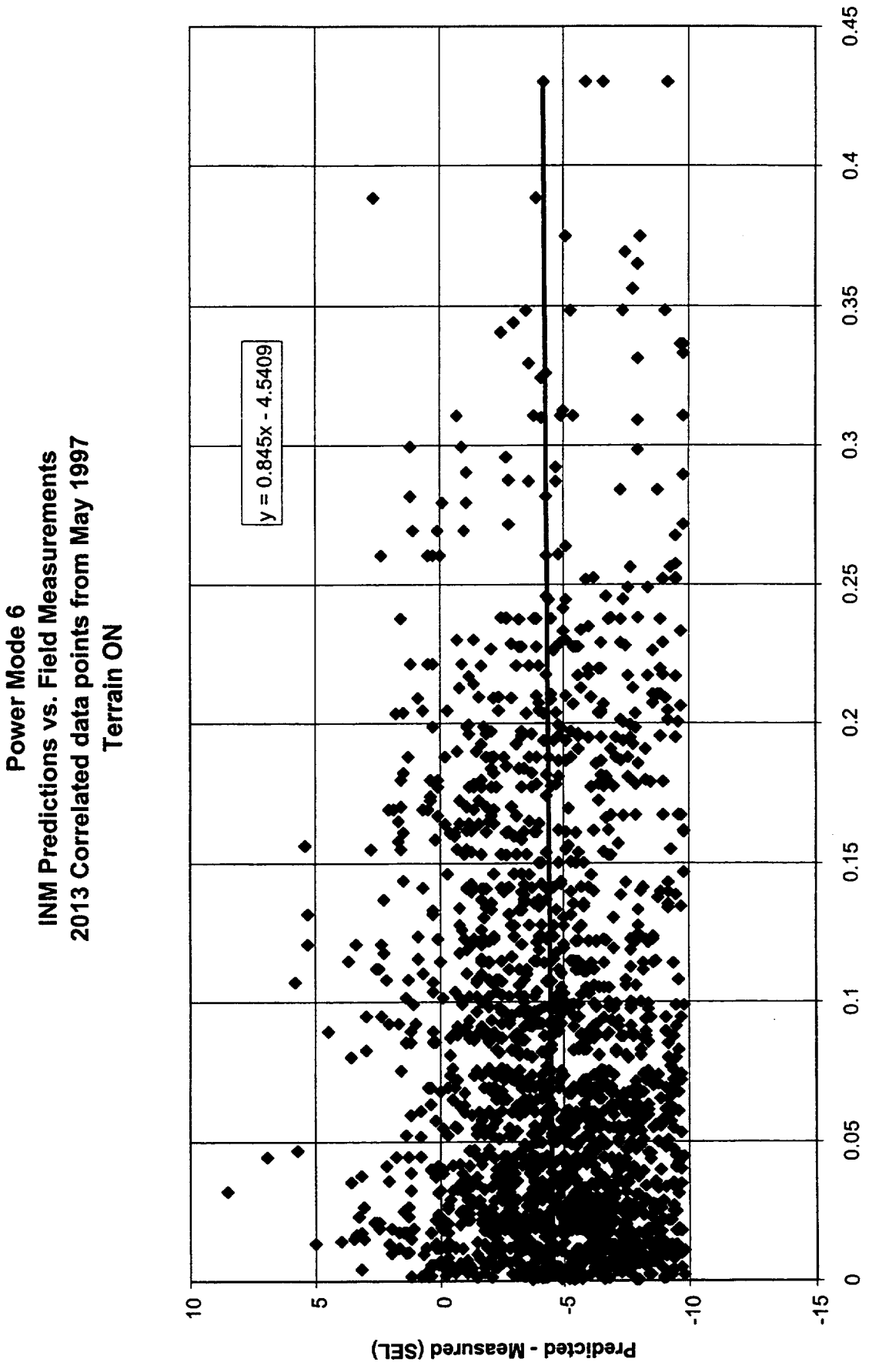

Figure 5-16. Maximum Allowable Weight Margin – Power Mode 6

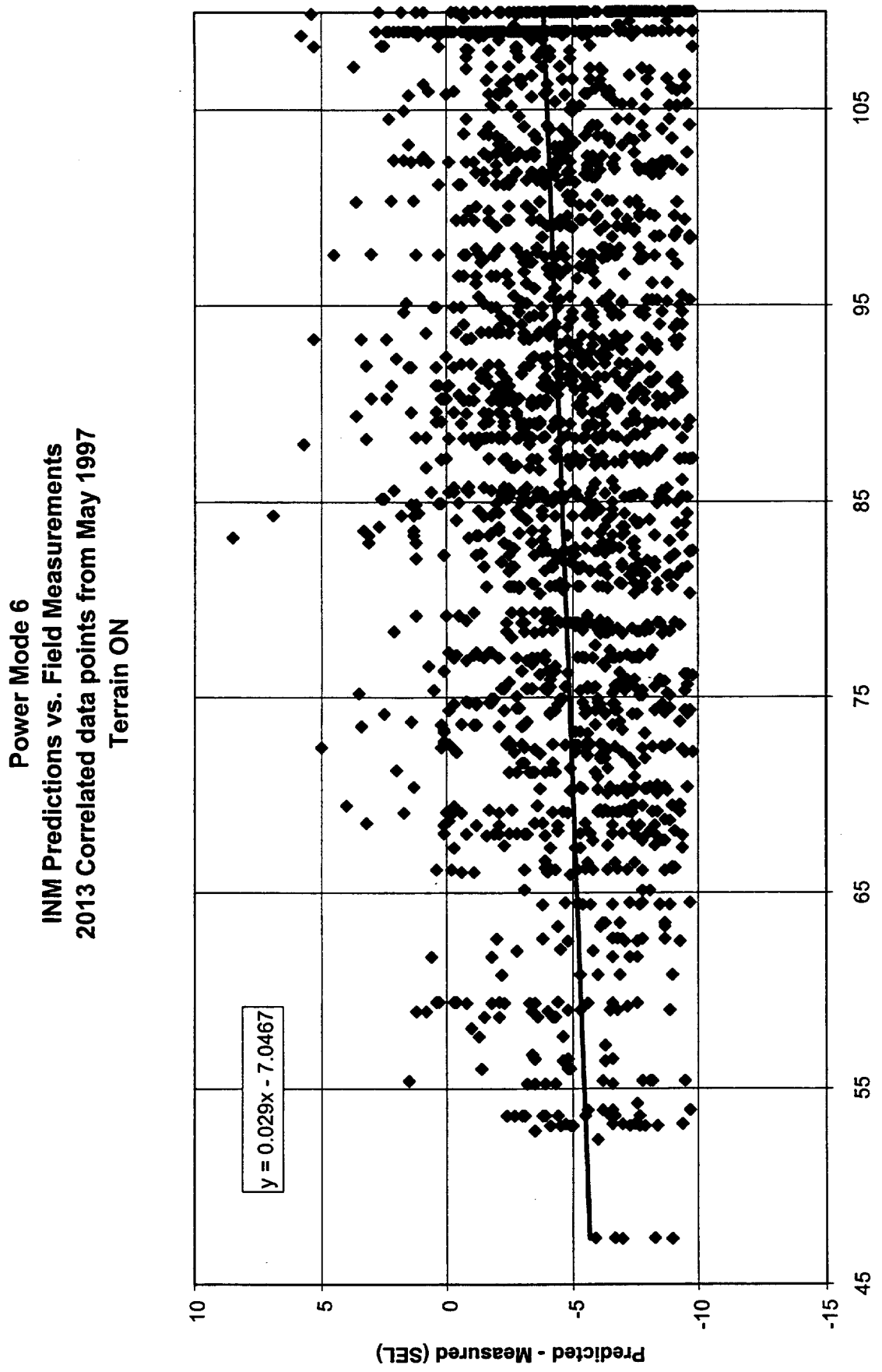

Figure 5-17. Derate Assumed Temperature – Power Mode 6

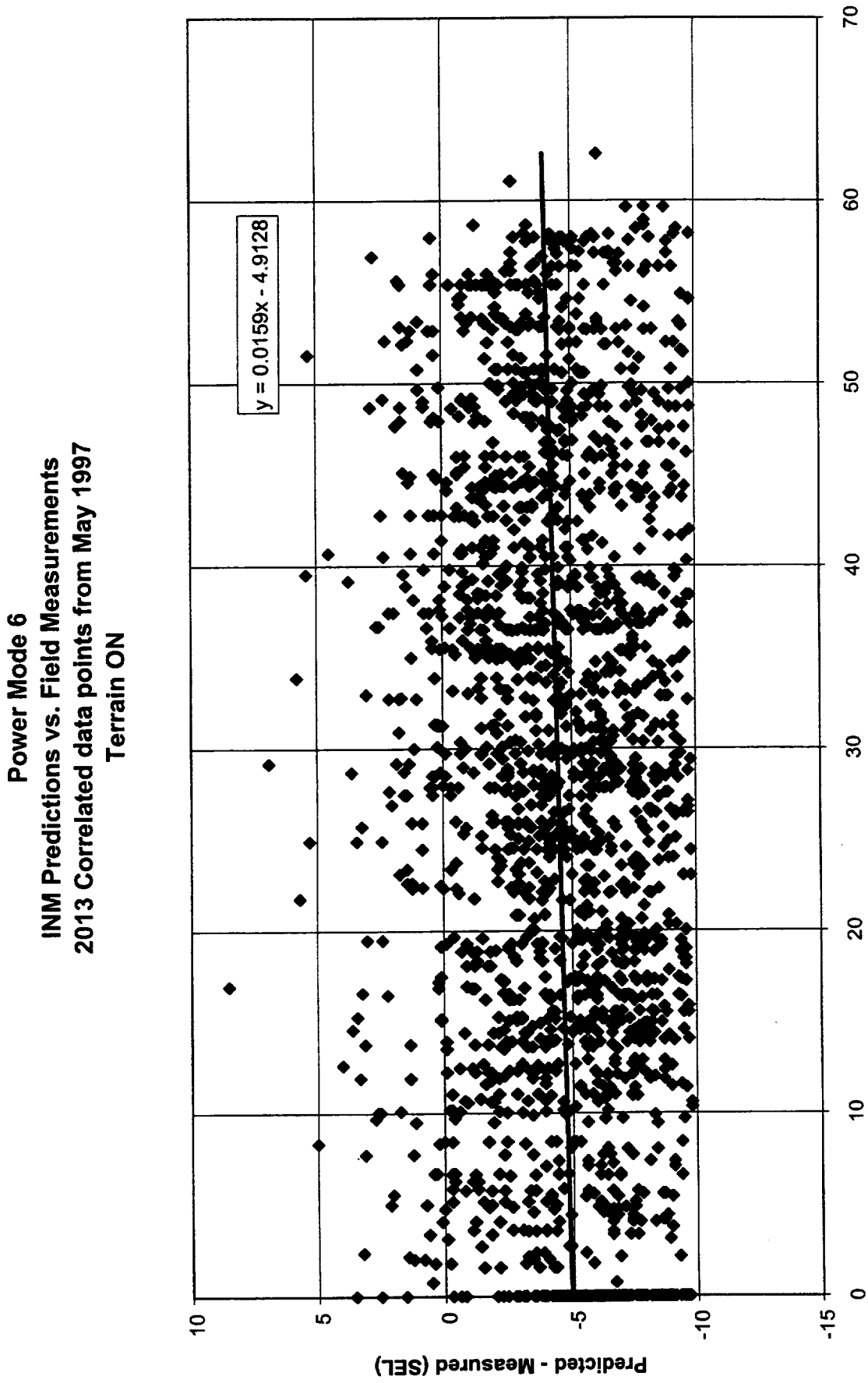

Figure 5-18. Thrust Derate Temperature Differential – Power Mode 6

Maneuver-state parameters are dictated by the aircraft motion and noise-source state at the point of closest approach, and should not be confused with departure-state parameters. These parameters include:

- Aircraft Speed (Figure 5-19)
- Compressibility Effects (Mach number) (Figure 5-20)
- Flight Thrust Level (Figure 5-21)
- Thrust Factor (Figure 5-22)

While aircraft speed and Mach number are undeniably related, there are subtle differences in correlation sensitivities due to local atmospheric conditions. These differences manifest themselves as a slightly stronger Mach dependence. This can be seen by the higher t-values for the Mach number statistical analysis (Section 5.4). This is due to compressibility and atmospheric effects, and leads to the observations that compressibility effects on noise source generation may be important. An investigation into the second segment thrust settings resulted in two independent parameters:

- Thrust (lbs) at point of closest approach (Figure 5-21)
- Thrust Factor

$$= \frac{\text{Takeoff Thrust} - \text{Closest Approach Point Thrust}}{\text{Takeoff Thrust}} \qquad \text{(Figure 5-22)}$$

Figure 5-21 shows the effects of aircraft type. Nondimensional variables presumably remove this aircraft type dependence to reveal the true thrust sensitivity shown in Figure 5-22.

Attempts to identify trends or effects relating to the initial segment derate condition once again indicated the fact that noise predictions farther away from the airport are independent of takeoff parameters. Similar to the Operational Parameters, a sensitivity to thrust factor – namely a decrease in correlation of decreasing thrust – indicates the following:

- INM's internal NPD data curves should be examined for accuracy at lower power settings and greater distances, and possibly expanded to include a large range of P-D.
- NPD data interpolation and extrapolation schemes should be examined and possibly improved.

5.4 Multiple Regression Analysis

Previous regression analyses indicated the importance of several variables falling into the following areas:

- Geometrical Parameters
- Atmospheric Conditions at the Source
- Aircraft Maneuvering Parameters

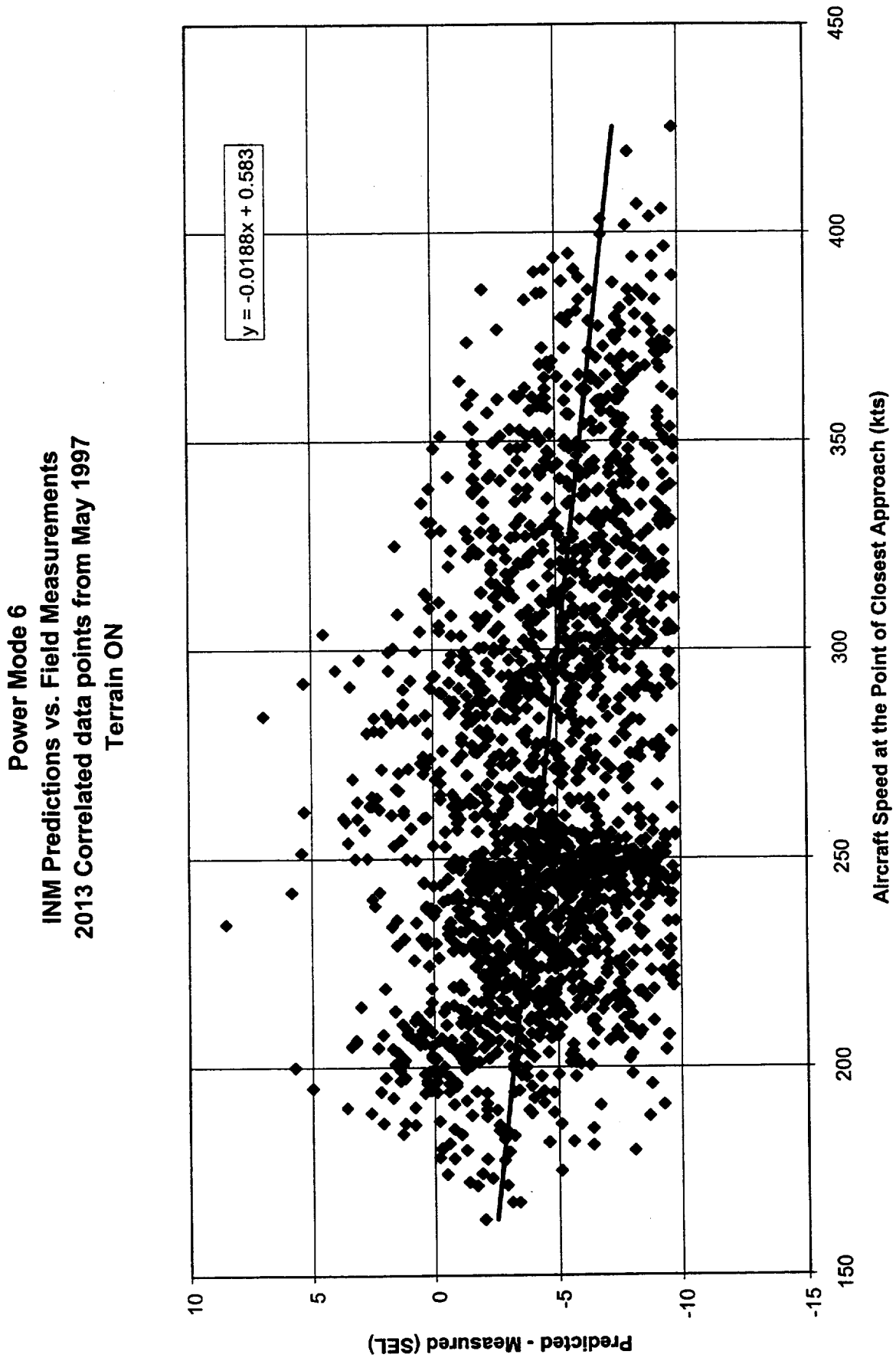

Figure 5-19. Aircraft Speed Knots at Point of Closest Approach – Power Mode 6

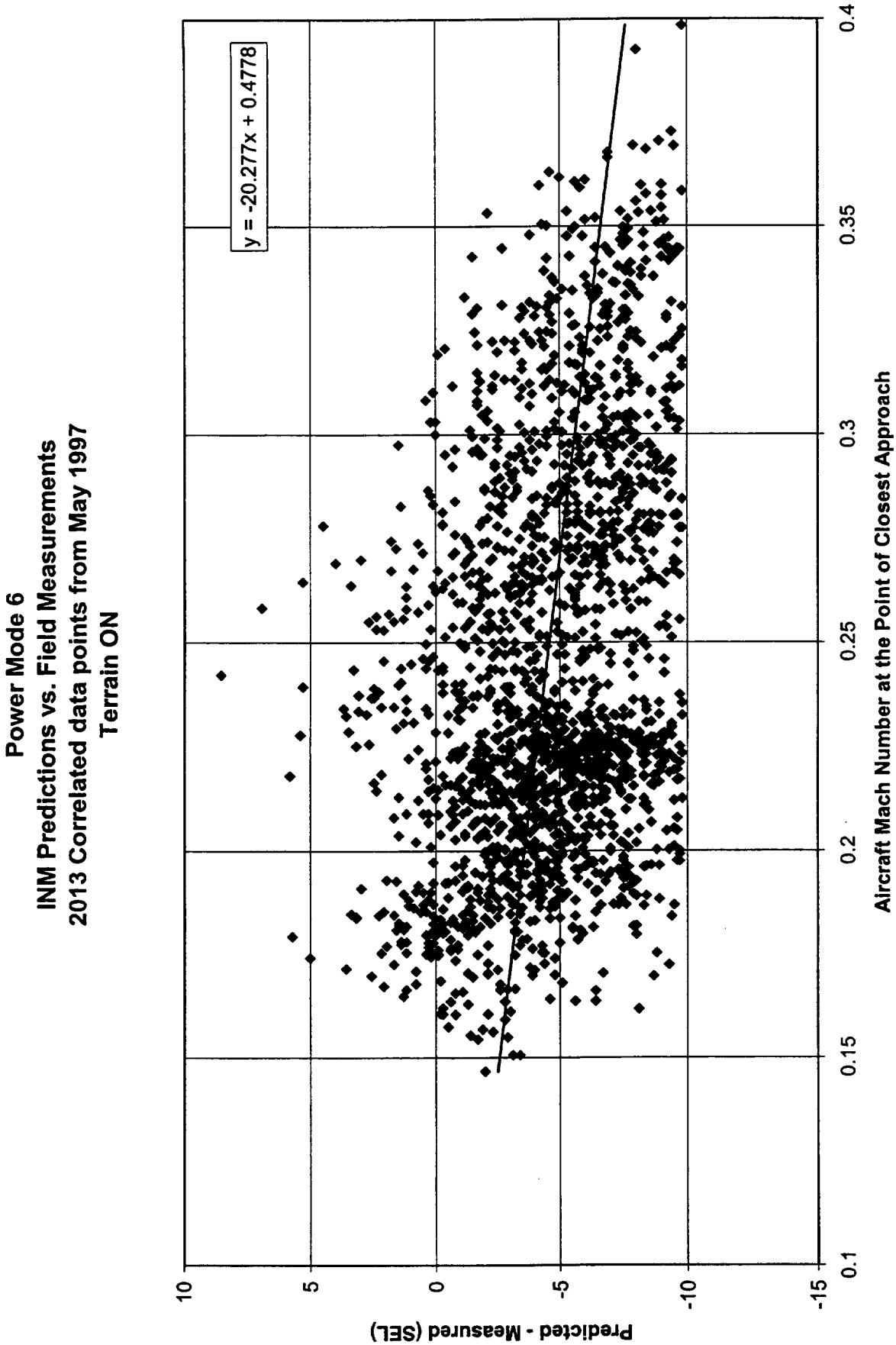

Figure 5-20. Mach Number at Point of Closest Approach – Power Mode 6

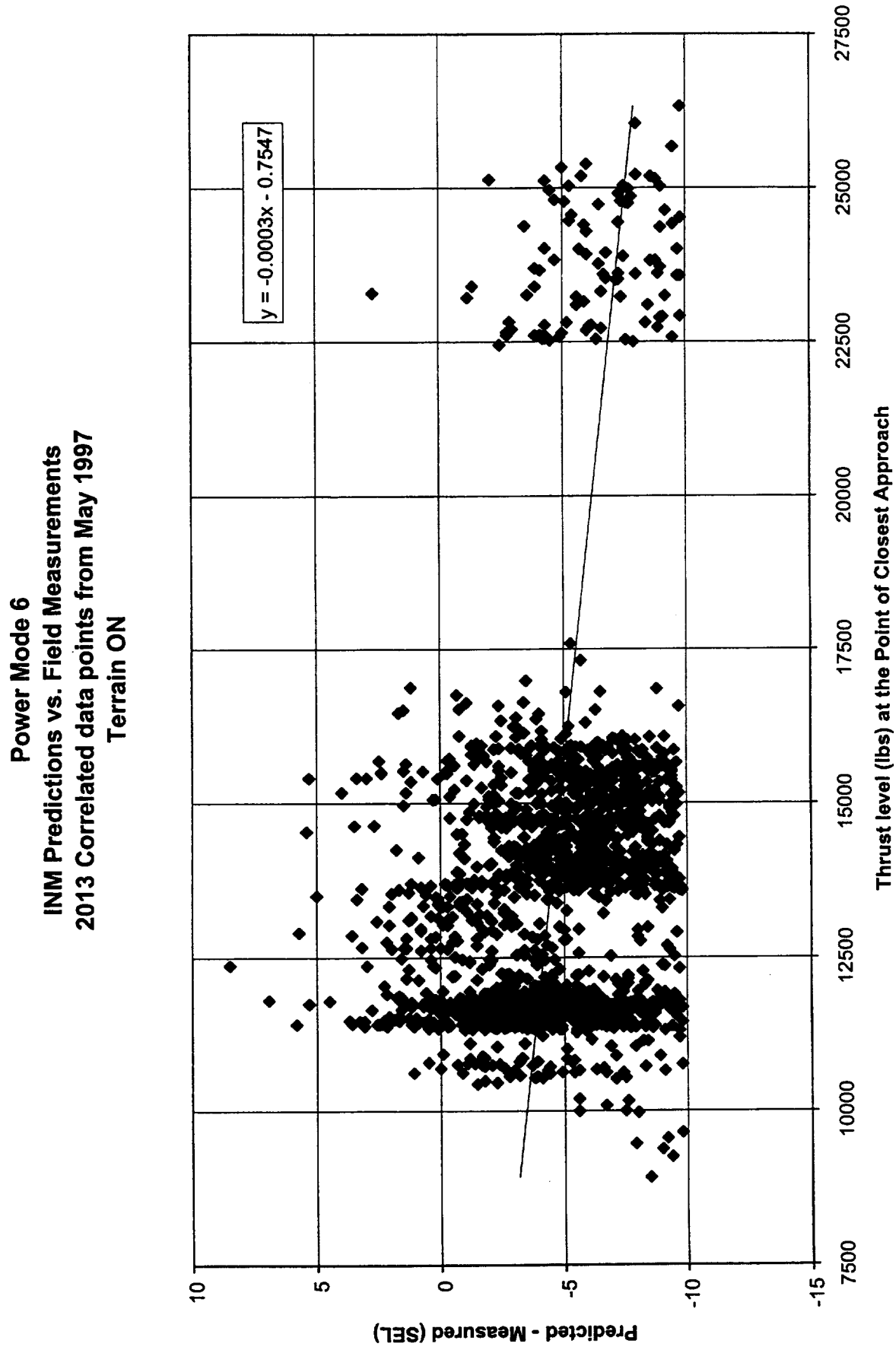

Figure 5-21. Thrust Level (lbs) at Point of Closest Approach – Power Mode 6

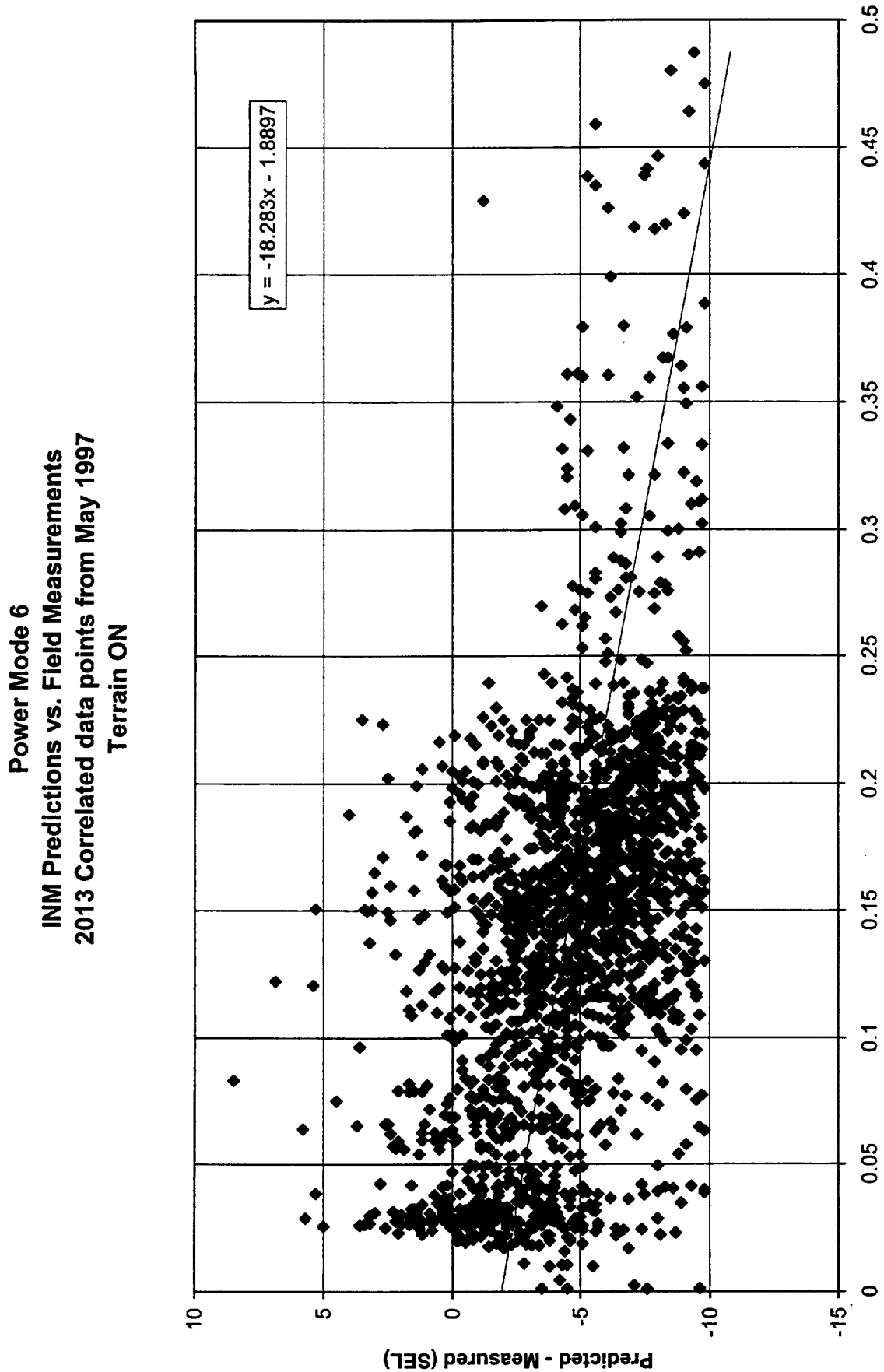

Figure 5-22. Thrust Factor at Point of Closest Approach – Power Mode 6

A multiple regression analysis counting the following three independent (although somewhat related) parameters was performed:

- Slant Range (feet) (Figure 5-22)
- Outside Air Temperature at the Point of Closest Approach (°F) (Figure 5-11)
- Aircraft Mach Number (Figure 5-20)

Only one parameter was chosen from each area. Slant range was selected as the geometrical parameter because it contains both altitude as determined by the source location, and a propagation distance, the relationship between source and receiver. Altitude only considers the source location with no regard to receiver proximity. Outside air temperature at the point of closest approach was the most reliable and predictable atmospheric parameter available from the weather balloon data. Atmospheric measurements made during the monitoring program execution indicated that ground level wind speed and direction varied considerably from one site to another. Although it is expected that this variation is less dramatic at the aircraft altitude, the researchers felt it more appropriate to use outside air temperature for the multiple regression analysis. As an aircraft maneuvering parameter, Mach number was selected. Mach includes compressibility effects due to the aircraft's actual altitude. Since engine operating conditions and hence the noise generation at the source is heavily dependent on operating state, Mach number was deemed the appropriate variable.

The results of this analysis are shown in the following regression equation:

$$\begin{aligned} \text{INM} - \text{MEAS} = {} & -9.1683 \\ & + -4.71602e-005 * \text{Slant Range} \\ & + 0.118217 * \text{Outside Air Temperature at Altitude} \\ & - 2.38207 * \text{Mach Number} \end{aligned}$$

Table 5-4 indicates, via interpretation of the t-value column, that of these three independent variables the most critical is Outside Air Temperature (OAT) at altitude. The Mach number parameter indirectly contains some OAT information in the form of the speed of sound. Also built into this parameter is the aircraft velocity. In this case, since Mach number is not driving the regression equation, the variation of speed of sound (with altitude manifesting itself in the aircraft's Mach number) appears to be less important than the outside air temperature at altitude. However, one can consider outside air temperature as a surrogate for altitude. The slant range parameter contains an altitude component. The magnitude of altitude at a particular point of closest approach is often diluted by large sideline distances. It would appear from the relative t-value predictions that it is the height of the aircraft, not the propagation distance, which is driving the results.

INM is based on NPD curves, which implicitly assume that sound power is independent of altitude. The observed effect may be due to altitude effects on engine noise generation, or possibly the effect of acoustic impedance at higher altitude. The NPD curves also assume air absorption for standard conditions. Air absorption for vertical propagation can vary significantly due to temperature/humidity stratifications and density gradients. These two factors should be investigated.

6 Conclusions and Recommendations

A noise study was conducted based on four consecutive weeks of noise measurements made during May and June 1997 at Denver International Airport in Colorado. Cooperation of United and Delta Airlines and the DIA Noise Abatement Office resulted in the creation of a database containing detailed information such as TOGW, thrust setting, and actual airframe/engine equipment use historical data. Analysis of numerous independent variables and correlation between noise measurements and INM predictions was completed using five power profile prediction techniques.

Detailed analysis of departure flight tracks using INM, and comparison with correlated measured noise data indicates the following:

- INM underpredicts the SEL for DIA departures by 4 to 10 dB depending on the Profile Power Prediction Method with a standard deviation of approximately 3.3 dB.
- Power Prediction based on actual detailed Installed Engine Fn/δ tables produces the most accurate results (Table 5-1).
- Primary independent variables affecting the correlation can be summarized as Geometric, Atmospheric, and Maneuver Parameters.
- Multiple regression analysis indicates that the strongest dependence is on Atmospheric Conditions at Altitude (Section 5.5).

Based on the results presented in Chapter 5 and an understanding of INM, the following recommendations for future analyses and possible prediction method improvements are made:

- From certification data, update the noise source data levels contained in the N-P-D database with improved lateral attenuation algorithms and for greater distances in order to avoid data extrapolations within INM.
- Atmospheric effects on both noise source generation and long-range propagation should be investigated in more detail, with a focus on the current atmospheric models in INM, and with the intent to develop methodologies for treating acoustic impedance on the noise source at the point of closest approach.
- Investigate the feasibility of generating improved thrust and performance prediction methods for use within INM, which more closely model the actual installed engine performance, considering such variables as local airport conditions, Mach number, and TOGW.

References

1. *Integrated Noise Model (INM) Version 5.0 User's Guide*, FAA-AEE-95-01, August 1995.
2. *Integrated Noise Model (INM) Version 4.11 User's Guide - Supplement*, DOT/FAA/EE/93-03, December 1993.
3. *Procedure for the Calculation of Airplane Noise in the Vicinity of Airports*, SAE AIR 1845, March 1986
4. Moulton, C. L., *Air Force Procedure for Predicting Aircraft Noise Around Airbases: Noise Exposure Model (NOISEMAP) User's Manual*, Wyle Research Report WR 89-20, also AAMRL-TR-90-011, February 1990
5. Page, J., Plotkin, K., Carey, J. and Bradley, K., *Validation of Aircraft Noise Models at Lower Levels of Exposure*, NASA Contractor Report 198315, February 1996.
6. Stusnick, E., Plotkin, K. J., Page, J. A., and Bradley, K. *Validation of Aircraft Noise Prediction Models at Low Levels of Exposure, Phase 2 Test Plan*, Wyle Research Technical Note TN 97-1, January 1997
7. *National Airspace System Automated Radar Terminal System III (ARTSIII)*, Department of Transportation, FAA Aeronautical Center N-9, March 1973.
8. United Airlines B727-222A Flight Manual, Takeoff Section.
9. United Airlines B737-200 (ADV-17, ADV-9, BASIC-7) Flight Manual, Takeoff Section.
10. United Airlines B737-322/522 Flight Manual, Takeoff Section.
11. United Airlines A319-131/A320-232 Flight Manual, Takeoff Section.
12. United Airlines DC-10-10/DC-10-30/DC-10-30F Flight Manual, Takeoff Section.
13. United Airlines B757-222/-222ER Flight Manual, Takeoff Section.
14. United Airlines B767-222/-222ER Flight Manual Takeoff Section.
15. United Airlines B777-222/222B Flight Manual, Takeoff fSection.
16. United Airlines, *Standard Performance Reference Handbook*, DENTK-Chet Collett, Coordinator-Airplane Performance Programs, 12 January 1996.
17. *Air Traffic Training Publication N-9*, NAS Operational Equipment, ARTS III, Air Traffic Branch, Federal Aviation Administration Academy, March 1973.
18. *ARTS III, Collection and Editing System (ACES) for Noise Monitoring,Technical Reference and User's Manual*, Dimensions International, Inc. February 1994.
19. *Procedure for the Calculation of Airplane Noise in the Vicinity of Airports*, SAE AIR 1845, March 1986.
20. Fleming, G.G., Olmstead J.R., D'Aprile, J.R., Gerbi, P.J, Gulding, J.M., and Plante, J.A.. *Integrated Noise Model (INM) Version 5.1 Technical Manual*, Report No. FAA-AEE-97-04, December 1997
21. Clarke, J.P., and Fleming G., e-mail communication to Page, J., Guilding, J., and Shepherd, K., Thrust Translation, 13 November 1997.
22. Bishop, D.E., and Mills, J.F., *Update of Aircraft Profile Data for the Integrated Noise Model Computer Program*, Report No. FAA-EE-91-02, March 1992
23. Plotkin, K.J., Hobbs, C.M., Stusnick, E., *Validation of Aircraft Noise Prediction Models at Low Levels of Exposure,* Volume 2: Lateral Array Studies, Wyle Research Report WR 98-11, March 1999
24. *Standard Values of Atmospheric Absorption as a Function of Temperature and Humidity*, SAE ARP 866A, 15 March 1975.

REPORT DOCUMENTATION PAGE

Form Approved
OMB No. 0704-0188

1. AGENCY USE ONLY (*Leave blank*)	2. REPORT DATE	3. REPORT TYPE AND DATES COVERED
	April 2000	Contractor Report

4. TITLE AND SUBTITLE
Validation of Aircraft Noise Prediction Models at Low Levels of Exposure

5. FUNDING NUMBERS
C NAS1-20103, Task 22

WU 538-03-15-01

6. AUTHOR(S)
Juliet A. Page, Christopher M. Hobbs, Kenneth J. Plotkin, and
Eric Stusnick

7. PERFORMING ORGANIZATION NAME(S) AND ADDRESS(ES)
The Boeing Company
2401 East Wardlow Road
Long Beach, CA 90807-4418

Wyle Laboratories (Subcontractor)
2001 Jefferson Davis Highway
Arlington, VA 22202-3604

8. PERFORMING ORGANIZATION REPORT NUMBER

9. SPONSORING/MONITORING AGENCY NAME(S) AND ADDRESS(ES)
National Aeronautics and Space Administration
Langley Research Center
Hampton, VA 23681-2199

10. SPONSORING/MONITORING AGENCY REPORT NUMBER
NASA/CR-2000-210112

11. SUPPLEMENTARY NOTES
Langley Technical Monitor: Kevin P. Shepherd

12a. DISTRIBUTION/AVAILABILITY STATEMENT
Unclassified-Unlimited
Subject Category 71 Distribution: Nonstandard
Availability: NASA CASI (301) 621-0390

12b. DISTRIBUTION CODE

13. ABSTRACT (*Maximum 200 words*)
Aircraft noise measurements were made at Denver International Airport for a period of four weeks. Detailed operational information was provided by airline operators which enabled noise levels to be predicted using the FAA's Integrated Noise Model. Several thrust prediction techniques were evaluated. Measured sound exposure levels for departure operations were found to be 4 to 10 dB higher than predicted, depending on the thrust prediction technique employed. Differences between measured and predicted levels are shown to be related to atmospheric conditions present at the aircraft altitude.

14. SUBJECT TERMS
Noise - Aircraft Noise Prediction

15. NUMBER OF PAGES
97

16. PRICE CODE
A05

17. SECURITY CLASSIFICATION OF REPORT	18. SECURITY CLASSIFICATION OF THIS PAGE	19. SECURITY CLASSIFICATION OF ABSTRACT	20. LIMITATION OF ABSTRACT
Unclassified	Unclassified	Unclassified	UL